International Journal of Corrosion

Atmospheric Corrosion

Guest Editors: Blanca M. Rosales, Rosa Vera, Oladis Troconis de Rincon, Alejandro Di Sarli, Jaime Alberto Rocha Valenzuela, and Johan Tidblad

Atmospheric Corrosion

International Journal of Corrosion

Atmospheric Corrosion

Guest Editors: Blanca M. Rosales, Rosa Vera,
Oladis Troconis de Rincon, Alejandro Di Sarli,
Jaime Alberto Rocha Valenzuela, and Johan Tidblad

Editorial Board

Contents

Hindawi Publishing Corporation
International Journal of Corrosion
Volume 2012, Article ID 174240, 3 pages
doi:10.1155/2012/174240

Editorial
Atmospheric Corrosion

Blanca M. Rosales,[1] Rosa Vera,[2] Oladis Troconis de Rincon,[3] Alejandro Di Sarli,[1] Jaime Alberto Rocha Valenzuela,[4] and Johan Tidblad[5]

[1] *CIDEPINT, CONICET, CCT, La Plata, Argentina*
[2] *Pontificia Universidad Católica de Valparaíso, Laboratorio de Corrosión, Instituto de Química, Valparaíso, Chile*
[3] *Universidad del Zulia, Centro de Estudios de Corrosión, Ciudad Universitaria, Maracaibo, Venezuela*
[4] *Research Institute of Metallurgy and Materials, University of San Andres, La Paz, Bolivia*
[5] *Swerea KIMAB, P.O. Box 55970, 102 16 Stockholm, Sweden*

Correspondence should be addressed to Blanca M. Rosales, brosales@fibertel.com.ar

Received 22 December 2011; Accepted 22 December 2011

The scope of this special issue is to gather the most varied research work performed on atmospheric corrosion.

According to the purpose of each project, different methodologies have been followed on diverse environments along the history. However, the nowadays generalised increase in the world pollutants contamination emphasises the need on working on transboundary research objectives. Uneven human interests determine the diversity of subjects where the money and effort inversions suggest producing the best results. In spite of that, cooperative projects have shown at present to have been the most promising systematic inversion in terms of new findings, sharing experience, time saving, and light shedding on unexpected phenomena and materials involved. They also resulted in different type of economical benefit to the respective societies in terms of personnel development, avoiding material looses, and producing direct profit incomes.

The paper "*Effects of air pollution on materials and cultural heritage: ICP materials celebrates 25 years of research*" gives an overview of all results from the International Cooperative Programme on effects on Materials including historic and cultural monuments (ICP Materials), which was launched in 1985. Since then, about twenty different materials have been exposed repeatedly in a network of test sites consisting of more than twenty sites with an extensive environmental characterisation and more than sixty official reports have been issued. Recent results on trends in corrosion, soiling, and pollution show that corrosion of carbon steel, zinc and limestone are today substantially lower than 25 years ago but while corrosion of carbon steel has decreased until today, corrosion of zinc, and limestone have remained more or less constant since the turn of the century. Unique data are given on measured HNO_3 concentrations from 2002-2003, 2005-2006, and 2008-2009 and the relative average decrease was about the same from 2002-2003 to 2005-2006 as it was from 2005-2006 to 2008-2009.

It reveals the many ways in which the research work of the European community countries produced not only the benefit of long term pollutants assessment and trends but also triggered efficient policies driving to reduce the most aggressive pollutant, the SO_2, in the atmosphere content. In 1979, the member states of the United Nations Economic Commission for Europe (UNECE) adopted the convention on long-range transboundary air pollution as a response to acid rain, brought on by contamination of the air, killing forests and lakes even in remote places far from industrial facilities. Already in 1980, Vladimir Kucera was approached by UNECE with a request to provide a short summary of the state of knowledge concerning the effects of sulphur compounds on materials. At present, the most preferable way to use the ICP data include, the economic evaluation of the "stock at risk" studies and discussion on the "use of results for policy purposes".

The paper "*Looking back on contributions in the field of atmospheric corrosion offered by the MICAT Ibero-American testing network*" summarises the joint experience of two European and twelve American countries analysing together the atmospheric corrosion of the four main base metals of structural alloys. The most extreme climes, from equator to 3 test sites in Antarctica, in natural and anthropogenic polluted atmospheres were the outdoor experience field for 6-year studies on metallic corrosion. The most advanced international techniques available (SEM, EDS, electrochemical polarisation, X-ray Diffraction, etc.) were applied to deepen the characterisation of thousands of test samples exposed in the 75 test stations network.

No less important was the objective of promoting international cooperation. The building of bridges of understanding and the establishing of Ibero-American research groups have been considered achievements of deep and lasting significance. It was taken advantage of existing synergies and above all sharing knowledge and providing training for other countries less developed in the study of atmospheric corrosion. This research project was the first time in Ibero-America that 14 countries had worked together towards a common goal in the field of corrosion.

Also, the just emergent clean technologies for anticorrosive protection were tested in the MICAT laboratories and outdoor test network in contrast with previous heavily contaminant protective materials. This also gave rise to another enormous multiplier effect in personnel qualification and strengthened the contact amongst the university and the production. Such entail was remarkably enlarged and appreciated. Not only professionals from universities and scientific institutions but also from industries gave their enthusiastic support to join experience and funds to those provided by the scientific sector in the Ibero-American region.

In that context, the paper "*Atmospheric corrosion of painted galvanized and 55% Al-Zn steel sheets. results of 12 years of exposure*", reflects the local technical need for basic science support to the manufacturing. The good correlation between visual inspection and the impedance electrochemical tests performed allowed explaining troubles observed in service and contributed to improve production quality. The laboratory and field normalized tests involved in this study were useful to understand the behavior of duplex systems exposed to natural weathering at La Plata test site, in Buenos Aires, Argentina. An almost constant corrosion rate of bare zinc and zinc-aluminum layers acting as galvanic coating of steel sheets was found during the 12-years exposure to the natural atmosphere. Both materials cathodically protected the steel substratum for 12 years. Respecting the comparative electrochemical study among the three painting systems applied on both S/Z or S/ZA sheets, different RcCc and RtCdl evolutions were obtained depending mainly on the paint. The best protective performance offered by the Polyurethane-based painting system was explained in principle taking into account its better barrier properties. The experimental results coming from the alkyd- and epoxy-based painting systems were not satisfactory due to their low resistance to the atmospheric conditions existing at La Plata station.

Also the paper "*Six-year evaluation of thermal sprayed coating Zn/Al in tropical marine environments*" reveals the impulse given at the Zulia University to the technical formation of specialists on the bases of applied research. Many of the cited bibliographic references are thesis work of different degree of students of that University Corrosion Centre. The main objective of this research was to evaluate the performance of thermosprayed coatings of zinc and aluminum (double layer) after 6 years of exposure, with and without the use of sealant (wash primer) in tropical marine environments of very high aggressiveness: La Voz (Cabo San Román/Falcón State) and Cruce del Lago de Maracaibo (Zulia State), in Venezuela. Carbon steel coupons were Zn/Al sprayed by flame process. The coupons were characterized by means of initial weight, thickness, metallographic, coating adherence, and roughness, being evaluated monthly by visual inspection during six years. After removal, the coupons were evaluated by microscopic analysis to determine the morphology of attack, microstructure, penetration of contaminants, composition, and morphology of corrosion products. The results showed that after six years, the double-layer system represents an excellent choice for corrosion protection of steel by combining the galvanic protection of zinc with the erosion resistance of aluminum. However, due to the erosion-corrosion effect, a sealant such as wash primer can be used in order to extend its service life.

In the paper "*Some clarifications regarding literature on atmospheric corrosion of weathering steels*", extensive research work has thrown light on the requisites for a protective rust layer to form on weathering steels (WS) in the atmosphere, one of the most important being the existence of wet/dry cycling. However, the abundant literature on WS behaviour in different atmospheres can sometimes be confusing and lacks clear criteria regarding certain aspects that are addressed in the present paper: What corrosion models best fit the obtained data? How long does it take for the rust layer to stabilize? What is the morphology and structure of the protective rust layer? What is an acceptable corrosion rate for unpainted WS? What are the guideline environmental conditions, time of wetness (TOW), SO_2, and Cl^- concentration for unpainted WS? The paper makes a review of the bibliography on this issue.

The same sophisticate instrumental techniques, usually applied to push beyond the present limits the scientific knowledge, may also be used by the industry to develop new and better products to improve our every-day-live quality. The long lasting research work on the most important construction materials impels the knowledge and development to a possible better built world.

Important equipment financed with official funds for scientific organisations are generally great national inversions which might be faster amortized providing very rentable solutions to unaffordable technical problems of other institutions or industries.

The research working plan for Ph.D. thesis, projects financed by the Official Scientific System, and so forth, should not be limited to basic or theoretical solutions but

training of young researchers must also involve the capability to solve real every-day problems faced by manufacturers.

Blanca M. Rosales
Rosa Vera
Oladis Troconis de Rincon
Alejandro Di Sarli
Jaime Alberto Rocha Valenzuela
Johan Tidblad

Hindawi Publishing Corporation
International Journal of Corrosion
Volume 2012, Article ID 824365, 24 pages
doi:10.1155/2012/824365

Review Article

Looking Back on Contributions in the Field of Atmospheric Corrosion Offered by the MICAT Ibero-American Testing Network

M. Morcillo, B. Chico, D. de la Fuente, and J. Simancas

Ingeniería de Superficies, Corrosión y Durabilidad, Centro Nacional de Investigaciones Metalúrgicas (CENIM, CSIC), Avenida Gregorio del Amo 8, 28040 Madrid, Spain

Correspondence should be addressed to M. Morcillo, morcillo@cenim.csic.es

Received 19 July 2011; Revised 10 October 2011; Accepted 25 October 2011

Academic Editor: Oladis Troconis de Rincon

The Ibero-American Map of Atmospheric Corrosiveness (MICAT) project was set up in 1988 sponsored by the International Ibero-American programme "Science and Technology for Development (CYTED)" and ended in 1994 after six years of activities. Fourteen countries were involved in this project: Argentina, Brazil, Chile, Colombia, Costa Rica, Cuba, Ecuador, Mexico, Panama, Peru, Portugal, Spain, Uruguay, and Venezuela. Research was conducted both at laboratories and in a network of 75 atmospheric exposure test sites throughout the Ibero-American region, thus considering a broad spectrum of climatological and pollution conditions. Although with its own peculiarities, the project basically followed the outline of the ISOCORRAG and ICP/UNECE projects, with the aim of a desirable link between the three projects. This paper summarizes the results obtained in the MICAT project for mild steel, zinc, copper, and aluminum specimens exposed for one year in different rural, urban, and marine atmospheres in the Ibero-American region. Complementary morphological and chemical studies were carried out using scanning electron microscopy (SEM) coupled with energy dispersive spectrometry (EDS), X-ray diffraction (XRD), and fourier transform infrared Spectroscopy (FTIR) techniques, in order to correlate climatic and atmospheric conditions and properties of the corrosion products.

1. Introduction

During the 2nd Ibero-American Congress on Corrosion and Protection held in Maracaibo (Venezuela) in September 1986, a round-table was organized to discuss the idea of an Ibero-American Map of Atmospheric Corrosion (MICAT). Representatives of the countries present at the meeting expressed their interest in participating in such a project.

Moves were then made to include this proposal in the Ibero-American Programme Science and Technology for Development (CYTED). A year later, in January 1988, the Technical and Managing Council of CYTED, gathered in Havana (Cuba), decided to approve the inclusion of the MICAT study into the CYTED Programme.

The primary aims of the MICAT study were [1, 2] as follows.

(1) To improve knowledge of the process of atmospheric corrosion in various climatic regions of Iberoamerica.

(2) By means of statistical treatment of the results to obtain mathematical expressions of the estimation of atmospheric corrosion as a function of climatic and pollution parameters.

(3) No less important was the objective of promoting international cooperation. In this respect, the building of bridges of understanding and the establishing of Ibero-American research groups have been achievements of deep and lasting significance, taking advantage of existing synergies and above all sharing knowledge and providing training for other countries less developed in the study of atmospheric corrosion. This research project was the first time in Ibero-America that 14 countries had worked together towards a common goal in the field of corrosion.

The MICAT project was officially launched in Caracas in August 1988 and came to an end in Lisbon in December 1994, with meetings in Rio de Janeiro (1989), San Jose Costa

Rica (1990), Marambio Argentine Antarctic Base (1991), Madrid (1992), and Santiago de Chile (1993).

Research was carried out in laboratories in the 14 participating countries (Argentina, Brazil, Colombia, Costa Rica, Chile, Ecuador, Mexico, Panama, Peru, Portugal, Spain, Uruguay, and Venezuela) and in a network of 72 atmospheric testing stations covering a broad spectrum of climatological and pollution conditions. Some 70 working groups comprising a total of 130 researchers took part in the project. The countries, organizations responsible, and contact persons are listed in Table 1.

The publication of preliminary results [3, 4] met with accolades throughout Ibero-America and received an NACE International award. A book has been published in Spanish and Portuguese [5] describing in more than 800 pages all the details and results obtained in the MICAT project. Likewise, several papers have been published in international journals, which describe in an ample way the main results obtained [6–17]. Some of the countries participating in the project have also published their own monographic studies: Spain [18], Argentina [19], Portugal [20], Mexico [21], and so forth.

This paper summarises the MICAT project's main contributions to knowledge of atmospheric corrosion.

2. Experimental

Although with its own peculiarities, the project basically followed the outline of the ISOCORRAG [22] and ICP/UNECE [23] projects, with the aim of a desirable link between the three projects. Standardized procedures ISO have been followed.

Figure 1 shows the location of the Ibero-American network of atmospheric corrosion test stations. The names and identification codes of the test are sites listed in Table 2. The network provides a variety of climatological and pollution conditions.

The atmosphere at each test site is characterized from meteorological and atmospheric pollution data (ISO 9223 [24]). The former include basically the temperature, relative humidity (RH) of the air, and rainfall. These parameters are recorded at the station itself most lie in meteorological stations of the Meteorological Service of the country in question—or at a neighbouring meteorological station. The recorded thermohydrograms are used to show the time of wetness (TOW), the fraction of the year in which RH > 80% and T > 0°C. The deposition rates of SO_2 and chloride are measured following ISO 9225 [25]. Average annual environmental data have been published elsewhere [14].

The materials investigated are structural metals, in the form of flat plate specimens, with the following features: steel (unalloyed, low carbon), zinc (98.5% min), copper (99.5% min), and aluminum (99.5% min). The test specimens are usually $10 \times 15\ cm^2$ and cut out from 1 mm thick sheets.

The exposure sequences include three one-year exposures, one two-year exposure, one three-year exposure, and one four-year exposure. In this paper only one-year exposures have been considered.

Four specimens of each material are exposed in each sequence, three of which are used to determine weight losses according ISO 9226 [26]. The removal of corrosion products by chemicals to determine the weight loss involves a loss of valuable information of the atmospheric corrosion process. Therefore, a fourth specimen of each sequence was used for laboratory studies: (a) analysis of the corrosion products by means of diverse experimental techniques: XRD, IR, Mössbauer spectroscopy, and so forth, and microscopical examination (surface and cross-section) of the morphology of the corrosion products layers.

2.1. Identification of Corrosion Products. The identification techniques used were basically the following: X-ray diffraction (XRD), infrared spectroscopy (IR), and Mössbauer Spectroscopy (only for the steel). In certain cases elemental information was also obtained by energy dispersive spectroscopy (EDS). The techniques used are complementary. The integration of all of them has permitted a more precise identification of the corrosion compounds formed.

2.2. Morphology of the Attack of the Base Metal and Microstructure of the Corrosion Products. This information was obtained from observation with the scanning electron microscope (SEM) of both the outer surface of the layer of corrosion products and cross-sections. In some cases elemental information was also obtained by EDS, as well as X-ray mappings of certain chemical elements of interest (mainly S and Cl).

3. Main Results and Discussion

In particular, attention is paid to the atmospheric corrosion of four reference metals: unalloyed carbon steel, zinc, copper, and aluminium.

The MICAT project gathered highly varied and complementary information that allowed an in-depth insight into the atmospheric corrosion mechanisms of these four metals. This data included atmospheric aggressivity factors (meteorological parameters, time of wetness (TOW), sulphur dioxide, and chloride deposition rates), the attack experienced by the materials in different atmospheres, the nature of the corrosion products formed on the metallic surface, the morphology of the corrosion films and products, and the morphology of the attack experienced by the base metals.

In order to address this analysis in a systematic way, reference was essentially made to international standard ISO 9223 [24], which classifies atmospheres by their TOW (τ) and the deposition rate of the most common pollutants: sulphur dioxide (P) and atmospheric salinity (S). Thus, the testing stations participating in the project were classified as shown in Table 3. Figure 2 gives an overview of the atmospheres considered in the research by S_xP_y categories according to ISO 9223 [24]. As can be seen, the MICAT atmospheres cover the spectrum of rural and pure marine atmospheres fairly well and are sufficiently representative of marine atmospheres with low to moderate SO_2 contents, but

Table 1: Organizations participating in the MICAT Project.

Country	Institution, organization	Contact person
Argentina	Instituto de Investigaciones Científicas y Técnicas de las Fuerzas Armadas (CITEFA)	B. M. Rosales
Brazil	Centro de Pesquisas de Energía Elétrica (CEPEL)	M. Marrocos
Chile	Universidad de Chile Instituto de Investigaciones y Ensayes de Materiales (IDIEM)	G. Joseph
Colombia	Universidad de Antioquia	A. Valencia
Costa Rica	Instituto Tecnológico de Costa Rica (ITCR)	J. F. Álvarez
Cuba	Centro de Investigaciones Químicas (CIQ)	A. Cabezas
Ecuador	Escuela Superior Politécnica del Litoral (ESPOL)	J. Peña
Mexico	Instituto de Investigaciones Eléctricas (IIE)	J. Uruchurtu
Panama	Universidad de Panamá	A. F. de Bósquez
Peru	Instituto de Investigación Tecnológica Industrial de Normas Técnicas (ITINTEC)	G. Salas
Portugal	Instituto Nacional de Engenharia e Tecnología Industrial (INETI)	E. M. Almeida
	Instituto Superior Técnico (IST)	M. G. S. Ferreira
Spain	Centro Nacional de Investigaciones Metalúrgicas (CENIM/CSIC)	M. Morcillo
Uruguay	Universidad de la República Oriental del Uruguay (UROU)	S. Rivero
Venezuela	Universidad Nacional Experimental Francisco Miranda (UNEFM)	M. R. Prato
	Universidad del Zulia	O. T. de Rincón

Figure 1: MICAT network of atmospheric corrosion stations.

Table 2: List of MICAT test sites.

Country	Code	Test site
Argentina	1	Camet
	2	V. Martelli
	3	Iguazú
	4	San Juan
	5	Jubani
	6	La Plata
Brazil	7	Caratinga
	8	Ipatinga
	9	Arraial do Cabo
	10	Cubatao
	11	Ubatuba
	12	São Paulo
	13	Río de Janeiro
	14	Belem
	15	Fortaleza
	16	Brasilia
	17	P. Afonso
	18	Porto Velho
Colombia	19	Isla Naval
	20	San Pedro
	21	Cotové
Costa Rica	22	Puntarenas
	23	Limón
	24	Arenal
	25	Sabanilla
Cuba	26	Ciq
	27	Cojímar
	28	Bauta
Chile	29	Cerrillos
	30	Valparaíso
	31	Idiem
	32	Petrox
	33	Marsh
	34	Isla de Pascua
Ecuador	35	Guayaquil
	36	Riobamba
	37	Salinas
	38	Esmeraldas
	39	San Cristóbal
Mexico	48	México
	49	Cuernavaca
	50	Potosí
	51	Acapulco
Panama	52	Panamá
	53	Colón
	54	Veraguas
Peru	55	Piura
	56	Villa Salvador
	57	San Borja
	58	Arequipa
	59	Cuzco
	60	Pucallpa
Portugal	62	Leixões
	63	Sines
	64	Pego
Spain	40	León
	41	El Pardo
	42	Barcelona, S
	43	Tortosa
	44	Granada
	45	Lagoas
	46	Labastida
	47	Artíes
Uruguay	65	Trinidad
	66	Prado
	67	Melo
	68	Artigas
	69	Punta del Este
Venezuela	70	El Tablazo
	71	Punto Fijo
	72	Coro
	73	Matanzas
	74	Barcelona, V
	75	Puerto Cabello

are short of atmospheres with only SO_2 pollution or mixed high contents of both pollutants.

3.1. Atmospheric Corrosion of Mild Steel

3.1.1. Mechanisms [27]. According to Kucera and Mattsson [28], two general stages may be distinguished in the atmospheric corrosion of iron: initiation and propagation.

Initiation. In a dry, clean atmosphere the steel surface becomes coated with a 20–50 Å thick oxide film that practically prevents further oxidation.

The initiation of corrosion on a clean metal surface in nonpolluted atmospheres is a very slow process, even in atmospheres saturated with water vapour. In this case, initiation may occur at surface inclusions such as MnS, which dissolve when the surface becomes wet [29, 30]. Another important factor for the initiation of corrosion is the presence of solid particles on the surface [31].

During the initiation period, anodic spots surrounded by cathodic areas are formed.

Table 3: Classification of MICAT test sites according to ISO 9223 [24].

Type of atmosphere	Denomination (ISO 9223) [24]	Deposition rate	
		Cl^- ($mg \cdot m^{-2} \cdot d^{-1}$)	SO_2 ($mg \cdot m^{-2} \cdot d^{-1}$)
Rural atmospheres	S_0P_0	$S \leq 3$	$P \leq 10$
Urban and industrial atmospheres	S_0P_1	$S \leq 3$	$10 < P \leq 35$
	S_0P_2	$S \leq 3$	$35 < P \leq 80$
Marine atmospheres*	S_1P_0	$3 < S \leq 60$	$P \leq 10$
	S_2P_0	$60 < S \leq 300$	$P \leq 10$
	S_3P_0	$300 < S \leq 1500$	$P \leq 10$
Mixed atmospheres	S_1P_1	$3 < S \leq 60$	$10 < P \leq 35$
	S_1P_2	$3 < S \leq 60$	$35 < P \leq 80$
	S_2P_1	$60 < S \leq 300$	$10 < P \leq 35$
	S_2P_2	$60 < S \leq 300$	$35 < P \leq 80$

*Due to the singular climatic characteristic of the marine Antarctic test sites, they have been considered as a separate group, whose results have been already published [16].

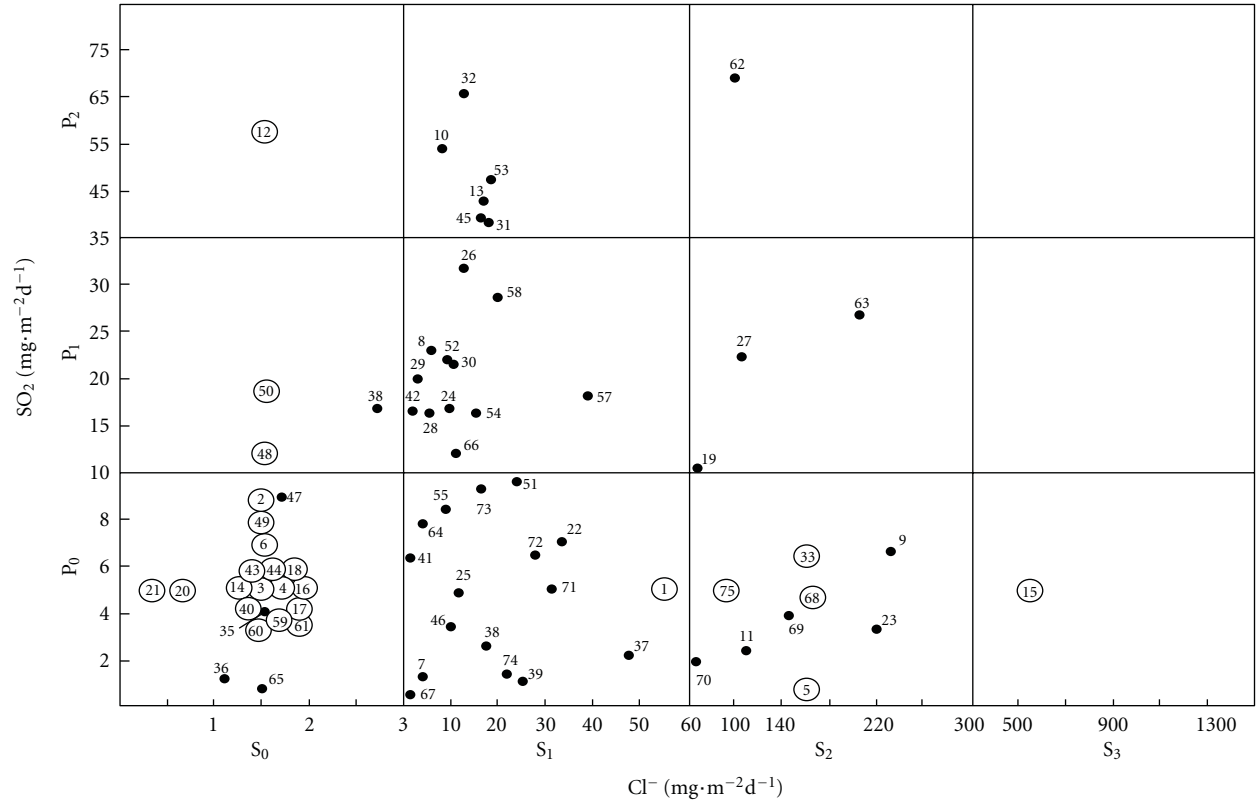

Figure 2: Classification of the test sites, according to ISO 9223 [24] and based on the SO_2 and Cl^- deposition rates (average of the first three years of exposure in the atmospheres). The test sites where the deposition rates have been estimated are surrounded with a circle.

Propagation. In the presence of an electrolyte film on the metal surface, conditions are created for propagation of the corrosion process.

The following equations may in principle describe the reactions taking place in the corrosion cells [28],

At the Anode:

$$Fe \longrightarrow Fe^{2+} + 2e^- \quad (1)$$

At the Cathode. The main cathodic reaction is considered to be reduction of oxygen dissolved in the electrolyte film:

$$\frac{1}{2}O_2 + H_2O + 2e^- \longrightarrow 2OH^- \quad (2)$$

This process causes a local increase in pH at the cathodes and promotes the precipitation of corrosion products at some distance from the anodes.

Electrochemical studies by Stratmann and Müller [32] showed for the first time that oxygen is reduced within the oxide layer and not at the metal/electrolyte interface.

As soon as ferric corrosion products have been formed, another cathodic process may take place:

$$Fe^{3+} + e^- \longrightarrow Fe^{2+} \tag{3}$$

Evans [33] developed an electrochemical model to explain the observed influence of changing wetness on the atmospheric corrosion of iron. He postulated that in periods of high water content within the porous structure of the rust, the anodic dissolution of iron is balanced by the cathodic reduction of Fe(III) oxides in the rust layer

$$Fe^{2+} + 8FeOOH + 2e^- \longrightarrow 3Fe_3O_4 \text{ (unstable)} + 4H_2O \tag{4}$$

The consensus in the early 1970s was that the main products of rust formed on mild steels in atmospheric corrosion were α-FeOOH, γ-FeOOH, Fe_3O_4, and X-ray amorphous matter. However, the mechanism of the formation of α-FeOOH, γ-FeOOH, and amorphous matter in atmospheric rusting was not completely understood. In particular, the composition of amorphous matter remains undetermined.

Misawa et al. [34] characterised X-ray amorphous matter as amorphous ferric oxyhydroxide $FeO_x(OH)_{3-2x}$ by XRD and IRS, formulating the following mechanism of atmospheric rusting.

(a) Rusting starts with the formation of γ-FeOOH in a neutral to slightly acidic solution. In the first stage of rusting the aerial oxidation of ferrous ions, dissolved from the steel into a slightly acidic thin water layer formed by rain on the steel surface, leads to the precipitation of γ-FeOOH. Fine weather accelerates the precipitation and crystallisation of γ-FeOOH by drying,

$$\begin{aligned} Fe &\xrightarrow{\text{dissolution}} Fe^{2+} \xrightarrow{\text{hydrolysis}} FeOH^+ \\ &\xrightarrow{\text{oxidation and precipitation}} \gamma\text{-FeOOH} \end{aligned} \tag{5}$$

(b) The γ-FeOOH content is higher in inner rust layers than in outer layers, which contain large amounts of amorphous ferric oxyhydroxide and α-FeOOH. This suggests that γ-FeOOH is formed on the steel surface and transformed to amorphous ferric oxyhydroxide and α-FeOOH from the outer part upon atmospheric rusting as follows.

It is known that fresh rain dissolving impurities including SO_2 in the atmosphere often shows a low pH value, such as pH 4. Such a low pH water layer dissolves γ-FeOOH and results in the precipitation of amorphous ferric oxyhydroxide with drying. The amorphous ferric oxyhydroxide transforms to α-FeOOH by deprotonation using hydroxyl ions provided by the rain,

$$\begin{aligned} \gamma\text{-FeOOH} &\xrightarrow{\text{Dissolution and precipitation}} \underset{\text{Amorphous ferric oxyhydroxide}}{FeO_x(OH)_{3-2x}} \\ &\xrightarrow{\text{Solid state transformation}} \alpha\text{-FeOOH} \end{aligned} \tag{6}$$

The wet-dry cycle accelerates these rusting process, especially precipitation and transformation with deprotonation and dehydration.

Stratmann et al. [35], in an electrochemical study of phase transitions in rust layers, experimentally showed that the oxidation of Fe_3O_4 to γ-FeOOH (reaction (7)), as proposed by Evans [33, 36] and Evans and Taylor [37], was not possible,

$$3Fe_3O_4 + \frac{3}{4}O_2 + \frac{9}{2}H_2O \longrightarrow 9FeOOH \tag{7}$$

Thus, in 1987 Stratmann et al. [35] proposed dividing the atmospheric corrosion mechanism of pure iron into the following three stages.

Stage 1: Wetting of the Dry Surface. As proposed by Evans [33, 36] and Evans and Taylor [37], a corrosion cell starts where the anodic dissolution of iron is balanced by the cathodic reduction of Fe(III) in the rust layer

$$\begin{aligned} &2\gamma\text{-FeOOH} + 2H^+ + 2e \longrightarrow 2Fe \cdot OH \cdot OH \\ &\text{(reduced surface layer on FeOOH crystals)} \end{aligned} \tag{8}$$

During this stage the cathodic O_2 reduction reaction is very slow compared to anodic iron dissolution. The metal dissolution rate is high, but the amount of dissolved iron is restricted to the amount of reducible FeOOH in the rust layer [38].

Stage 2: Wet Surface. Once the reducible FeOOH has been used up, the O_2 reduction reaction becomes the cathodic reaction as in (2).

The metal dissolution rate is determined by the diffusion limited current density of the O_2 reduction reaction on the pore surfaces. Because the pores in the rust layer are filled with electrolyte, the corrosion rate is quite slow during stage 2, as the diffusion rate is lower in the electrolyte than in the gas phase.

Electrochemical studies by Stratmann and Müller [32] showed for the first time that oxygen is reduced within the oxide scale and not at the metal/electrolyte interface. This implies that the electronic structure of the oxides will strongly influence the reduction of oxygen and therefore also the corrosion rate. The atmospheric corrosion rate is determined for thin films by the electronic properties of the rust layer, and the corrosion rate immediately decreases as the oxides are reoxidised [39].

Stage 3: Drying-Out of the Surface. During drying-out, the rate of the diffusion limited O_2 reduction reaction is extremely fast due to thinning of the electrolyte film on the inner surface of the rust layer. Accordingly, the corrosion rate is very high, O_2 reduction again being the cathodic reaction.

In addition to this, O_2 can reoxidise the reduced Fe^{2+} formed in stage 1

$$2Fe \cdot OH \cdot OH + 2O_2 \longrightarrow 2FeOOH + H_2O \tag{9}$$

As a consequence of the high corrosion rate, stage 3 seems to dominate the metal loss during the whole wet-dry cycle.

In the third stage, the reduced layer of γ-FeOOH and the other ferrous species are reoxidised by oxygen, leading to the formation of goethite and the regeneration of lepidocrocite. The electrolyte film is used up, stopping the corrosion process completely. It is during this final stage that the rust layer composition changes, leading to a different intensity in the corrosion process for the next wet-dry cycle.

Misawa [34] notes that the main constituent of rust in a rural (unpolluted) atmosphere is γ-FeOOH, while in an atmosphere containing SO_2 a large amount of α-FeOOH is detected.

The atmospheric corrosion process is stimulated by SO_2, which is adsorbed and oxidised in the rust layer to SO_4^{2-}. In the corrosion cells, sulphate accumulates at the anodes and thus creates so-called sulphate nests in the rust, which were first described by Schwarz [40].

When the surface becomes wetted by rain, dew, or moisture adsorption, the sulphate nests in combination with the surrounding area form corrosion cells. The electrolyte is mostly very concentrated and has low water activity. Anodes are located inside the sulphate nests.

The sulphate nest becomes enclosed within a semipermeable membrane of hydroxide formed through oxidative hydrolysis of the iron ions. Diffusion causes transfer of sulfate ions into the nest. This will stabilise the existence of the nest.

Hydrolysis of the ferrous sulphate formed in these nests controls their propagation. The osmotic pressure can cause them to burst, thus increasing the corrosion rate. The nests are covered by a membrane containing FeOOH. The higher the amorphous FeOOH content, the greater the stability of this membrane and the more unlikely it is to burst due to the effect of osmotic pressure and the repeated wetting and drying of the rust layer.

In atmospheres polluted with chlorides the corrosion of carbon steel proceeds in local cells which resemble the sulphate nests mentioned above [41]. They may arise around chloride particles deposited on the surface, where the concentrated chloride solution locally destroys the FeOOH passivating film. In the anodic areas so formed, the chlorides are concentrated by migration while the rust-coated surrounding area acts as a cathode. However, unlike in the case of atmospheres polluted with SO_2, nests are not formed. No amorphous oxide/hydroxide membrane is formed. It is fairly common to find iron chlorides among the iron corrosion products, which tend to accumulate at the steel/rust interface by migration.

In marine atmospheres, in addition to γ-FeOOH and α-FeOOH, akaganeite (β-FeOOH) and magnetite (Fe_3O_4) are also formed. The latter species tends to be concentrated in the innermost zones of the rust layer, where it is hardest for oxygen to reach. In contrast, akaganeite forms in the most superficial zones of the rust layer.

Sea chlorides from natural airborne salinity together with SO_2 play an important role in determining the magnitude of atmospheric steel corrosion. However, the scientific literature contains relatively little information on atmospheric corrosion in this type of mixed atmospheres.

The diversity of industrial environments, with the possible presence of other pollutants that may influence the corrosion process, has given rise to several papers on the effect of both pollutants (SO_2 and chlorides), acting together. Thus, Ericsson [42] speaks of a synergic effect of the combined influence of SO_2 and sodium chloride while others speak of a competitive absorption effect [43].

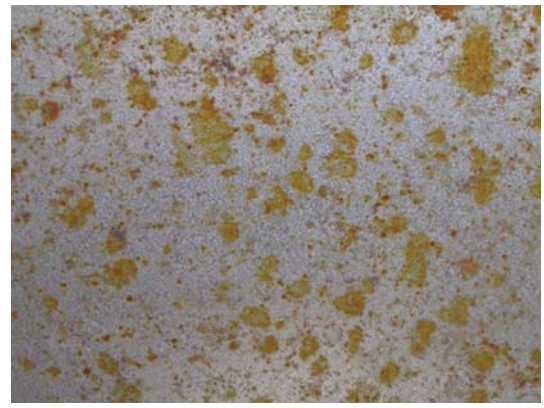

Figure 3: Appearance of the mild steel surface after one year of outdoor exposure in Cuzco.

3.2. Main Results Obtained in the MICAT Project. Table 4 displays information obtained in the MICAT project [6, 7] and Table 5 gives a list of the main corrosion products identified.

There follows a summary of mild steel behaviour in the MICAT project testing station network covering different types of atmospheres according to ISO 9223 (Table 3).

Unpolluted Atmospheres (S_0P_0):

(i) S_0P_0 rural atmospheres, with very low chloride and SO_2 pollution, showed significantly different time of wetness (TOW) and environmental characteristics, such as soil particulate pollution and background pollution. As a consequence of these differences, a relatively wide range of steel corrosion rates could be observed, from 1.4 to 28.2 $\mu m \cdot y^{-1}$, after one year of exposure. The steel corrosion product layers were constituted by lepidocrocite or lepidocrocite and goethite.

(ii) An extremely low first-year corrosion rate of steel (Ave. 1.4 $\mu m \cdot y^{-1}$) in the atmosphere of Cuzco (Peru) was found, perhaps the lowest ever reported in the literature [44].

The low atmospheric corrosion of steel in this Peruvian city was evident by inspecting the surface of steel exposed to the atmosphere for one year (Figure 3). The surface was not fully rusted and only showed scattered corrosion spots. This suggests that the metal surface does not go beyond the early steps of the atmospheric corrosion process, where the attack is limited to a few anodic areas while the rest of the metal surface remains unaltered.

Different hypotheses were put forward to try to explain this singular behaviour: very short TOW, steel composition,

Table 4: MICAT test sites characteristics. Data for mild steel.

Type of atmosphere (Table 3)	Id. (Table 2)	Name	Deposition rate ($mg \cdot m^{-2} \cdot d^{-1}$)		Time of wetness (TOW)	1st-year corrosion rate (μm)	Atmospheric corrosivity (ISO 9223) [24]	Corrosion products (see Table 5)
			Cl^-	SO_2				
S_0P_0	60	Cuzco	(*)	(*)	τ_4	1,4	C2	—
	47	Artíes	1,7	9,0	τ_3	3,9	C2	L, G
	4	San Juan	(*)	(*)	τ_3	4,9	C2	—
	3	Iguazú	(*)	(*)	τ_5	5,7	C2	L
	65	Trinidad	1,5	0,7	τ_4	6,7	C2	—
	36	Riobamba	1,1	1,2	τ_4	8,4	C2	L
	44	Granada	(*)	6,2	τ_3	8,5	C2	L, G
	16	Brasilia	(*)	(*)	τ_4	12,9	C2	L
	49	Cuernavaca	(*)	7,9	τ_3	13,4	C2	L, G
	61	Pucallpa	(*)	(*)	τ_5	14,3	C2	L, G
	2	V. Martelli	(*)	9,0	τ_4	14,7	C2	L
	59	Arequipa	(*)	(*)	τ_2	15,4	C2	L
	20	San Pedro	(*)	0,6	τ_5	17,0	C2	L, G
	14	Belem	(*)	(*)	τ_5	19,4	C2	L, G
	21	Cotové	(*)	0,3	τ_4	19,6	C2	L, G
	43	Tortosa	(*)	5,3	τ_4	20,2	C2	L, G
	40	León	(*)	(*)	τ_3	20,8	C2	L, G
	35	Guayaquil	1,5	3,0	τ_4	22,6	C2	L
	6	La Plata	(*)	6,9	τ_4	28,1	C3	—
S_0P_1	48	México	(*)	13.6	τ_3	9.7	C2	—
	50	S. L. Potosí	(*)	18.9	τ_3	31.1	C3	—
S_0P_2	12	São Paulo	(*)	57.8	τ_5	20.6	C2	L, G
S_1P_0	67	Melo	3,8	0,7	τ_5	12,8	C2	—
	41	El Pardo	3,9	6,4	τ_4	11,3	C2	L, G
	7	Caratinga	5,8	1,3	τ_4	11,1	C2	L, G, Mg
	64	Pego	6,0	7,9	τ_4	28,5	C3	L, G
	55	Chiriquí	8,7	8,2	τ_4	23,0	C2	G, L, Mg
	46	Labastida	9,8	3,6	τ_4	15,0	C2	L, G,
	25	Sabanilla	11,3	4,9	τ_5	16,6	C2	L, G
	73	Matanzas	15,9	9,3	τ_4	23,0	C2	—
	24	Arenal	16,7	9,2	τ_5	69,3	C4	L, G, M
	74	Barcelona,V	21,8	1,5	τ_4	18,5	C2	L, G
	51	Acapulco	23,8	9,6	τ_4	22,1	C2	L, G, M
	39	S. Cristóbal	25,0	1,1	—	34,5	C3	—
	72	Coro	27,5	6,5	τ_4	14,8	C2	—
	71	Punto Fijo	31,0	5,0	τ_4	21,4	C2	L, G
	22	Puntarenas	33,4	7,1	τ_4	61,6	C4	L, G, Mg
	37	Salinas	47,3	2,3	τ_4	55,4	C4	—
	1	Camet	55,1	(*)	τ_5	49,5	C3	L, G
S_2P_0	70	El Tablazo	63,3	6,0	τ_4	29,3	C3	L, G
	75	P. Cabello	—	(*)	τ_5	37,3	C3	L, G, A
	11	Ubatuba	113	2,6	τ_4	302,0	C5	L, G, A, M
	69	P. del Este	144	4,0	τ_4	53,0	C4	—
	23	Limón	220	3,5	τ_5	371,5	>C5	L, G, M
	9	A. do Cabo	229	6,7	τ_4	165,4	C5	G, M, L, Mg
S_3P_0	15	Fortaleza	>300	(*)	τ_4	118.3	C5	—

Table 4: Continued.

Type of atmosphere (Table 3)	Id. (Table 2)	Name	Deposition rate ($mg \cdot m^{-2} \cdot d^{-1}$)		Time of wetness (TOW)	1st-year corrosion rate (μm)	Atmospheric corrosivity (ISO 9223) [24]	Corrosion products (see Table 5)
			Cl^-	SO_2				
S_1P_1	42	Barcelona, S	4,4	16,7	τ_3	17,4	C2	L, G
	54	Veraguas	14,8	16,5	τ_4	20,0	C2	L, G, Mg
	52	Panamá	9,8	21,7	τ_4	27,6	C3	L, G, Mg
	26	Ciq	12,0	31,6	τ_4	30,4	C3	G, L
	58	San Borja	20,0	29,0	τ_5	30,8	C3	L, G
	66	Prado	10,8	12,1	τ_4	33,3	C3	—
	28	Bauta	6,4	16,4	τ_4	33,8	C3	L, G
	57	V. Salvador	38,0	18,0	τ_5	35,1	C3	L, M
	30	Valparaíso	10,0	23,6	τ_5	35,5	C3	—
	29	Cerrillos	4,5	20,0	τ_4	36,3	C3	L, G
	8	Ipatinga	6,8	23,0	τ_4	49,4	C3	L, G
S_1P_2	45	Lagoas	16,7	39,5	τ_4	28,2	C3	L, G
	53	Colón	16,8	47,4	τ_5	108,1	C5	G, L
	13	Río Janeiro	16,4	43,5	τ_4	110,5	C5	L, G
	10	Cubatão	8,1	54,5	τ_4	158,9	C5	L, G, M
	32	Petrox	12,8	65,2	τ_5	167,2	C5	—
S_2P_1	19	Isla Naval	60,7	10,3	τ_5	33,5	C3	L, G, A
	27	Cojímar	104	22,5	τ_4	193,2	C5	M, L, G
	63	Sines	203	27,0	τ_4	365,0	>C5	L, G, A, M, Mg
S_2P_2	62	Leixões	97,6	69,2	τ_4	72,4	C4	L, G, M

(*) apparently nonpolluted.
(—) not available.

Table 5: Steel corrosion products identified in the MICAT project.

Code	Name	Composition
	Hydroxides	
L	Lepidocrocite	γ-FeOOH
G	Goethite	α-FeOOH
A	Akaganeite	β-FeOOH
	Oxides	
M	Magnetite	Fe_3O_4
Mg	Maghemite	γ-Fe_2O_3

and low atmospheric pollution. From the results obtained, it seems that the atmosphere of Cuzco is almost unpolluted, which may account for the extremely low corrosion rates found. Some authors [45, 46] suggest that the presence of strong oxidants such as hydrogen peroxide and ozone can favour the formation of a passivating layer over the steel surface, thereby inhibiting the atmospheric corrosion process. In this respect, the great height of Cuzco (3219 m) may account for increased amounts of ozone.

SO_2-Polluted Atmospheres (S_0P_1, S_0P_2):

(i) The scarce data obtained in the MICAT project for steel samples exposed in urban atmospheres ($SO_2 \leq 60\ mg \cdot m^{-2} \cdot d^{-1}$ of SO_2), only 3 test sites, yields results which are not significantly different to those obtained in rural atmospheres. However, it was confirmed by Mössbauer spectroscopy that the α-FeOOH/γ-FeOOH ratio increases when SO_2 pollution increases.

Pure Marine Atmospheres (S_1P_0, S_2P_0, S_3P_0):

(i) In S_1P_0 marine atmospheres (low chloride deposition rates) mild steel presented corrosivity categories from C2 to C4, and the corrosion surface layer exhibited a morphology characterized by cotton balls of acicular iron corrosion products (Figure 4(a)). The relatively compact corrosion product layers were composed of lepidocrocite, goethite, and occasionally traces of maghemite and/or magnetite.

(ii) In S_2P_0 marine atmospheres, corrosion product layers exhibited more open structures (Figure 4(b)) and a greater tendency to flaking, showing higher corrosivity categories (C3–C5). When $S > 60\ mg \cdot m^{-2} \cdot d^{-1}$ of Cl^- and TOW $\geq \tau_4$, the presence of akaganeite (β-FeOOH) can be seen among the corrosion products. The surface morphology of corrosion layers corresponds to generalized honeycomb structures.

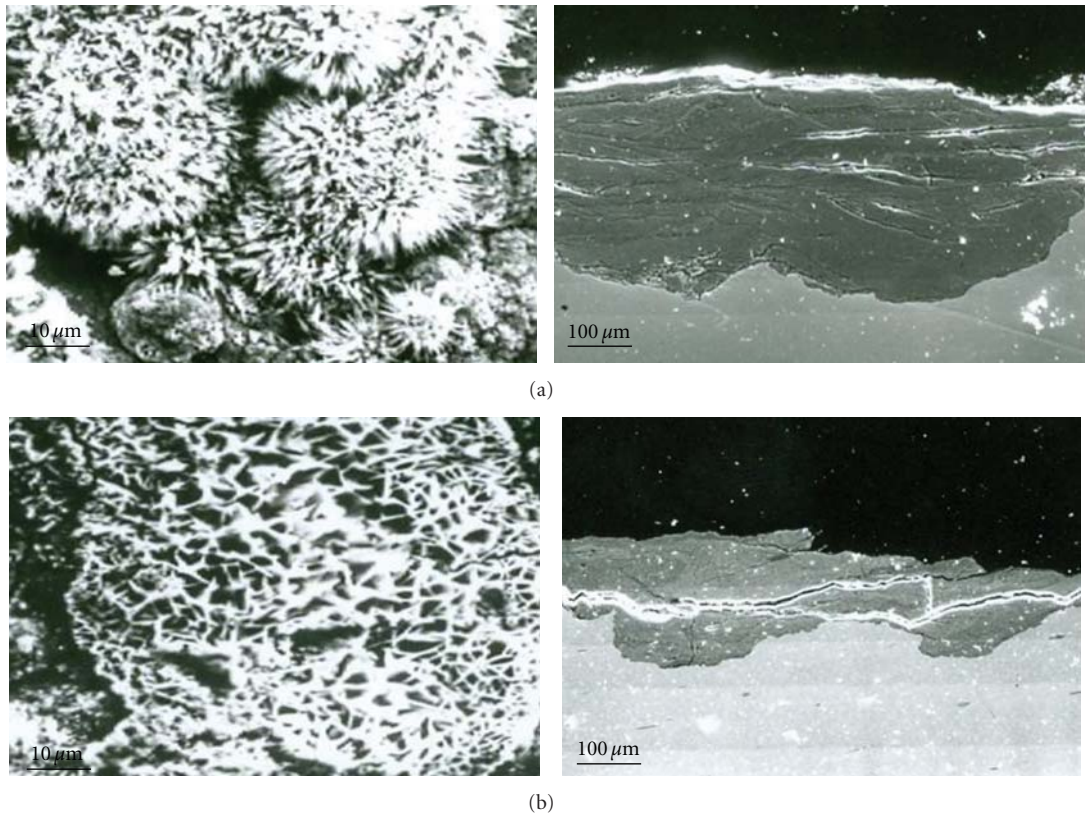

Figure 4: SEM micrographs of corrosion product layers formed on mild steel in pure marine atmospheres: (a) Puntarenas (S_1P_0) and (b) Arraial do Cabo (S_2P_0).

Mixed Marine Atmospheres (S_1P_1, S_2P_2, S_2P_1, S_2P_2):

(i) They showed different corrosivity categories (from C2 to > C5), depending on their SO_2 and Cl^- pollution levels. Most of iron corrosion products were identified: L, G, A, M, Mg (Table 5).

(ii) The cracking effect in the corrosion product layer seems to increase with SO_2 pollution and TOW while the contribution of chloride ions into the open structures seems to play a detrimental effect on atmospheric corrosion resistance.

3.3. Atmospheric Corrosion of Zinc

3.3.1. Mechanisms [47]. A prerequisite for atmospheric corrosion to occur is that a moisture layer be present on the zinc surface. This layer acts as a solvent for atmospheric constituents and a medium for electrochemical reactions. The atmospheric corrosion of zinc is influenced principally by the time of wetness and the presence of atmospheric constituents such as CO_2, SO_x, and Cl^-. When the moisture layer evaporates, a film of corrosion products precipitates.

Unlike in the atmospheric corrosion of iron, the corrosion products formed on zinc include the respective characteristic anion of the environment where the metal is exposed: CO_3^{2-}, SO_4^{2-}, Cl^-, and so forth, giving rise to different basic chemical compounds: carbonates, sulphates, chlorides, and so forth. Zinc exposed to the atmosphere is particularly sensitive to wetting and drying cycles, which are largely dependent on the climatology. These alternating periods have a considerable influence on certain characteristics of the corrosion products, such as their amount and compactness.

As other metals zinc corrodes in the atmosphere in a discontinuous process, electrochemical in nature, each time the metallic surface is wet. Quintana et al. [48] point out the importance of the temperature-humidity complex in the atmospheric corrosion of zinc. Both metal temperature and time of wetness influence the morphology of the corrosion products formed.

A ZnO (zincite) film is the first thin layer to form from the reaction of zinc with atmospheric oxygen [49]. According to Schikorr [50] these films have a relatively minor protective effect. In the presence of water, zincite is promptly transformed into hydroxides. Many studies agree that upon initial exposure zinc rapidly forms a thin film of zinc hydroxide. In continued exposure this film is transformed into various other atmospheric corrosion products [51].

Carbonates are formed as a result of the reaction of zinc hydroxide with atmospheric CO_2. Although several compounds have been detected, the most common are $ZnCO_3$ (smithsonite) and $Zn_5(CO_3)_2(OH)_6$ (hydrozincite). However, hydrozincite is sometimes difficult to detect by XRD.

SO_2 concentration in the atmosphere is a major factor in controlling the rate of corrosion of zinc; the zinc corrosion film has been shown to strongly absorb SO_2 during

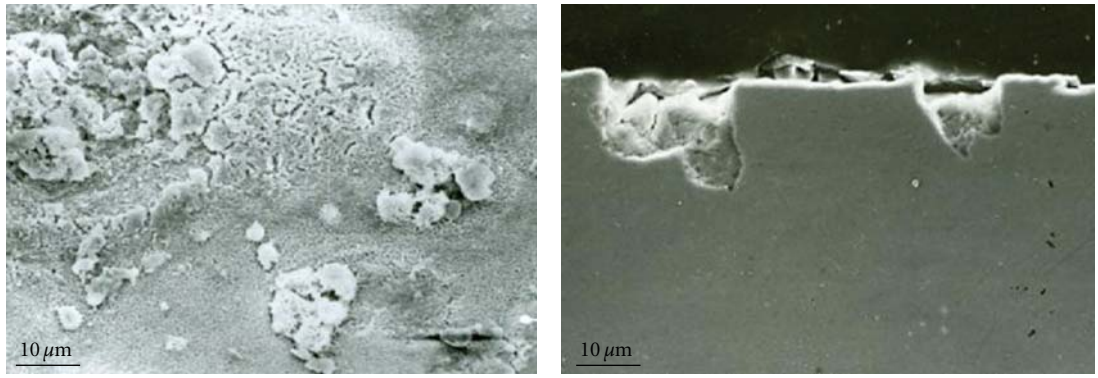

(a) (b)

Figure 5: Morphology of corrosion product layers formed on zinc in unpolluted atmospheres: (a) Villa Martelli (surface view) and (b) La Plata (cross-section view).

dry deposition. Likewise, deposition of acidic condensates produces a fall in pH and the rate of zinc attack again increases [52]. There is an approximately linear relationship between zinc corrosion rate and sulphur dioxide concentration in the atmosphere [53]. In SO_2-polluted atmospheres the formation of basic zinc sulphates and zinc hydroxysulfate takes place. Different compounds may be formed $[6Zn(OH)_2 \cdot ZnSO_4 \cdot 4H_2O]$, $[Zn_7(OH)_{12} \cdot SO_4 \cdot 4H_2O]$, $[Zn_2(OH)_2 \cdot ZnSO_4]$, $[Zn_2(OH)_2SO_4]$, $3Zn(OH)_2 \cdot ZnSO_4 \cdot 4H_2O]$, $[Zn_4(OH)_6SO_4 \cdot 4H_2O]$, and so forth, whose precipitation contributes [54] to the inhibition of the atmospheric corrosion of zinc. However, in this type of atmospheres the condensed moisture is acidic and corrodes zinc at a rapid rate. The corrosion products are dissolved and washed off by the acid rain.

Chloride in marine atmospheres also increases the atmospheric corrosion of zinc. There is also a linear relationship between the corrosion rate and salinity [55] in the atmosphere. In the case of pure marine atmospheres, the protective hydrozincite is attacked by chlorides, leading to its transformation into zinc hydroxychloride (simonkolleite). Basic chlorides are scarcely soluble and are not washed off by the rainwater, remaining in the layer of corrosion products.

When SO_2 is also present in marine atmospheres, Svenson and Johansson [54] note that an inhibiting effect is sometimes observed due to the formation of sodium zinc chlorohydroxysulfate $[NaZn_4Cl(OH)_6SO_4 \cdot 6H_2O]$ or zinc chlorohydroxysulfate $[Zn_4Cl_2(OH)_4 \cdot SO_4 \cdot 5H_2O]$.

3.3.2. Main Results Obtained in the MICAT Project. Table 6 displays information obtained in the MICAT project [8, 9] and Table 7 gives a list of the main corrosion products identified.

There follows an analysis of zinc behaviour in the MICAT project testing station network covering different types of atmospheres according to ISO 9223 (Table 3).

Unpolluted Atmospheres (S_0P_0):

(i) Zinc displays a wide range of first-year corrosion rate values: 0.11–3.30 $\mu m \cdot y^{-1}$.

(ii) Zincite (ZnO) and hydrozincite $[Zn_5(CO_3)_2(OH)_6]$ are the detected corrosion products on zinc surfaces exposed in rural atmospheres. The zinc surface corrosion layers show isolated white products (zincite) on a generalized and relatively uniform clear grey layer (hydrozincite) (Figure 5(a)).

(iii) Pitting corrosion is observed (Figure 5(b)), possibly as a consequence of particulate settlement causing corrosion attack on zinc due to differential aeration. This feature was also observed by Askey et al. [56].

SO_2-Polluted Atmospheres (S_0P_1, S_0P_2):

(i) In Sao Paulo (57.8 $mg \cdot m^{-2} \cdot d^{-1}$ of SO_2) the characteristic morphology and nature of corrosion products, rounded agglomerates of smithsonite, are observed (Figure 6(a)).

Pure Marine Atmospheres (S_1P_0, S_2P_0, S_3P_0):

(i) In low SO_2 polluted ($\leq$10 $mg \cdot m^{-2} \cdot d^{-1}$ of SO_2) marine atmospheres corrosion of zinc is a direct function of the chloride pollution level and TOW. S_1P_0 atmospheres showed zinc corrosion rates of 0.19–2.73 $\mu m \cdot y^{-1}$ and corrosivity categories, based on first-year corrosion rates, of C2–C4. In these atmospheres, the corrosion products formed after one-year exposure were zincite and hydrozincite. Only after exposure at the site with the highest chloride deposition rate (55.1 $mg \cdot m^{-2} \cdot d^{-1}$of Cl^-) very small simonkolleite crystals were detected during SEM observations.

Simonkolleite shows a similar structure to hydrozincite, differing only in its interlayer structure content [57]. Both products show a layered structure of zinc cations in octahedral and tetragonal configurations with a ratio of 3 : 2. Hydrozincite shows OH^- ions as its interlayer content. Simonkolleite shows chlorine atoms localized on the corner of the zinc tetrahedron, electric neutrality through the H–Cl bonds remaining relatively weak. It displays hexagonal cells as its

Table 6: MICAT test sites characteristics. Data for zinc.

Type of atmosphere (Table 3)	Id. (Table 2)	Name	Deposition rate ($mg \cdot m^{-2} \cdot d^{-1}$)		Time of wetness (TOW)	1st-year corrosion rate (μm)	Atmospheric corrosivity (ISO 9223) [24]	Corrosion products (see Table 7)
			Cl^-	SO_2				
S_0P_0	44	Granada	(*)	6,2	τ_3	0,11	C2	Z, H
	35	Guayaquil	1,5	3,0	τ_4	0,21	C2	Z
	4	San Juan	(*)	(*)	τ_3	0,21	C2	Z, H
	59	Arequipa	(*)	(*)	τ_2	0,23	C2	Z, H
	43	Tortosa	(*)	5,3	τ_4	0,25	C2	Z, H
	47	Artíes	1,7	9,0	τ_3	0,28	C2	Z, H
	40	León	(*)	(*)	τ_3	0,37	C2	Z, H
	60	Cuzco	(*)	(*)	τ_4	0,40	C2	Z, H
	65	Trinidad	1,5	0,7	τ_4	0,55	C2	—
	6	La Plata	(*)	6,9	τ_4	0,91	C3	H, Z
	61	Pucallpa	(*)	(*)	τ_5	1,01	C3	Z, H
	2	V. Martelli	(*)	9,0	τ_4	1,19	C3	Z, H
	14	Belem	(*)	(*)	τ_5	1,10	C3	—
	49	Cuernavaca	(*)	7,9	τ_3	1,36	C3	—
	3	Iguazú	(*)	(*)	τ_5	1,36	C3	—
	16	Brasilia	(*)	(*)	τ_4	1,78	C3	Z, H
	20	San Pedro	(*)	0,6	τ_5	3,29	C4	Z
	21	Cotové	(*)	0,3	τ_4	3,30	C4	Z
S_0P_1	48	México	(*)	13.6	τ_3	0,82	C3	Z, H
	50	S.L. Potosí	(*)	18.9	τ_3	1.77	C3	Z
S_0P_2	12	São Paulo	(*)	57.8	τ_5	1.21	C3	Z, HZC, H
S_1P_0	67	Melo	3,8	0,7	τ_5	0,69	C2	—
	41	El Pardo	3,9	6,4	τ_4	0,19	C2	Z, H
	7	Caratinga	5,8	1,3	τ_4	0,67	C2	Z
	64	Pego	6,0	7,9	τ_4	1,15	C3	Z
	46	Labastida	9,8	3,6	τ_4	0,31	C2	Z, H
	25	Sabanilla	11,3	4,9	τ_5	—	—	H, ZC
	73	Matanzas	15,9	9,3	τ_4	2,73	C4	—
	74	Barcelona,V	21,8	1,5	τ_4	2,01	C3	—
	51	Acapulco	23,8	9,6	τ_4	1,79	C3	S, Z, H
	72	Coro	27,5	6,5	τ_4	0,30	C2	—
	71	Punto Fijo	31,0	5,0	τ_4	0,57	C2	—
	22	Puntarenas	33,4	7,1	τ_4	—	—	H, HZC
	1	Camet	55,1	(*)	τ_5	1,63	C3	—
S_2P_0	70	El Tablazo	63,3	6,0	τ_4	—	—	—
	11	Ubatuba	113	2,6	τ_4	7,07	C5	S, H
	69	P. del Este	144	4,0	τ_4	2,89	C4	—
	23	Limón	220	3,5	τ_5	—	—	H, S, HZC
	75	P. Cabello	—	(*)	τ_5	4,34	C5	—
	9	A. do Cabo	229	6,7	τ_4	4,87	C5	Z, S
S_3P_0	15	Fortaleza	>300	(*)	τ_4	5,46	C5	—

Table 6: Continued.

Type of atmosphere (Table 3)	Id. (Table 2)	Name	Deposition rate ($mg \cdot m^{-2} \cdot d^{-1}$)		Time of wetness (TOW)	1st-year corrosion rate (μm)	Atmospheric corrosivity (ISO 9223) [24]	Corrosion products (see Table 7)
			Cl^-	SO_2				
S_1P_1	42	Barcelona, S	4,4	16,7	τ_3	0,56	C2	Z,H
	52	Panamá	9,8	21,7	τ_4	1,06	C3	—
	66	Prado	10,8	12,1	τ_4	1,10	C3	—
	26	Ciq	12,0	31,6	τ_4	1,20	C3	S, ZC
	28	Bauta	6,4	16,4	τ_4	1,22	C3	H, S
	8	Ipatinga	6,8	23,0	τ_4	1,23	C3	Z
	58	San Borja	20,0	29,0	τ_5	1,61	C3	Z, H
	56	Piura	(*)	(*)	τ_3	1,63	C3	—
	29	Cerrillos	4,5	20,0	τ_4	1,77	C3	Z
	57	V. Salvador	38,0	18,0	τ_5	2,46	C4	Z, H
S_1P_2	45	Lagoas	16,7	39,5	τ_4	0,45	C2	Z, H
	10	Cubatão	8,1	54,5	τ_4	1,25	C3	H
	13	Río Janeiro	16,4	43,5	τ_4	1,47	C3	H
	31	Idiem	16,8	43.3	τ_5	3,93	C4	Z
	32	Petrox	12,8	65,2	τ_5	8,58	>C5	Z
S_2P_1	63	Sines	203	27,0	τ_4	4,03	C4	H, BZC, S
	19	Isla Naval	60,7	10,3	τ_5	5,89	C5	S
	27	Cojímar	104	22,5	τ_4	7,09	C5	S, ZC, H
S_2P_2	62	Leixões	97,6	69,2	τ_4	2,51	C4	H,S,ZH

(*) apparently olluted.
(—) not available.

Table 7: Zinc corrosion products identified in the MICAT project.

Code	Name	Composition
	Oxides	
Z	Zincite	ZnO
	Hydroxides	
ZH	Zinc hydroxide	$Zn(OH)_2$
	Carbonates	
ZC	Smithsonite	$ZnCO_3$
H	Hydrozincite	$Zn_5(CO_3)_2(OH)_6$
HZC	Hydrated zinc carbonate	$4ZnO \cdot CO_2 \cdot 4H_2O$
BZC	Basic zinc carbonate	$Zn_4CO_3(OH)_6 \cdot H_2O$ or $ZnCO_3 \cdot 3Zn(OH)_2 \cdot H_2O$
	Chlorides	
S	Simonkolleite	$Zn_5(OH)_8\ Cl_2 \cdot H_2O$

main structure [58]. Many of the S_1P_0 atmospheres did not lead to simonkolleite formation, possibly owing to the relatively low Cl^- content to substitute OH^- ions in the hydrozincite structure, preferably in acidic or almost neutral media, simonkolleite being more stable at high chloride concentrations.

(ii) S_2P_0 atmospheres showed significantly higher zinc corrosion rates (2.89–7.07 $\mu m \cdot y^{-1}$) and as a consequence higher corrosivity categories (C4 and C5), being hydrozincite and simonkolleite the common corrosion products. The atmospheres in this group with high TOWs (τ_5) yielded open structures of corrosion product layers with very good simonkolleite crystallization and consequently higher corrosivity categories (Figure 6(b)).

Mixed Marine Atmospheres (S_1P_1, S_1P_2, S_2P_1, S_2P_2):

(i) Marine atmospheres with SO_2 deposition rates in excess of 10 $mg \cdot m^{-2} \cdot d^{-1}$ of SO_2 never display any evidence of residual zinc sulphates on the surface of the corrosion product layers because even if they form they are always washed off by rainfall.

(ii) When $Cl^- < 60\ mg \cdot m^{-2} \cdot d^{-1}$ of Cl^-, the corrosion products do not display any evidence of simonkolleite. Zinc corrosion rates vary between 0.45 (C2) and 8.58 (C5) $\mu m \cdot y^{-1}$, strongly depending on TOW and pollution levels. However, chloride pollution of more than 60 $mg \cdot m^{-2} \cdot d^{-1}$ of Cl^- promotes the formation of simonkolleite.

3.4. Atmospheric Corrosion of Copper

3.4.1. Mechanisms [59]. Several stages may be identified in the evolution of the visual appearance of exposed copper from its initial state to its final patination. Prior to exposure to an outdoor atmosphere, new freshly cleaned copper is a salmon-pink colour, but after just a few weeks of exposure it turns a dull-brown shade.

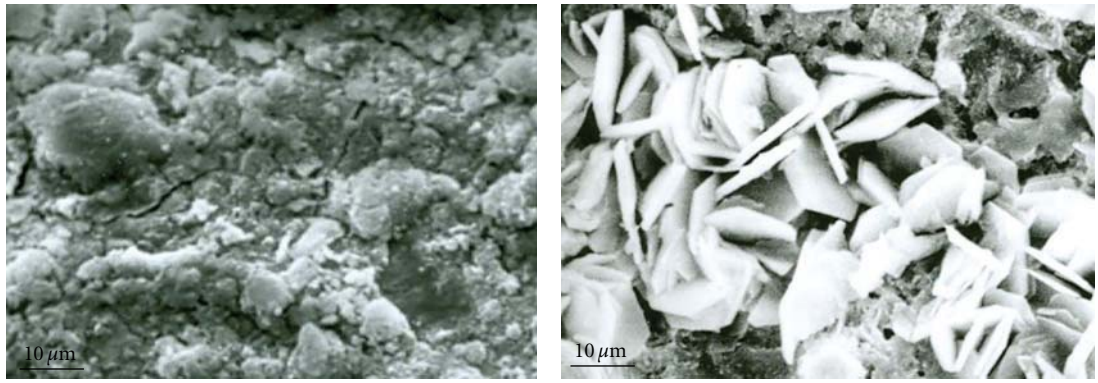

(a) (b)

Figure 6: Morphology of corrosion product layers formed on zinc exposed in the SO_2-polluted atmosphere of Sao Paulo (a) and marine atmosphere of Puerto Cabello (b).

At room temperature, copper in contact with clean air instantaneously becomes coated with a thin invisible film of cuprous oxide (cuprite) through a direct oxidation mechanism [60].

Copper corrosion in the atmosphere follows an electrochemical mechanism whereby the metal dissolves anodically forming cuprous and cupric ions:

$$\begin{aligned} Cu &\longrightarrow Cu^{+} + e^{-} \\ Cu &\longrightarrow Cu^{2+} + 2e^{-} \end{aligned} \tag{10}$$

In the first days of exposure to the atmosphere the copper surface often exhibits a mottled appearance (dark spots). These dark spots are comprised of submicron crystallites of a uniform size. With time the crystallites grow in size with a characteristic cubo-octahedral appearance.

With increased exposure time these spots increase in surface coverage and cause the specimens to change from their metallic colour to more familiar "copper" colours due to a thin surface oxide. After a few months the copper surface develops a uniform primary protective film of cuprite (Cu_2O), which has a matt brown colour and continues to darken with exposure (blackening).

In the following corrosion stages, which can last up to 20 y depending on the environmental conditions, a green-blue patina with a layered structure corresponding to brochantite (mainly rural and urban atmospheres) or atacamite (marine atmospheres) is formed. In the latter case the time to formation is considerably shorter. During this stage, although the copper looks brown, there is an initial "incubation period" in which brochantite forms on the cuprite surface as isolated islands that gradually join together.

Dissolution of SO_2 in the moisture layer leads to the formation of sulphite (SO_3^{2-}) and sulphate (SO_4^{2-}) ions and acidification of the medium. In the presence of excess acidity (H^+) cuprite dissolves according to the reaction:

$$Cu_2O + 2H^{+} \longrightarrow Cu^{2+} + Cu^{0} + H_2O \tag{11}$$

A similar process takes place with the Cl^-, SO_4^{2-}, and H^+ values typically found in meteorological precipitation. Atacamite appears from the direct reaction of Cl^- with Cu^{2+} ions according to the reaction:

$$4Cu^{2+} + 2Cl^{-} + 6H_2O \longrightarrow [Cu_4Cl_2(OH)_6] + 6H^{+} \tag{12}$$

and brocantite can form according to the reaction:

$$4Cu^{2+} + 6H_2O + SO_4^{2-} \longrightarrow [Cu_4(SO_4)(OH)_6] + 6H^{+} \tag{13}$$

In rural and urban atmospheres, the formation of brochantite occurs as discrete isolated clumps of crystals on the cuprite base layer, with brochantite "islands" (Figure 7(a)) increasing in number and size with increasing exposure time [61].

Posnjakite $[Cu_4SO_4(OH)_6 \cdot H_2O]$ is formed initially but is then either dissolved or converted to brochantite $[Cu_4SO_4(OH)_6]$ the most common sulphate-containing phase in copper patinas [62]. Weak indications of posnjakite are typically seen on specimen surfaces exposed to urban and rural atmospheres for one year or more.

With exposure time a continuous brochantite layer forms and hides the underlying cuprite layer, giving the specimens a green appearance (Figure 7(b)). This brochantite layer gradually increases in thickness.

In chloride environments (marine) the initial corrosion product phase to be formed is cuprite, with paratacamite $[Cu_2Cl(OH)_3]$, an isomorphic compound of atacamite, appears as a secondary phase growing on the cuprite. Atacamite also appears after longer exposures. Both atacamite and paratacamite present a green-blue colouring characteristic of the copper patinas formed in marine atmospheres (Figure 7(c)).

Once the patina is established it remains stable, and copper corrosion occurs at an ever diminishing rate. Patinated copper typically consists of (a) the underlying copper metal, (b) a thin layer (5–20 μm) of cuprite, and (c) a top layer of basic copper sulphate (brochantite) or basic copper chloride (atacamite).

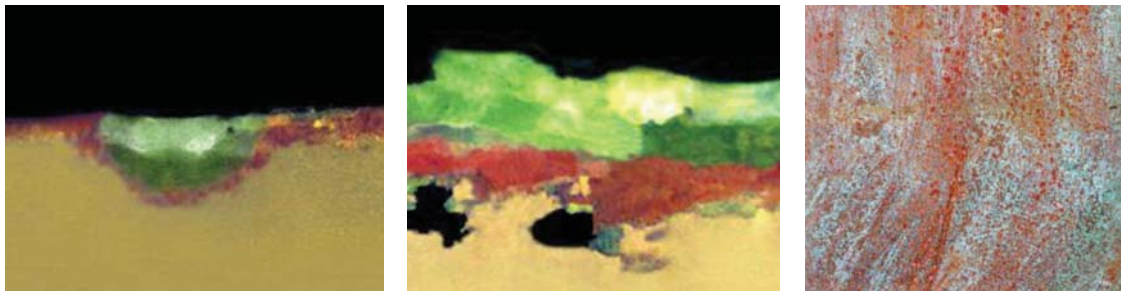

(a) (b) (c)

Figure 7: (a) Brochantite formation at discrete isolated clamps of crystals on the cuprite base layer formed in an urban atmosphere (cross-section view) [54]. (b) Brochantite formation on the cuprite base layer formed in a marine atmosphere (cross-section view) [54]. (c) Surface view of brochantite formation on the cuprite base layer formed in the marine atmosphere of Cojimar.

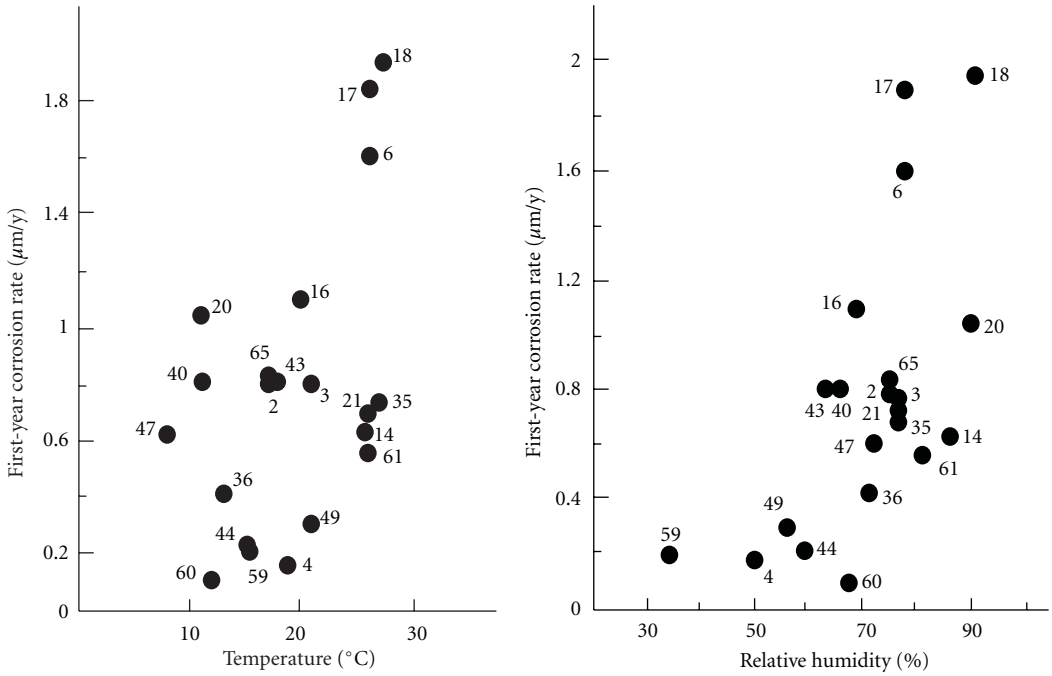

Figure 8: First-year copper corrosion rate versus temperature (a) and relative humidity (b) in rural atmospheres.

When environmental SO_2 reaches a competitive level with the chloride aerosol the patina formed is a complex mixture of basic cupric chlorides (paratacamite and atacamite) and basic cupric sulphates (antlerite and brochantite).

3.4.2. Main Results Obtained in the MICAT Project. Table 8 displays information obtained in the MICAT project [10] and Table 9 gives a list of the main corrosion products identified.

There follows an analysis of copper behaviour in the MICAT project testing station network covering different types of atmospheres according to ISO 9223 (Table 3).

Unpolluted Atmospheres (S_0P_0):

(i) From a preliminary analysis of Table 8, there is an enormous variation in the corrosion values found during the first year of exposure (from $0.09\,\mu m\cdot y^{-1}$ in Cuzco to $1.57\,\mu m\cdot y^{-1}$ in La Plata), which seems to indicate the importance of climatic conditions on the corrosion of this material in rural atmospheres.

To consider this question, an analysis was made of the annual average temperatures (T) and relative humidities (RH) recorded at the test sites. To this end, Figure 8 displays the variation of first-year corrosion rates with the average annual T and RH values. The figures seem to suggest that low T and low RH tend to promote low copper corrosion rates, while high RH and high T (provided there is sufficient TOW of the metallic surface) tend to intensify copper corrosion in these types of atmospheres. This is in agreement with the observations of Kucera and Mattsson, who note that low temperatures and dryness of the atmosphere

Table 8: MICAT test sites characteristics. Data for copper.

Type of atmosphere (Table 3)	Id. (Table 2)	Name	Deposition rate ($mg \cdot m^{-2} \cdot d^{-1}$)		T °C	RH %	Time of wetness (TOW)	1st-year corrosion rate (μm)	Atmospheric corrosivity (ISO 9223) [24]	Corrosion products (see Table 9)
			Cl^-	SO_2						
S_0P_0	60	Cuzco	(*)	(*)	12.2	67	τ_4	0,09	C1	—
	4	San Juan	(*)	(*)	18.8	50	τ_3	0,17	C2	Cu
	59	Arequipa	(*)	(*)	15.6	34	τ_2	0,20	C2	—
	44	Granada	(*)	6,2	15.6	59	τ_3	0,22	C2	Cu
	49	Cuernavaca	(*)	7,9	21.0	56	τ_3	0,30	C2	—
	36	Riobamba	1,1	1,2	—	—	τ_4	0,43	C2	—
	61	Pucallpa	(*)	(*)	26.1	81	τ_5	0,56	C2	—
	47	Artíes	1,7	9,0	7.8	72	τ_3	0,62	C3	Cu, Br, Po
	14	Belem	(*)	(*)	26.4	86	τ_5	0,64	C3	Cu, At, Ca
	35	Guayaquil	1,5	3,0	25.9	76	τ_4	0,71	C3	—
	21	Cotové	(*)	0,3	27.0	76	τ_4	0,73	C3	Cu
	3	Iguazú	(*)	(*)	21.2	75	τ_5	0,77	C3	Cu
	2	V. Martelli	(*)	9,0	16.9	74	τ_4	0,79	C3	Cu, Po, Br, At
	40	León	(*)	(*)	11.2	65	τ_3	0,81	C3	Cu
	43	Tortosa	(*)	5,3	17.4	63	τ_4	0,81	C3	Cu
	65	Trinidad	1,5	0,7	16.7	74	τ_4	0,83	C3	—
	20	San Pedro	(*)	0,6	11.5	90	τ_5	1,05	C3	Cu
	16	Brasilia	(*)	(*)	20.4	68	τ_4	1,12	C3	Cu, Po
	6	La Plata	(*)	6,9	16.8	77	τ_4	1,57	C4	Cu
	17	P. Alfonso	(*)	(*)	25.9	77	—	1.86	C4	—
	18	Porto Velho	(*)	(*)	26.6	90	—	1.94	C4	—
S_0P_1	48	México	(*)	12.0	15.4	64	τ_3	0.12	C3	Cu
	50	S. L. Potosí	(*)	18.9	18.0	58	τ_3	0.54	C2	Cu
S_0P_2	12	São Paulo	(*)	57.8	19.6	75	τ_5	0.56	C4	Cu, Br, Ca
S_1P_0	67	Melo	3,8	0,7	17.4	80	τ_5	1,27	C3	—
	41	El Pardo	3,9	6,4	15.0	55	τ_4	0,81	C3	Cu, Po
	7	Caratinga	5,8	1,3	21.2	74	τ_4	0,99	C3	Cu, Po
	64	Pego	6,0	7,9	16.9	70	τ_4	1,43	C4	Cu, Po
	46	Labastida	9,8	3,6	12.0	73	τ_4	0,95	C3	Cu
	25	Sabanilla	11,3	4,9	19.9	83	τ_5	1,23	C3	Cu
	73	Matanzas	15,9	9,3	27.7	75	τ_4	0,95	C3	—
	74	Barcelona,V	21,8	1,5	26.7	78	τ_4	0,35	C2	—
	51	Acapulco	23,8	9,6	24.6	80	τ_4	1,23	C3	Cu, At
	39	S. Cristóbal	25,0	1,1	27.5	74	—	1,52	C4	—
	72	Coro	27,5	6,5	26.5	77	τ_4	2,35	C4	—
	71	Punto Fijo	31,0	5,0	27.6	76	τ_4	3,19	C5	—
	22	Puntarenas	33,4	7,1	28.0	80	τ_4	2,98	C5	Cu, At
	37	Salinas	47,3	2,3	23.3	80	τ_4	2,33	C4	—
	1	Camet	55,1	(*)	14.1	79	τ_5	2,23	C4	Cu
S_2P_0	11	Ubatuba	113	2,6	22.1	80	τ_4	3,29	C5	Cu, At
	69	P. del Este	144	4,0	16.5	78	τ_4	2,51	C4	—
	23	Limón	220	3,5	25.4	88	τ_5	3,68	C5	Cu, At
	9	A. do Cabo	229	6,7	24.5	78	τ_4	4,12	C5	Cu, At
	75	P. Cabello	—	(*)	26.7	82	τ_5	4,50	C5	—
	70	El Tablazo	63,3	6,0	27.7	77	τ_4	5,80	>C5	—

Table 8: Continued.

Type of atmosphere (Table 3)	Id. (Table 2)	Name	Deposition rate ($mg \cdot m^{-2} \cdot d^{-1}$) Cl^-	Deposition rate ($mg \cdot m^{-2} \cdot d^{-1}$) SO_2	T °C	RH %	Time of wetness (TOW)	1st-year corrosion rate (μm)	Atmospheric corrosivity (ISO 9223) [24]	Corrosion products (see Table 9)
S_3P_0	15	Fortaleza	>300	(*)	26.4	74	τ_4	3,80	C5	Cu, Co, At, Po
S_1P_1	42	Barcelona, S	4,4	16,7	16.1	61	τ_3	0,71	C3	Cu, Po
	29	Cerrillos	4,5	20,0	14.2	71	τ_4	0,73	C3	Cu
	30	Valparaíso	10,0	23,6	14.0	82	τ_5	0,87	C3	—
	8	Ipatinga	6,8	23,0	23.2	90	τ_4	1,21	C3	Cu
	52	Panamá	9,8	21,7	26.9	71	τ_4	1,24	C3	—
	66	Prado	10,8	12,1	17.0	76	τ_4	1,38	C4	—
	26	Ciq	12,0	31,6	25.2	79	τ_4	1,45	C4	Cu
	58	San Borja	20,0	29,0	19.4	84	τ_5	1,62	C4	Cu
	28	Bauta	6,4	16,4	24.0	81	τ_4	1,80	C4	Cu, At, An, Br, Po
	57	V. Salvador	38,0	18,0	19.6	84	τ_5	1,98	C4	Cu
S_1P_2	45	Lagoas	16,7	39,5	15.9	70	τ_4	1,23	C3	Cu
	10	Cubatao	8,1	54,5	22.7	74	τ_4	2,86	C5	Cu, Br, Ca
	31	Idiem	16,8	43,3	12.2	82	τ_5	4,79	C5	Cu
	32	Petrox	12,8	65,2	12.2	82	τ_5	5,35	C5	Cu, Br
	13	Río Janeiro	16,4	43,5	21.4	80	τ_4	7,01	>C5	Cu, Br
S_2P_1	63	Sines	203	27,0	18.4	61	τ_4	3.61	C5	Cu, At, La
	19	Isla Naval	60,7	10,3	27.8	86	τ_5	4.72	C5	Cu
	27	Cojímar	104	22,5	25.1	79	τ_4	4.89	C5	Cu, At
S_2P_2	62	Leixões	97,6	69,2	17.0	59	τ_4	4.32	C5	Cu, Pa, At, Sc, Cc

(*) apparently nonpolluted.
(—) not available.

considerably delay the time of formation of patinas on copper [28].

SO_2-Polluted Atmospheres (S_0P_1, S_0P_2):

(i) According to Barton [63] it is necessary to reach a minimum SO_2 level in the atmosphere ($\sim 60\ mg \cdot m^{-2} \cdot d^{-1}$ of SO_2) for this pollutant to significantly influence copper corrosion, provided there is humidity on the surface. This critical value coincides with that found in the Sao Paulo atmosphere ($57.8\ mg \cdot m^{-2} \cdot d^{-1}$ of SO_2).

(ii) Sao Paulo is a highly polluted Ibero-American city with a heavy road traffic. Volatil organic compounds (VOC) in the Sao Paulo atmosphere, mainly carboxylic acids, were measured by Souza et al. [64]. Photochemical production appeared to be a very likely source of the gaseous acetic and formic acids, although direct emissions mainly motor exhaust of vehicles also contributed to their presence in air.

It is well known that copper is corroded in presence of organic acids [62, 65]. In a recent research, Echevarría et al. [66] found that copper corrosion increased at high relative humidities and concentrations of propionic acid.

The appearance of cuprous sulphide (chalcocite, Cu_2S) in the first year of exposure in the Sao Paulo atmosphere, which in subsequent years is transformed into cupric sulphur (covellite, CuS), seems to indicate the presence in this atmosphere of considerable amounts of sulphide ions, and the conversion in time of brocantite into antlerite. The first transformation confirms the research of Vernon and Whitby [67] who suggest calcocite as an initial formation that subsequently oxidises to covellite. However, the conversion of brocantite into antlerite contradicts some evidence [61] which suggested the formation of antlerite in the first stages of patination, experimentally confirming the hypothesis formulated by Baboian and Cliver [68], according to which acid rain converts brocantite into less protective antlerite formations.

Pure Marine Atmospheres (S_1P_0, S_2P_0, S_3P_0):

(i) A critical threshold for atmospheric salinity, $\sim 20\ mg \cdot m^{-2} \cdot d^{-1}$ of Cl^-, seems to differentiate copper behavior in these types of atmospheres. Below

Table 9: Copper corrosion products identified in the MICAT project.

Code	Name	Composition
	Oxides	
Cu	Cuprite	Cu_2O
	Sulphates	
Sc	Copper (II) sulphate	$CuSO_4 \cdot H_2O$
An	Antlerite	$Cu_3(SO_4)(OH)_4$
Br	Brochantite	$Cu_4(SO_4)(OH)_6$
La	Langite	$Cu_4(SO_4)(OH)_6 \cdot 2H_2O$
Po	Posnjakite	$Cu_4(SO_4)(OH)_6 \cdot 2H_2O$
	Chlorides	
Cc	Copper (II) chloride	$CuCl(OH)$
At	Atacamite	$Cu_2Cl(OH)_3$
Pa	Paratacamite	$Cu_2Cl(OH)_3$
	Sulphides	
Ca	Chalcocite	Cu_2S
Co	Covellite	CuS

the threshold, copper behaves as in rural atmospheres with corrosion rates of $<2\,\mu m \cdot y^{-1}$. Above the threshold, copper corrosion accelerates notably with atmospheric salinity.

(ii) In Figure 9, the variation of the first-year copper corrosion rate with salinity in pure marine atmospheres is shown. It must be pointed out that copper corrosion in atmospheres with salinities of $<20\,mg \cdot m^{-2} \cdot d^{-1}$ of Cl^- is close to copper corrosion in rural atmospheres (an average of $0.77\,\mu m \cdot y^{-1}$). Salinities $> 20\,mg \cdot m^{-2} \cdot d^{-1}$ Cl^- notably accelerate copper attack.

(iii) Copper hydroxysulfates are frequently detected in the corrosion product layers, accompanying the basic copper chlorides typical of these types of atmospheres.

Mixed Marine Atmospheres (S_1P_1, S_1P_2, S_2P_1, S_2P_2):

(i) The presence of both pollutants (Cl^- and SO_2) leads to the abundant formation of basic salts, both sulfates (brochantite) and chlorides (atacamite), which noticeably compact the corrosion product layers.

(ii) Copper corrosion also accelerates in these types of atmospheres after a critical threshold of $20\,mg \cdot m^{-2} \cdot d^{-1}$ of Cl^-, increasing with Cl^- and SO_2 contents in the atmosphere.

(iii) Basic chlorides and sulfates coexist in the atmospheric corrosion products. The threshold of $20\,mg \cdot m^{-2} \cdot d^{-1}$ of Cl^- defines what will be the main constituent of the patinas; below this value the predominant phase is basic sulfates and above it basic chlorides.

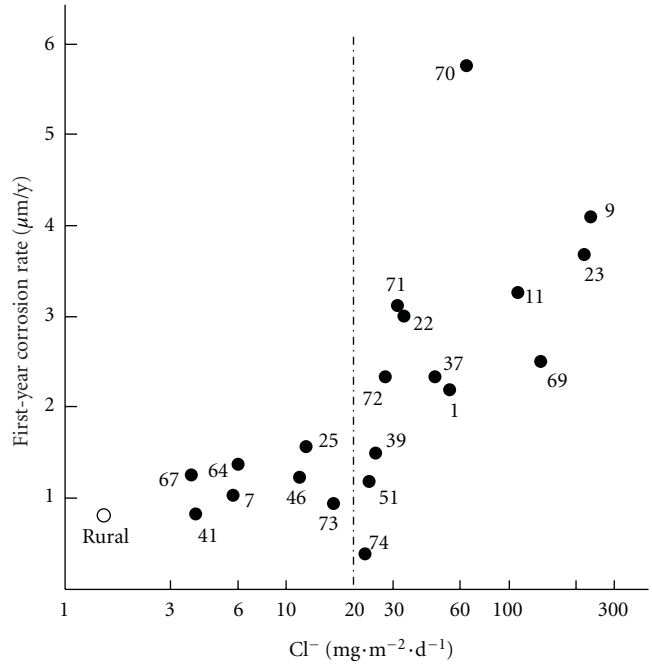

Figure 9: First-year copper corrosion rate versus Cl^- deposition rate in marine (S_1P_0, S_2P_0, and S_3P_0) atmospheres. In the graph, the average value of corrosion rate in rural atmospheres (O) is shown.

3.5. Atmospheric Corrosion of Aluminium

3.5.1. Mechanisms [69]. Unlike other metals, whose corrosion causes a general loss of thickness of the material, aluminium corrosion tends to be localised, with the formation of numerous cavities (pits) spread across the entire surface, leaving large areas of the metal between them intact. In this case the concept of mean penetration becomes meaningless, and it is preferable to express corrosion as mass loss per unit of surface area.

All studies agree that upon its initial exposure aluminium quickly forms a thin film of aluminium oxide. Under continued exposure this film may grow and be transformed into various other atmospheric products, γ-alumina (Al_2O_3) is the first component formed upon exposure to the atmosphere, with an initial depth of 2-3 nm [70]. In a few months in the air, this oxide becomes covered by a thin layer of boehmite [γ-AlOOH], which is subsequently covered by bayerite [$Al(OH)_3$], also written as [$Al_2O_3 \cdot 3H_2O$] [71].

As with other metals, the atmospheric corrosion of aluminium is strongly influenced by the presence or absence of moisture. A crucial consequence of the existence of a water layer on the metal surface is that it provides a medium for the mobilisation of aluminium cations and also for deposited anions.

At the bottom of the pit the environment is acid, and aluminium acts anodically, oxidising according to the reaction:

$$Al \longrightarrow Al^{3+} + 3e^- \quad (14)$$

Table 10: MICAT test sites characteristics. Data for aluminium.

Type of atmosphere (Table 3)	Id. (Table 2)	Name	Deposition rate ($mg \cdot m^{-2} \cdot d^{-1}$)		Time of wetness (TOW)	1st year corrosion rate (μm)	Atmospheric corrosivity (ISO 9223) [24]	Corrosion products (see Table 11)
			Cl^-	SO_2				
S_0P_0	59	Arequipa	(*)	(*)	τ_2	0,01	C1	—
	65	Trinidad	1,5	0,7	τ_4	0,01	C1	—
	60	Cuzco	(*)	(*)	τ_4	0,02	C1	N
	35	Guayaquil	1,5	3,0	τ_4	0.03	C1	N
	61	Pucallpa	(*)	(*)	τ_5	0.03	C1	N
	44	Granada	(*)	6,2	τ_3	0.04	C1	N
	4	San Juan	(*)	(*)	τ_3	0,08	C1	N
	43	Tortosa	(*)	5,3	τ_4	0,08	C1	N
	47	Artíes	1,7	9,0	τ_3	0,11	C1	N
	2	V. Martelli	(*)	9,0	τ_4	0,12	C1	N
	40	León	(*)	(*)	τ_3	0,13	C1	N
	21	Cotové	(*)	0,3	τ_4	0,14	C1	—
	6	La Plata	(*)	6,9	τ_4	0,15	C1	N
	3	Iguazú	(*)	(*)	τ_5	0,20	C1	N
	20	S. Pedro	(*)	0,6	τ_5	0,20	C1	—
	14	Belem	(*)	(*)	τ_5	0,22	C1	N
	49	Cuernavaca	(*)	7,9	τ_3	0,24	C1	—
	16	Brasilia	(*)	(*)	τ_4	0,27	C1	N
S_0P_1	48	México	(*)	12	τ_3	0,12	C1	—
	50	S.L. Potosí	(*)	18.9	τ_3	0.54	C2	—
S_0P_2	12	São Paulo	(*)	57.8	τ_5	0.56	C2	N
S_1P_0	67	Melo	3,8	0,7	τ_5	0,06	C1	—
	41	El Pardo	3,9	6,4	τ_4	0,07	C1	N
	7	Caratinga	5,8	1,3	τ_4	0,17	C1	N
	64	Pego	6,0	7,9	τ_4	0,35	C2	N
	46	Labastida	9,8	3,6	τ_4	0,18	C1	N
	25	Sabanilla	11,3	4,9	τ_5	0,14	C1	N
	73	Matanzas	15,9	9,3	τ_4	0,28	C1	—
	74	Barcelona,V	21,8	1,5	τ_4	0,16	C1	—
	39	S.Cristóbal	25,0	1,1	—	0,52	C2	N
	72	Coro	27,5	6,5	τ_4	0,75	C3	—
	71	Punto Fijo	31,0	5,0	τ_4	0,49	C2	—
	51	Acapulco	23,8	9,6	τ_4	1,63	C3	—
	22	Puntarenas	33,4	7,1	τ_4	1,93	C3	A
	37	Salinas	47,3	2,3	τ_4	1,12	C3	—
	1	Camet	55,1	(*)	τ_5	0,57	C2	N
S_2P_0	11	Ubatuba	113	2,6	τ_4	1,17	C3	A
	69	P. del Este	144	4,0	τ_4	1,68	C3	—
	23	Limón	220	3,5	τ_5	0,86	C3	A
	9	A. do Cabo	229	6,7	τ_4	1,68	C3	A
	75	P. Cabello	—	(*)	τ_5	1,64	C3	—
S_3P_0	15	Fortaleza	>300	(*)	τ_4	1.58	C3	A

Table 10: Continued.

Type of atmosphere (Table 3)	Id. (Table 2)	Name	Deposition rate ($mg \cdot m^{-2} \cdot d^{-1}$)		Time of wetness (TOW)	1st year corrosion rate (μm)	Atmospheric corrosivity (ISO 9223) [24]	Corrosion products (see Table 11)
			Cl^-	SO_2				
S_1P_1	66	Prado	10,8	12,1	τ_4	0,27	C1	—
	8	Ipatinga	6,8	23,0	τ_4	0,39	C2	A
	52	Panamá	9,8	21,7	τ_4	0,43	C2	—
	42	Barcelona, S	4,4	16,7	τ_4	0,68	C3	N
	29	Cerrillos	4,5	20,0	τ_4	0,68	C3	N
	28	Bauta	6,4	16,4	τ_4	0,99	C3	N
	26	Ciq	12,0	31,6	τ_4	1,11	C3	N
	58	San Borja	20,0	29,0	τ_5	1,32	C3	N
	57	V. Salvador	38,0	18,0	τ_5	1,57	C3	N
	30	Valparaíso	10	23.6	τ_5	3.56	C4	—
S_1P_2	45	Lagoas	16,7	39,5	τ_4	0,33	C2	N
	13	Río Janeiro	16,4	43,5	τ_4	0,74	C3	A
	10	Cubatão	8,1	54,5	τ_4	0,78	C3	A
	31	Idiem	16,8	43.3	τ_5	5,21	C5	—
	32	Petrox	12,8	65,2	τ_5	5,43	C5	—
S_2P_1	19	Isla Naval	60,7	10,3	τ_5	1.67	C3	N
	27	Cojímar	104	22,5	τ_4	3.01	C4	N
	63	Sines	203	27,0	τ_4	3.79	C4	A, Sb
S_2P_2	62	Leixões	97,6	69,2	τ_4	4.09	C4	A, Sb, Ca

(*) apparently nonpolluted.
(—) not available
(N) not detected any corrosion product.

Table 11: Aluminium corrosion products identified in the MICAT project.

Code	Name	Composition
	Oxides	
A	Alumina	γ-Al_2O_3
	Sulphates	
Sb	Aluminium basic sulphate	$Al_x(SO_4)_y(OH)_z$
	Chlorides	
Ca	Aluminium chloride	$AlCl_3 \cdot 6H_2O$

The pit edges act as cathodes and the environment there is alkaline, giving rise to the cathodic reaction as in (2).

Al^{3+} ions, which are practically insoluble in water, combine with oxyhydryl ions from the dissociation of water to form aluminium hydroxide [$Al(OH)_3$]:

$$Al^{3+} + 3OH^- \longrightarrow Al(OH)_3 \quad (15)$$

Aluminium hydroxide is not soluble and precipitates in the form of a gelatinous white mass, normally known as alumina, although generally it is bayerite.

There is agreement that the normal corrosion reaction consists of combining with water to form aluminium hydroxide (which constitutes the corrosion product and covers the pit in the form of voluminous bulges) and hydrogen [72]:

$$2Al + 6H_2O \longrightarrow 2[Al(OH)_3] + 3H_2 \quad (16)$$

The formation of hydrogen gas and its accumulation in the outermost strata of the base aluminium gives rise to the formation of blisters on the metallic surface, which coincide with the existence of pitting of the base aluminium.

The formation of pits on the surface is the most common type of corrosion found in aluminium alloys exposed to the atmosphere, above all in marine atmospheres. In the case of certain highly aggressive industrial atmospheres there are references which indicate the possibility of generalised attack.

The effect of the relative humidity (RH) of the air is of little consideration when aluminium is exposed to pure atmospheres. In fact, the corrosion of aluminium and its alloys depends primordially on the atmosphere being contaminated (in general by sulphur dioxide or chlorides), and only in such cases does the time of wetness intervene decisively in the corrosion process.

Little is known about the influence of temperature on the atmospheric corrosion of aluminium. According to Mikhailovskii et al. [73], temperature variations seem to have

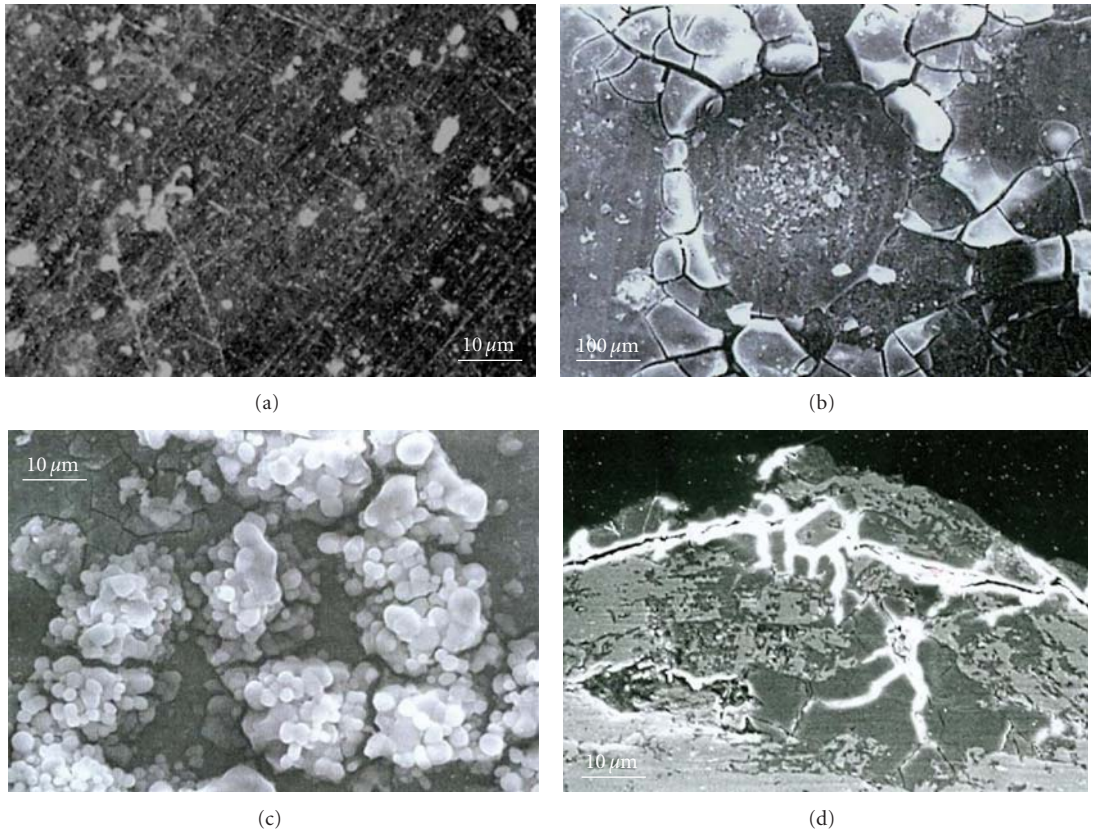

(a) (b)

(c) (d)

Figure 10: (a) Soiling of aluminium surface by dust particles. (b) Pitting of aluminium surface caused by sea-borne chlorides. Great formation of corrosion products (c) and strong pitting (d) caused by severe attack of aluminium in SO_2-polluted marine atmospheres.

little influence on the corrosion of aluminium and its alloys over a broad temperature range when the surface is wetted by precipitated humidity (rain, fog, dew).

From an analysis of the available information [74] it is seen that the corrosion of aluminium is considerably accelerated in industrial atmospheres. This conclusion is in line with Speeding [75], who reports that the aluminium corrosion rate is seven-times higher in an industrial atmosphere than in a rural environment. The amount of SO_2 absorbed on the aluminium surface increases notably with humidity, giving rise to the formation of sulphuric acid, which causes the destruction of the thin natural oxide film that spontaneously coats the metal, and thus accelerating the attack. Amorphous aluminium sulphate hydrate is observed to be the most abundant corrosion product on aluminium exposed to marine and industrial atmospheres [76].

Chloride ions are a significant cause of aluminium surface degradation in atmospheric exposure [77]. Chloride ions tend to perforate and destroy the natural oxide films that protect aluminium. Thus, according to Berukshitis and Klark [78], chlorides in the atmosphere constitute a specific medium for aluminium corrosion, which in their experiments was seen to be up to 22-times higher in a marine atmosphere than in a rural atmosphere.

3.5.2. Main Results Obtained in the MICAT Project. Table 10 displays information obtained in the MICAT project [11–13], and Table 11 gives a list of the main corrosion products identified.

There follows an analysis of aluminium behaviour in the MICAT project testing station network covering different types of atmospheres according to ISO 9223 (Table 3).

Unpolluted Atmospheres (S_0P_0). In unpolluted rural atmospheres aluminium does not present significant attack, only some soiling by dust particles (Figure 10(a)), loss of shine, and perhaps some isolated pitting, preferentially on the downward surfaces protected from the rain not detected with the naked eye. The corrosion values found ($<0.30\,g\cdot m^{-2}\cdot y^{-1}$) are mainly a result of metal attack by the chemical reagent used for gravimetric weight loss determination rather than by the action of the atmosphere.

SO_2-Polluted Atmospheres (S_0P_1, S_0P_2):

(i) Unfortunately, the MICAT project involved a very small number of testing stations of this type: only two atmospheres corresponding to category S_0P_1 (Mexico City and San Luis Potosí) and one atmosphere corresponding to category S_0P_2 (Sao Paulo). With so few stations it is risky to make generalisations about aluminium behaviour in these atmospheres. Bearing this in mind, an indication is given of the most relevant findings, supplemented with other published information.

Aluminium attack in these two types of atmospheres, although significant, is only low ($<0.6\,g\cdot m^{-2}\cdot y^{-1}$), which may indicate that SO_2 in the atmosphere does not have a significant effect on the atmospheric corrosion of aluminium at concentrations below $60\,mg\cdot m^{-2}\cdot d^{-1}$ of SO_2, confirming the experience of Rozenfeld [79], possibly due to the low adsorption of SO_2 by aluminium surfaces [80].

As in the rural atmospheres, the presence of very small amounts of corrosion products, aggravated by their location at isolated points on the surface, hinders their identification by the analytical techniques used in this research.

Pure Marine Atmospheres (S_1P_0, S_2P_0, S_3P_0). In pure marine atmospheres there seems to be a critical threshold for atmospheric salinity, around $20\,mg\cdot m^{-2}\cdot d^{-1}$ Cl^-, which differentiates the corrosion behavior of aluminium. Below this threshold aluminium behaves in a similar way as in rural atmospheres, that is, practical absence of attack. Above it, aluminium undergoes pitting from the first year of exposure (Figure 10(b)) being more ostensible the greater the atmospheric salinity.

Mixed Atmospheres (S_1P_1, S_1P_2, S_2P_1, S_2P_2). Aluminium corrosion in mixed atmospheres (polluted by Cl^- and SO_2) depends both on the chloride concentration and the SO_2 pollution level in the atmosphere. Aluminium attack can increase considerably Figures 10(c) and 10(d), undergoing strong pitting from the start of exposure. There is a synergic effect through the combined action of the two pollutants.

4. General Conclusion

The 72 Ibero-American Atmospheric testing stations, covering a broad spectrum of climatological and pollution conditions, were divided into subgroups according the classification of atmospheric aggressiveness (ISO 9223 [24]) as function of meteorological (TOW) and atmospheric pollution (SO_2 and Cl^-). The groups were as follows: unpolluted atmospheres, SO_2-polluted atmospheres, pure marine atmospheres, and mixed atmospheres.

In each of these subgroups and for each of the reference metals (low carbon steel, zinc, copper, and aluminium) the corrosion extent for the first year of exposure and the nature of the corrosion products formed were evaluated. Generalizations were made based on observed trends.

Acknowledgment

The authors wish to express their gratitude to the Programa Ibero-Americano de Ciencia y Tecnología para el Desarrollo (CYTED) for financial support granted for the international coordination of MICAT project.

References

[1] L. Uller and M. Morcillo, "The setting-up of an Iberoamerican map of atmospheric corrosion. MICAT Study—CYTED-D," in *Proceedings of the 11th International Corrosion Congress*, vol. 2, pp. 2.35–2.45, Associazione Italiana di Metallurgia, Florence, Italy, 1990.

[2] L. Uller and M. Morcillo, "Mapa Iberoamericano de Corrosao Atmosférica. Projecto MICAT Estudo—CYTED-D," *Corrosao e Proteccao de Materiais*, vol. 10, pp. 7–12, 1991.

[3] M. Morcillo, L. Uller, B. Rosales et al., "Ibero-American map of atmospheric corrosiveness (MICAT). Preliminary results," *Corrosao e Proteccao de Materiais*, vol. 11, pp. 6–12, 1992.

[4] M. Morcillo, L. Uller, B. Rosales et al., "Ibero-American map of atmospheric corrosiveness (MICAT). Preliminary results," *Revista Iberoamericana de Corrosión y Protección*, vol. 23, p. 79, 1992.

[5] M. Morcillo, E. Almeida, B. Rosales, J. Uruchurtu, and M. Marrocos, *Corrosion y Protección de Metales en las Atmósferas de Iberoamérica. Parte I—Mapas de Iberoamérica de Corrosividad Atmosférica (Proyecto MICAT, XV.1/CYTED)*, CYTED, Madrid, Spain, 1998.

[6] E. Almeida, M. Morcillo, B. Rosales, and M. Marrocos, "Atmospheric corrosion of mild steel Part I—rural and urban atmospheres," *Materials and Corrosion*, vol. 51, no. 12, pp. 859–864, 2000.

[7] E. Almeida, M. Morcillo, and B. Rosales, "Atmospheric corrosion of mild steel Part II—Marine atmospheres," *Materials and Corrosion*, vol. 51, no. 12, pp. 865–874, 2000.

[8] E. Almeida, M. Morcillo, and B. Rosales, "Atmospheric corrosion of zinc Part 1: Rural and urban atmospheres," *British Corrosion Journal*, vol. 35, no. 4, pp. 284–288, 2000.

[9] E. Almeida, M. Morcillo, and B. Rosales, "Atmospheric corrosion of zinc Part 2: Marine atmospheres," *British Corrosion Journal*, vol. 35, no. 4, pp. 289–296, 2000.

[10] M. Morcillo, E. Almeida, M. Marrocos, and B. Rosales, "Atmospheric corrosion of copper in Ibero-America," *Corrosion*, vol. 57, no. 11, pp. 967–980, 2001.

[11] M. Morcillo, E. Almeida, and B. Rosales, "Degradation of aluminium in rural atmospheres," *Aluminium*, vol. 76, 2000.

[12] M. Morcillo, E. Almeida, and B. Rosales, "Corrosion of aluminium in pure marine atmospheres," *Aluminium*, vol. 76, 2000.

[13] M. Morcillo, E. Almeida, and B. Rosales, "Corrosion of aluminium in SO_2—polluted marine atmospheres," *Aluminium*, vol. 76, 2000.

[14] M. Morcillo, "Atmospheric corrosion in Ibero-america: the MICAT project," in *Atmospheric Corrosion*, W. W. Kirk and H. H. Lawson, Eds., pp. 257–275, American Society for Testing and Materials, Philadelphia, Pa, USA, ASTM STP 1239, 1995.

[15] L. Mariaca-Rodriguez, E. Almeida, and A. de Bosquez, "Marine atmospheric corrosion of reference metals in tropical climates of Latin-America," in *Marine Corrosion in Tropical Environments*, S. W. Dean, G. H. D. Delgadillo, and J. B. Bushman, Eds., pp. 3–17, American Society Testing and Materials, West Conshohocken, PA, 2000.

[16] M. Morcillo, B. Chico, D. de la Fuente et al., "Atmospheric corrosion of reference metals in Antarctic sites," *Cold Regions Science and Technology*, vol. 40, no. 3, pp. 165–178, 2004.

[17] M. Morcillo, E. Almeida, B. Chico, and D. De la Fuente, "Analysis of ISO standard 9223 (classification of corrosivity of atmospheres) in the light of information obtained in the Ibero-America micat project," in *Outdoor Atmospheric Corrosion*, American Society for Testing and Materials, West Conshohocken, Pa, USA, ASTM STP 1421, 2002.

[18] M. Morcillo and S. Feliu, *Mapas de España de Corrosividad Atmosférica*, CYTED, Madrid, Spain, 1993.

[19] B. M. Rosales, *Mapas de Corrosividad Atmosférica de Argentina*, CITEFA, Buenos Aires, Argentina, 1977.

[20] M. E. M. Almeida and M. G. S. Ferreira, *Corrosao Atmosferica. Mapas de Portugal*, INETI, Lisboa, Portugal, 1998.

[21] L. Mariaca, J. Genescá, J. Uruchurtu, and L. Salvador, *Corrosividad Atmosférica (MICAT-México)*, Plaza y Valdés, México, 1999.

[22] D. Knotkova and L. Vrobel, "ISOCORRAG—the international testing program within ISO/TC 156/WG 4," in *Proceedings of the 11th International Corrosion Congress*, pp. 5.581–5.590, Associazione Italiana di Metallurgia, Florence, Italy, 1990.

[23] V. Kucera, A. T. Coote, J. F. Henriksen, D. Knotkova, C. Leygraf, and U. Reinhardt, "Effects of acidifying air pollutants on materials including historic and cultural monuments. An International cooperative programme within UNECE," in *Proceedings of the 11th Internacional Corrosion Congress*, vol. 2, pp. 2.433–2.442, Associazione Italiana di Metallurgia, Florence, Italy, 1990.

[24] ISO 9223, *Corrosion of Metals and Alloys. Clasiffication of Corrosivity of Atmospheres*, International Standard Organization, Geneve, Switzerland, 1991.

[25] ISO 9225, *Corrosion of Metals and alloys. Corrosivity of Atmospheres. Methods of Measurement of Pollution*, International Standards Organization, Geneve, Switzerland, 1991.

[26] ISO 9226, *Corrosion of Metals and Alloys. Corrosivity of Atmospheres. Method for Determination of Corrosion Rate of Standard Specimens for the Evaluation of Corrosivity*, International Standards Organization, Geneve, Switzerland, 1991.

[27] M. Morcillo, D. de la Fuente, I. Díaz, and H. Cano, "Atmospheric corrosion of mild steel. A review," *Revista de Metalurgia*, vol. 47, no. 5, pp. 426–444, 2011.

[28] V. Kucera and E. Mattsson, "Atmospheric corrosion," in *Corrosion Mechanisms*, F. Mansfeld, Ed., pp. 211–284, Marcel Dekker, New York, NY, USA, 1987.

[29] H. Okada and H. Shimada, "Relation between manganese sulfides and rust initiation," *Corrosion*, vol. 30, pp. 97–101, 1974.

[30] E. S. Ayllón, S. L. Granese, C. Bonazzola, and B. Rosales, "Corrosión atmosférica de aleaciones de fe y Zn en ambientes poluidos.," *Revista Iberoamericana de Corrosión y Protección*, vol. 17, pp. 205–211, 1986.

[31] W. H. J. Vernon, "A laboratory study of the atmospheric corrosion of metals. Part II.—Iron: The primary oxide film. Part III.—the secondary product or rust (influence of sulphur dioxide, carbon dioxide, and suspended particles on the rusting of iron)," *Transactions of the Faraday Society*, vol. 31, pp. 1668–1700, 1935.

[32] M. Stratmann and J. Müller, "The mechanism of the oxygen reduction on rust-covered metal substrates," *Corrosion Science*, vol. 36, no. 2, pp. 327–359, 1994.

[33] U. R. Evans, "Electrochemical mechanism of atmospheric rusting," *Nature*, vol. 206, no. 4988, pp. 980–982, 1965.

[34] T. Misawa, K. Asami, K. Hashimoto, and S. Shimodaira, "The mechanism of atmospheric rusting and the protective amorphous rust on low alloy steel," *Corrosion Science*, vol. 14, no. 4, pp. 279–289, 1974.

[35] M. Stratmann, K. Bohnenkamp, and T. Ramchandran, "The influence of copper upon the atmospheric corrosion of iron," *Corrosion Science*, vol. 27, no. 9, pp. 905–926, 1987.

[36] U. R. Evans, "The economic advantages of a sound painting scheme," *Transactions of the Institute of Metal Finishing*, vol. 37, pp. 1–7, 1960.

[37] U. R. Evans and C. A. J. Taylor, "Mechanism of atmospheric rusting," *Corrosion Science*, vol. 12, no. 3, pp. 227–246, 1972.

[38] M. Stratmann, K. Bohnenkamp, and H. J. Engell, "An electrochemical study of phase-transitions in rust layers," *Corrosion Science*, vol. 23, no. 9, pp. 969–985, 1983.

[39] M. Stratmann and H. Streckel, "On the atmospheric corrosion of metals which are covered with thin electrolyte layers-I. Verification of the experimental technique," *Corrosion Science*, vol. 30, no. 6-7, pp. 681–696, 1990.

[40] M. Schwarz, "Untersuchungen über dir Wirkung des Eisen (II)-sulfates beim atmosphärischen Rosten una beim Unterrosten von Anstrichen. Teil I," *Werkstoffe und Korrosion*, vol. 16, no. 1, pp. 93–103, 1965.

[41] J. F. Henriksen, "The distribution of NaCl on Fe during atmospheric corrosion," *Corrosion Science*, vol. 9, no. 8, pp. 573–577, 1969.

[42] R. Ericsson, "Influence of sodium chloride on the atmospheric corrosion of steel," *Werkstoffe und Korrosion*, vol. 29, no. 6, pp. 400–403, 1978.

[43] F. Corvo, "Atmospheric corrosion of steel in a humid tropical climate. Influence of pollution, humidity, temperature, rainfall and sun radiation," *Corrosion*, vol. 40, no. 4, pp. 170–175, 1984.

[44] M. Morcillo, S. Flores, G. Salas, and M. Valencia, "An extremely low corrosion rate of steel in the atmosphere of Cuzco (Peru)," *Atmospheric Environment. Part A*, vol. 27, no. 13, pp. 1959–1962, 1993.

[45] F. Mansfeld and R. Vijayakumar, "Atmospheric corrosion behavior in Southern California," *Corrosion Science*, vol. 28, no. 9, pp. 939–946, 1988.

[46] T. E. Graedel, "On the involvement of H_2O_2 and SO_2 in the atmospheric corrosion of steel," *Journal of the Electrochemical Society*, vol. 135, no. 4, pp. 1035–1036, 1988.

[47] D. de la Fuente, J. G. Castaño, and M. Morcillo, "Long-term atmospheric corrosion of zinc," *Corrosion Science*, vol. 49, no. 3, pp. 1420–1436, 2007.

[48] P. Quintana, L. Veleva, W. Cauich, R. Pomes, and J. L. Peña, "Study of the composition and morphology of initial stages of corrosion products formed on Zn plates exposed to the atmosphere of southeast Mexico," *Applied Surface Science*, vol. 99, no. 4, pp. 325–334, 1996.

[49] I. Odnevall and C. Leygraf, "Reaction sequences in atmospheric corrosion of zinc," in *Atmospheric Corrosion*, W. W. Kirk and H. H. Lawson, Eds., pp. 215–229, American Society Testing and Materials, West Conshohocken, Pa, USA, 1995.

[50] G. Schikorr, "Korrosionsverhalten von Zink und Zinküberzügen an der AtmosphäreVorgetragen auf der Diskussionstagung "Atmosphärische Korrosion der Metalle"," *Werkstoffe und Korrosion*, vol. 15, pp. 537–543, 1964.

[51] T. E. Graedel, "Corrosion mechanisms for zinc exposed to the atmosphere," *Journal of the Electrochemical Society*, vol. 136, no. 4, pp. C193–C203, 1989.

[52] V. E. Carter, "Atmospheric corrosion of non-ferrous metals," in *Corrosion Processes*, R. N. Parkins, Ed., pp. 77–113, Applied Science, London, UK, 1982.

[53] H. Guttman, "Effects of atmospheric factors on the corrosion of rolled zinc," in *Metal Corrosion in the Atmosphere*, pp. 223–239, American Society for Testing and Materials, Philadelphia, Pa, USA, ASTM STP 435, 1968.

[54] J. E. Svensson and L. G. Johansson, "A laboratory study of the initial stages of the atmospheric corrosion of zinc in the presence of NaCl; Influence of SO_2 and NO_2," *Corrosion Science*, vol. 34, no. 5, pp. 721–740, 1993.

[55] C. J. Slunder and W. K. Boyd, *Zinc: Its Corrosion Resistance*, ILZRO, New York, NY, USA, 1983.

[56] A. Askey, S. B. Lyon, G. E. Thompson et al., "The effect of fly-ash particulates on the atmospheric corrosion of zinc and mild steel," *Corrosion Science*, vol. 34, no. 7, pp. 1055–1081, 1993.

[57] I. Odnevall, *Atmospheric corrosion of field exposed zinc*, Ph.D. thesis, Royal Institute of Technology, Stockholm, Sweden, 1994.

[58] J. R. Vilche, F. E. Varela, G. Acuña et al., "A survey of Argentinean atmospheric corrosion: I—Aluminium and zinc samples," *Corrosion Science*, vol. 37, no. 6, pp. 941–961, 1995.

[59] D. de la Fuente, J. Simancas, and M. Morcillo, "Morphological study of 16-year patinas formed on copper in a wide range of atmospheric exposures," *Corrosion Science*, vol. 50, no. 1, pp. 268–285, 2008.

[60] E. Mattsson and R. Holm, "Copper and copper alloys," in *Metal Corrosion in the Atmosphere*, pp. 187–210, American Society for Testing and Materials, Philadelphia, Pa, USA, ASTM STP 435, 1968.

[61] T. E. Graedel, K. Nassau, and J. P. Franey, "Copper patinas formed in the atmosphere-I. Introduction," *Corrosion Science*, vol. 27, no. 7, pp. 639–649, 1987.

[62] T. E. Graedel, "Copper patinas formed in the atmosphere—II. A qualitative assessment of mechanisms," *Corrosion Science*, vol. 27, no. 7, pp. 721–740, 1987.

[63] K. Barton, "Personal Communication," in *Corrosion in Natural Environments*, D. Knotkova, B. Bosek, and J. Vlickova, Eds., p. 52, merican Society for Testing and Materials, Philadelphia, Pa, USA, ASTM STP 558, 1974.

[64] S. R. Souza, P. C. Vasconcellos, and L. R. F. Carvalho, "Low molecular weight carboxylic acids in an urban atmosphere: Winter measurements in São Paulo City, Brazil," *Atmospheric Environment*, vol. 33, no. 16, pp. 2563–2574, 1999.

[65] A. V. Echavarría, F. E. Echeverría, C. Arroyave, E. Cano, and J. M. Bastidas, "Carboxilic acids in the atmosphere and their effect on the degradation of metals," *Corrosion Reviews*, vol. 21, no. 5-6, pp. 395–413, 2003.

[66] A. Echavarría, F. Echeverría, H. Gil, and C. Arroyave, "Influence of environmental factors in the atmospheric corrosion of copper in the presence of propionic acid," *Journal of the Chilean Chemical Society*, vol. 54, no. 3, pp. 212–217, 2009.

[67] W. H. J. Vernon and L. Whitby, "The open-air corrosion of copper. Part II. The mineralogical relationships of corrosion products," *Journal of the Institute of Metals*, vol. 44, pp. 389–408, 1930.

[68] R. Baboian and E. B. Cliver, "Corrosion on the statue of liberty," *Materials Performance*, vol. 25, no. 3, pp. 80–81, 1986.

[69] D. de la Fuente, E. Otero-Huerta, and M. Morcillo, "Studies of long-term weathering of aluminium in the atmosphere," *Corrosion Science*, vol. 49, no. 7, pp. 3134–3148, 2007.

[70] H. P. Godard, *The Corrosion of Light Metals*, John Wiley & Sons, New York, NY, USA, 1967.

[71] M. S. Hunter and P. Fowle, "Natural and thermally formed oxide films on aluminum," *Journal of the Electrochemical Society*, vol. 103, pp. 482–485, 1656.

[72] H. P. Godard, "An insight into the corrosion behavior of aluminum," *Materials Performance*, vol. 20, no. 7, pp. 9–15, 1981.

[73] Y. N. Mikhailovskii, G. B. Klark, L. A. Shuvakhina, V. V. Agafonov, and N. I. Zhuravlena, "Calculation of atmospheric corrosion rate of aluminum and its alloys in various climatic zones according to meteorological parameters," *Protection of Metals*, vol. 9, no. 3, pp. 240–246, 1973.

[74] S. Feliu and M. Morcillo, *Corrosión y Protección de los Metales en la Atmósfera*, Barcelona, Spain, 1982.

[75] P. L. Spedding, "Corrosion by atmospheric sulphur dioxide ," *Australasian Corrosion Engineering*, vol. 15, no. 8, pp. 27–36, 1971.

[76] T. E. Graedel, "Corrosion mechanisms for aluminum exposed to the atmosphere," *Journal of the Electrochemical Society*, vol. 136, no. 4, pp. C204–C212, 1989.

[77] R. T. Foley, "Localized corrosion of aluminum alloys: a review," *Corrosion*, vol. 42, no. 5, pp. 277–288, 1986.

[78] G. K. Berukshitis and G. B. Klark, "Atmospheric corrosion of steel, zinc, cadmium, copper and aluminum in different coastal and continental regions," in *Corrosion of Metal and Alloys*, G. B. Tomashov and E. N. Mirolubev, Eds., pp. 281–297, Israel Program for Scientific Translations, Jerusalem, Israel, 1966.

[79] I. L. Rozenfeld, *Atmospheric Corrosion of Metals*, NACE, Houston, Tex, USA, 1972.

[80] T. Sydberger and N. G. Vannerberg, "The influence of the relative humidity and corrosion products on the adsorption of sulfur dioxide on metal surfaces," *Corrosion Science*, vol. 12, no. 10, pp. 775–784, 1972.

Hindawi Publishing Corporation
International Journal of Corrosion
Volume 2012, Article ID 419640, 16 pages
doi:10.1155/2012/419640

Research Article

Atmospheric Corrosion of Painted Galvanized and 55%Al-Zn Steel Sheets: Results of 12 Years of Exposure

C. I. Elsner,[1,2] P. R. Seré,[1] and A. R. Di Sarli[1]

[1] *CIDEPINT, Centro de Investigación y Desarrollo en Tecnología de Pinturas (CICPBA-CCT CONICET-La Plata), Avenida 52 s/n entre 121 y 122, B1900AYB La Plata, Argentina*
[2] *Facultad de Ingeniería, Universidad Nacional de La Plata, Avenida 1 esq. 47, B1900TAG La Plata, Argentina*

Correspondence should be addressed to A. R. Di Sarli, ardisarli@gmail.com

Received 28 July 2011; Accepted 1 November 2011

Academic Editor: Blanca M. Rosales

Zinc or 55%Al-Zn alloy-coated steel sheets, either bare or covered by different painting systems, have been exposed for 12 years to the action of the urban atmosphere at the CIDEPINT station located in La Plata (34° 50′ South, 57° 53′, West), province of Buenos Aires, Argentina. The samples exposed surface was evaluated through periodical visual inspections, standardized adhesion tests, and electrochemical impedance measurements. The ambient variables monitored were average annual rains and temperatures, time of wetness, sulphur and chloride concentration, relative humidity, and speed and direction of the winds. It was found that in this atmosphere, the corrosion resistance of the bare 55% Al-Zn/steel sheets was higher than of the galvanized steel, and the polyurethane painting system was more protective than the alkyd and epoxy ones, which degraded after 6-7 years of exposure.

1. Introduction

Exposed to specific aggressive media, metal or alloy stability depends upon the protective properties of the surface film formed, because its chemical composition, conductivity, adherence, solubility, hygroscopicity, and morphological characteristics determine the film capacity to work as a controlling barrier [1]. In such a sense, steel galvanic protection by means of zinc or zinc alloys is a common example, owing not only to the fact that the zinc, being electrochemically more active than the steel, corrodes preferentially, but also to the barrier effect of the corrosion products precipitated on the metallic surface. In particular, the coatings based on zinc are widely used to protect steel structures against atmospheric corrosion [2], because of the protective properties afforded by an insoluble film of basic carbonate. However, if the exposure conditions are such that there is changes of the ambient variables like atmospheric conditions, UV radiation intensity, type and level of pollutants, wet-dry cycles, depletion of air but high humidity, or a medium containing strongly aggressive species like chloride or sulphate ions, the zinc could dissolve forming soluble, less dense, and scarcely protective corrosion products, which sometimes lead to localized corrosion [2–5]. This condition can be reached during the storage and transportation of galvanized steel sheets or when they are exposed to marine and/or industrial environments [6]. Aluminium coatings have overcome these two factors. Nevertheless, as they cannot provide cathodic protection to exposed steel in most environments, early rusting occurs at coating defects and cut edges; besides, these coatings are also subjected to crevice corrosion in marine environmental [7].

For years, many attempts to improve the corrosion resistance of zinc and aluminium coatings through alloying were carried out. Although the protective effect of combinations of these two elements was known, they were not used until the discovery that silicon inhibits the fast alloying reaction with steel [8]. Thus, the alloy commercially known as Galvalume or Zincalum arose, and its composition: 55% Al, 1.6% Si, the rest zinc, was selected from a systematic study, providing an excellent combination of galvanic protection and low corrosion rate.

When a higher degree of protection of these metallic surfaces is of concern, properly chosen painting systems can provide a more effective corrosion-inhibiting barrier and also a better aesthetic appearance [9]. Some exposure conditions are so aggressive that both protective systems

(metallic + organic coatings) must be applied to get longer effectiveness. Such a combination, referred to as a duplex system, has demonstrated a synergistic effect when compared to the individual coating systems. This better corrosion protection is attributed to the double action afforded by the zinc or 55%Al-Zn layer (cathodic protection + blockage of its defects by the corrosion products), and also by the pigmented paint system (barrier effect + steel corrosion-inhibition) [10]. Besides, this duplex system requires less reconditioning and repairs of coating systems after transportation and assembly on site.

The mechanism responsible for the protective action of paint coatings is highly complex because it depends upon the simultaneous action of different factors. Irrespective of their intended function (functional, decorative, or protective), the paint must adhere satisfactorily to the underlying substrate [11, 12].

The organic film permeability is important in metallic substrate corrosion, since this property is directly connected to the permeation of environmental corrosion-inducing chemicals through the polymeric matrix, the chemical composition of the latter, and the presence of pores, voids, or other defects in the coating. It is important to note that particularly water and oxygen can permeate the film, at least to some extent, even if none of the intrinsic structural defects are present. For these reasons, the painted metal's resistance to degradation produced by weathering is a very important variable, since it defines the material's durability. Within this concept, the corrosion and resistance to weathering (degradation due to UV radiation, oxygen, humidity, etc.) are separately evaluated. The corrosion resistance depends upon the permeability (barrier effect) of the primer and galvanic layer as well as of the inhibitive capacity of the contained anticorrosive pigments. The weathering degradation (loss of gloss and/or adhesion, chalking, cracking, blistering, etc.) takes place at shorter times and depends mainly on the topcoat paint properties.

The still unsolved paint delamination or blistering problem, due to a bad bond at the substrate/paint interface, depends upon the chemical nature and crosslinking degree of the polymer as well as the metal substrate and its surface treatment [13]. In principle, paint adhesion can be improved by providing the substrate with a pretreatment layer, followed by applying a corrosion inhibiting primer + intermediate and/or topcoat paints. In line with this definition, the primer is considered the critical element in most paint systems because it is mainly responsible for preserving the metallic state of the substrate, and it must also anchor the total paint coating to the steel. Most coatings adhere to the metal via purely physical attractions (e.g., hydrogen bonds) that develop when two surfaces are brought closely together [14, 15]. Paint vehicles with polar groups (–OH, –COOH, etc.) have good wetting properties and show excellent physical adhesion characteristics (epoxies, alkyds, oil paints, etc.). Much stronger chemically bonded adhesion is possible when the primer can actually react with the metal, as is the case of several pretreatments [16–18].

Paint life depends on several factors such as the metallic substrate, the selected paint system, and the paint-substrate interface [19]. Paint selection is generally based on the aggressive medium properties, while the metal treatment before painting has a substantial impact on the useful life of the selected system.

The susceptibility to degradation of painted metals is estimated by accelerated laboratory tests and natural atmospheric exposure for several years [20–31]. Although the extrapolation of accelerated test results do not compare linearly to the actual performance of the coatings in their service life, it can supply useful information related to the rate and form of the corrosion-inhibiting system degradation. In most cases, such information can help to improve the paint formulation and/or the painting scheme design. Consequently, a comparative evaluation of the protective performance of either bare or covered with three different painting systems is reported in this paper. The corrosion resistance of these samples was tested by exposure for 12 years to the action of the urban atmosphere at the CIDEPINT station located in La Plata (34° 50′ South, 57° 53′, West), province of Buenos Aires, Argentina.

The evolution of the samples exposed surface was evaluated through periodical visual inspections, adhesion tests according to the ASTM D-3359/09 standard, and electrochemical impedance measurements applied to samples immersed for 1 h in 0.5 M Na_2SO_4 solution. The ambient variables monitored were average annual rains and temperatures, time of wetness, sulphur and chloride concentration, relative humidity, and speed and direction of the winds.

2. Experimental Details

A total of 280 commercial-grade steel sheets (15 × 8 × 0.2 cm) hot-dip coated with zinc or 55%Al-Zn plates were used as the metallic substrate. They were degreased by immersion in 5% Na_2CO_3 solution and then rinsed with distilled water to eliminate any possible surface contamination.

The commercial-grade protective painting systems (Table 1) were applied by brushing to maintain the same conditions for all the samples. After applying the painting system, the painted plates were placed in a dessicator cabinet at controlled temperature (30 ± 2°C) until completely dry. Next, measurements of dry film thickness (Table 1) were taken with an Elcometer 300 coating thickness gauge, using a bare sanded plate and standards of known thickness as references. Plates were exposed at 45° from the horizontal and they were oriented East allowing a maximum insolation on them. The test site was formed by wooden structures, where the flat plates were set on. Location coordinates, meteorological data, atmospheric pollutants, time of wetness and corrosion category of the place of location according to ISO 9223 are given in Figure 1 and Tables 2 and 3, respectively. All environmentally data were available from the Seismology and Meteorological Department of the Astronomic and Geophysics Science Faculty of the National University of La Plata, placed very near CIDEPINT Station.

To check reproducibility, a total of 280 samples including bare or painted steel/zinc or steel/55%Al-Zn sheets were exposed to natural weathering in La Plata station for 12 years.

Table 1: Mean thicknesses (μm).

Metal/paint system	Metallic coating	Primer	Topcoat	Total thickness
S/Z/AS	18 ± 0.9	22 ± 0.9	52 ± 2.6	92 ± 4.5
S/ZA/AS	20 ± 0.9	22 ± 0.9	52 ± 2.6	94 ± 4.5
S/Z/ES	18 ± 0.9	4 ± 0.2	87 ± 2.6	109 ± 5.1
S/ZA/ES	20 ± 0.9	4 ± 0.2	87 ± 2.6	111 ± 5.1
S/Z/PS	18 ± 0.9	4 ± 0.2	48 ± 2.6	70 ± 3.5
S/ZA/PS	20 ± 0.9	4 ± 0.2	48 ± 2.6	72 ± 3.5

Note: S/Z/AS: galvanized steel/alkyd-based paint system; S/ZA/AS: steel/55%Al-Zn alloy/alkyd-based paint system; S/Z/ES: galvanized steel/epoxy-based paint system; S/ZA/ES: steel/55%Al-Zn alloy/epoxy-based paint system; S/Z/PS: galvanized steel/polyurethane-based paint system; S/ZA/PS: steel/55%Al-Zn alloy/polyurethane-based paint system.

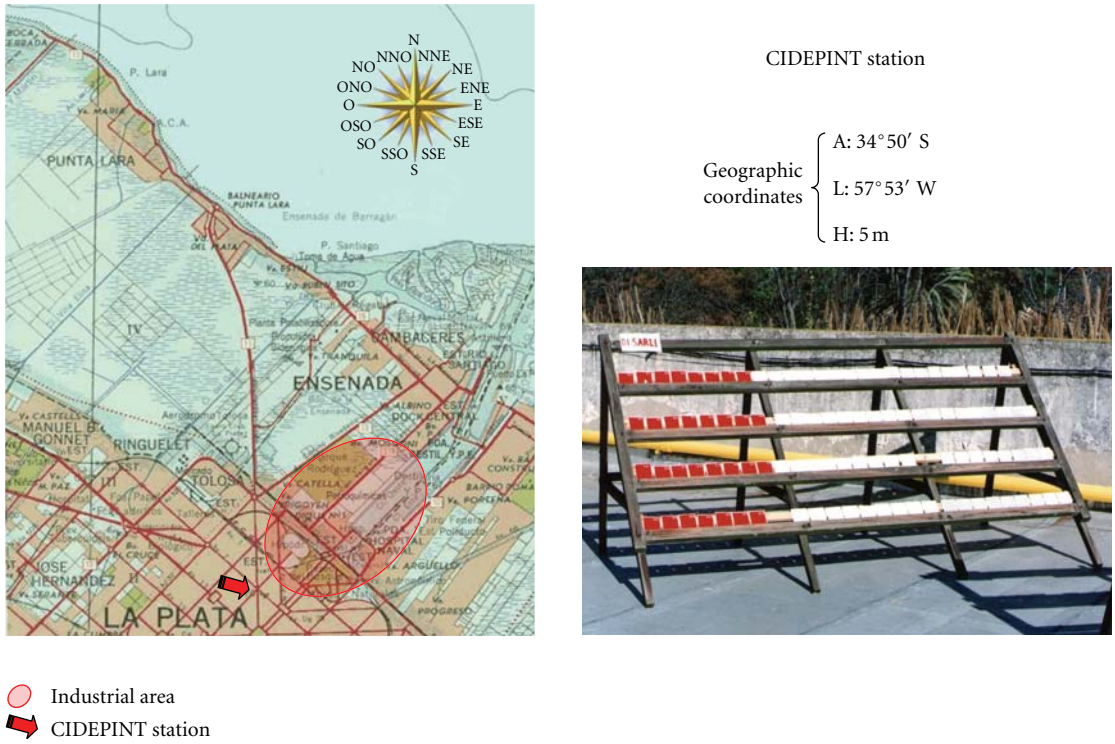

Figure 1: Location of the CIDEPINT station in La Plata, Buenos Aires, Argentina.

The painted samples were build-up with the three painting systems mentioned in Table 1, and their edges were masked with a thick wax base coating to avoid edge effect.

Gravimetric determinations for measuring weight-loss of bare steel/metallic coating samples were carried out in triplicate for each material tested.

The visual inspections and samplings took place according to the following program: during the first year each 1st, 3rd, 6th, 9th, 12th month, and then each 2nd, 4th, 8th, and 12th year. At the same times, adhesion tests according to the Test Tape ASTM D-3359/09 Standard on replicates of each type of painted samples were also performed.

2.1. Electrochemical Measurements. For the impedance measurements periodically carried out on other replicates of each type of samples, a cylindrical clamp-on acrylic (polymethyl methacrylate) cell was positioned on the painted panel by an O-ring defining a surface area of 15.9 cm^2. An aperture in the top of this three electrode electrochemical cell contained a Pt-Rh mesh counter-electrode with negligible impedance, oriented parallel to the working electrode (painted metal surface). A glass-linear Saturated $Hg/HgSO_4$ tipped Reference Electrode was positioned, together with the counter-electrode, close to the exposed painted steel surface panel. For further easy comparison with previous information, all the potential data in the text and figures were referred to the Saturated Calomel Electrode (SCE). Before the electrochemical impedance spectrum of each replicate was obtained, the sample was subjected to 1 hour of wetting in 0.5 M Na_2SO_4 solution. Impedance spectra were obtained from a Solartron 1255 FRA coupled to a Solartron EI 1286 and a PC, all controlled by the Zplot software. Impedance spectra collected in the frequency range $10^{-2} \leq f(Hz) \leq 10^6$ were analyzed and interpreted on the basis of equivalent electrical

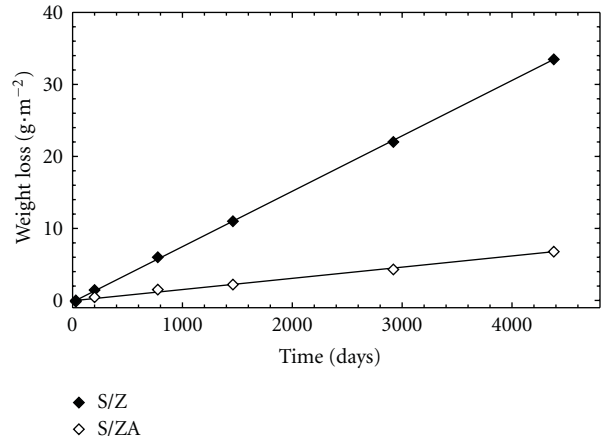

Figure 2: Plots showing the time dependence of the weight loss suffered by the bare S/Z and S/ZA sheets.

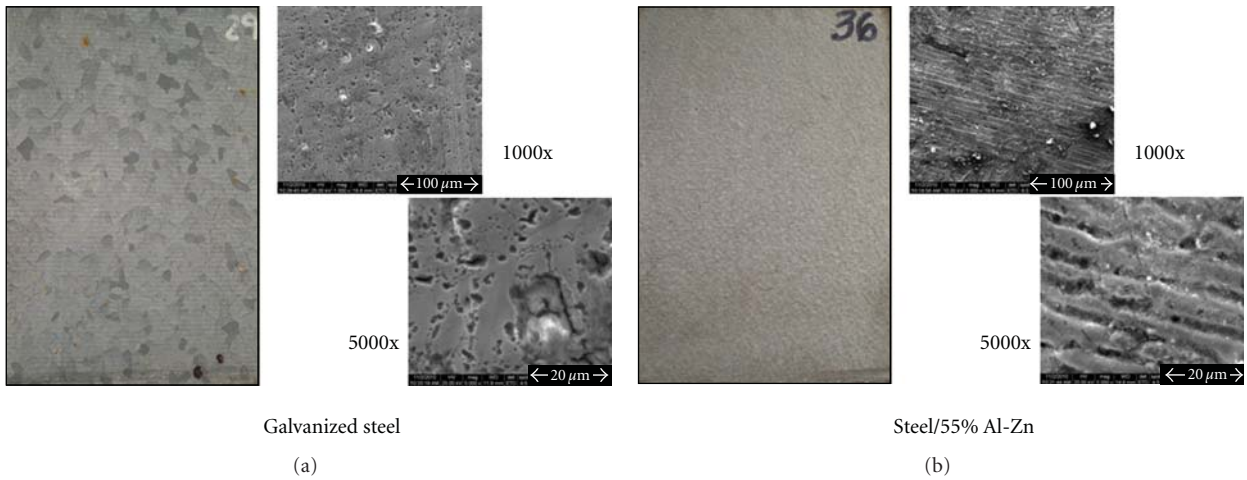

Figure 3: Photographs and SEM images of the bare metallic coatings after 12 years of exposure.

circuits, optimizing the values of the circuit parameters by using Boukamp' program [32].

All the electrochemical experiments were carried out at laboratory temperature (23 ± 2°C) and with the electrochemical cell in a Faraday cage to reduce external interferences as much as possible.

To improve the experimental data reliability, three replicates of each sample type were measured in all the tests.

3. Experimental Results and Discussion

3.1. Atmospheric Exposure Test

3.1.1. Corrosion of the Metallic Coatings. It is known that all the materials degrade under the influence of atmospheric factors such as oxygen, humidity, and/or pollutants (SO_2, NaCl, NO_x, etc.). Another important degradation source is the sun radiation, particularly its UV rays. All these influences compose the so-called "Macroclimate" of a determined zone [33]. In change, "Microclimate" is defined as the specific climate formed around an object and it results of vital importance to understand the atmospheric mechanisms causing the materials degradation. Among the parameters used to define it are the surface time of wetness (TOW), the heating by sun radiation, mainly the infrared, and the acidic nature ions (SO_3^{2-}, NO_2^-, Cl^-) gathering within the aqueous layer deposited on the object. On the other hand, the atmospheric corrosion process is the sum of partial corrosion processes taking place each time an electrolyte layer deposits on the surface metal. The rain, snow, fog, and/or humidity condensation produced by temperature changes are the main promoters of atmospheric corrosion. In such sense, the value of some climatological variables characterizing the average exposure conditions corresponding to the station used in the present work are shown in Tables 2 and 3. The aggressiveness of La Plata station was attributed to its high relative humidity, severe and lengthy TOW as well as surface runoff supported by the tested replicates.

Hot-dip zinc is widely used as a coating for carbon steel because of its good corrosion resistance and relatively low price [34]. Due to its practical use, zinc atmospheric corrosion has been studied in field exposures as well as in laboratory with controlled environments [35, 36]. Zincite, ZnO, is the first product formed when the naked metal is

Table 2: Meteorological data for the 12 years of exposure in the CIDEPINT Station, La Plata, Argentina.

Year	Mean temperature (°C)	Mean relative humidity (%)	Precipitation (mm)	Days of rain
1	16.5	80.8	943.1	90.0
2	16.8	80.7	1042.8	94.0
3	16.3	80.4	927.0	93.0
4	15.8	81.8	1342.1	90.0
5	16.4	84.4	1316.6	98.0
6	16.0	82.7	1611.8	107.0
7	15.8	81.1	924.5	98.0
8	16.1	80.8	881.7	88.0
9	15.9	79.4	926.6	91.0
10	16.0	79.0	1083.4	81.0
11	15.4	77.5	1153.2	85.0
12	16.3	78.3	775.1	70.0

Table 3: Average levels of chemical agents, time of wetness and corrosion category of CIDEPINT Station.

Year	Deposition rate of SO_2 ($mg \cdot m^{-2} \cdot d^{-1}$)	Deposition rate of chloride ($mg \cdot m^{-2} \cdot d^{-1}$)	Time of wetness fraction	Corrosion category according to ISO 9223
1	6.22	Negligible	0.61	$P_0S_0\tau_4/C_2$
2	7.25	Negligible	0.62	$P_0S_0\tau_4/C_2$
3	6.81	Negligible	0.61	$P_0S_0\tau_4/C_2$
4	6.53	Negligible	0.65	$P_0S_0\tau_5/C_2$
5	7.42	Negligible	0.63	$P_0S_0\tau_5/C_2$
6	6.94	Negligible	0.69	$P_0S_0\tau_5/C_2$
7	7.60	Negligible	0.59	$P_0S_0\tau_4/C_2$
8	8.12	Negligible	0.57	$P_0S_0\tau_4/C_2$
9	7.93	Negligible	0.61	$P_0S_0\tau_4/C_2$
10	6.82	Negligible	0.62	$P_0S_0\tau_4/C_2$
11	7.45	Negligible	0.62	$P_0S_0\tau_4/C_2$
12	8.01	Negligible	0.55	$P_0S_0\tau_4/C_2$

exposed to the air, creating a protective film that inhibits corrosion process. Under humidity conditions higher than 80%, zinc is oxidized forming zinc hydroxide. If the pH on the surface is high enough, this hydroxide can react with atmospheric components such as CO_2, SO_x, and Cl^-, forming, in the hydroxide/air interface, the corresponding zinc basic salts [37]. Some of these products form a compact film that protects the metal against later corrosive attacks [38]. An important intermediate in the subsequent formation of other corrosion products is hydrozincite $Zn_4CO_3(OH)_6 \cdot H_2O$ [39, 40]. If the pH of the humid surface is low, neither hydroxide nor basic salts are formed [37]. In presence of SO_2 polluted air, the main corrosion product is hydroxysulfate $Zn_4SO_4(OH)_6 \cdot 4H_2O$, and in presence of Cl^- contamination, the precipitation of insoluble hydroxychloride $Zn_5(OH)_8Cl_2 \cdot H_2O$ is possible.

The hot-dip aluminium-zinc alloy, known as Zincalume, actually contains about 55% aluminium, 1.5% silicon, and the balance zinc. A microstructure of the alloy-coated steel which forms on cooling is essentially two phase, comprising about 80% by volume of a dendritic aluminium-rich phase and the remainder an interdendritic zinc-rich phase with a thin intermetallic layer next to the steel substrate. When the coating corrodes initially, the zinc phase corrodes preferentially until the formation of corrosion products reduces further activity in these areas. During the initial stage of corrosion, the coating behaves like zinc coating. In the later stages of corrosion when the coating is essentially comprised of zinc corrosion products carried in an aluminium-rich matrix, the corrosion becomes more characteristic of the aluminium-rich phase, resulting in a lower corrosion rate, more typical of aluminium [41, 42].

Weight-loss measurements provide the most reliable figure concerning the aggressiveness of a given atmosphere, so that the corresponding corrosion data approach to the service conditions more than any other test. In the present case, as it is shown in Figure 2 both materials presented a linear relationship between its weight-loss and the weathering time and, considering the 12 years exposure, the galvanized coating exhibited a degree of corrosion 4.94 times greater than that of the 55%Al-Zn coating.

In general, the zinc coating suffered uniform corrosion with the development of a layer of corrosion products, mainly ZnO and $Zn_4CO_3(OH)_6 \cdot H_2O$, but in particular

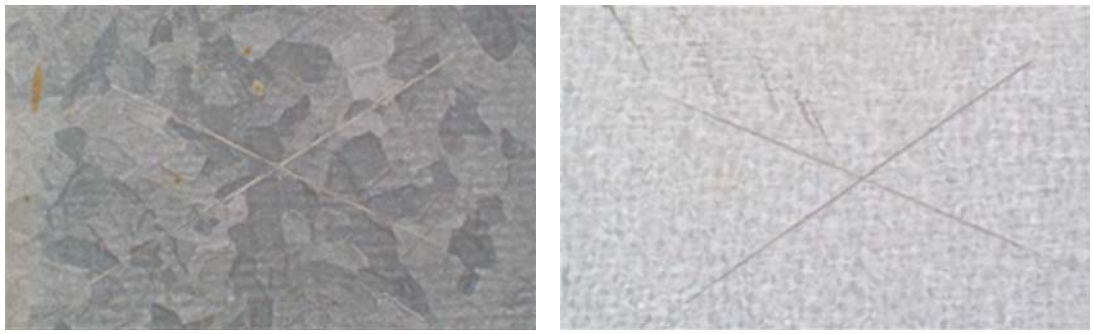

Galvanized steel (a) Steel/55% Al-Zn (b)

Figure 4: Photographs of the scribed area of bare metallic coatings after 12 years of exposure.

places of the surface, the accumulation of atmospheric dust produced localized corrosion as it is possible to see in the SEM images shown in Figure 3. On the other hand, on the 55%Al-Zn coating and due to the complex structure of the alloy, the development of localized corrosion was observed as a consequence of the preferential dissolution of the interdendritic Zn-rich phase, which provoked loss of surface' brightness and the development of thin dark lines related to the aluminium corrosion process.

During all the weathering period, both metallic coatings were able to afford cathodic protection to the substrate as it is shown in Figure 4.

These results can be explained by considering the climatic conditions prevailing during the outdoor exposure prior to samples removal, that is, level of sulphur compounds, wet/dry cycles, high TOW, and pluvial precipitations dissolving the zinc corrosion products and releasing zinc ions from the corroded surface, which are dispersed to the environment. This phenomenon is known today as a metal runoff process [43–50].

3.1.2. Duplex Systems. As a direct way of evaluating the anticorrosive performance of organic coatings, the exposure test to natural atmospheres either for intact or scribed painted surfaces is, without any doubt, the best.

Experimental results coming from exposure tests to natural weather conditions are further representative of the protective and aesthetic properties provided by the topcoat paint. In such a sense, the results obtained from visual inspections periodically carried out for 12 years of exposure in La Plata station confirmed that weathering of the considered duplex systems proceeds very slowly. The periodical visual inspection put in evidence that no sample presented underrusting, peeling, cracking, or checking. From the 4th year weathering and due to the effect of the UV radiation, the Epoxy paint systems showed significant deterioration by chalking, and the topcoat Alkyd paint began to show significant changes of color, brightness, and chalking that led to the exposure of the primer from the 8th year of test. In any case, blistering or filiform corrosion near the scribed cross was observed. Examples of this behavior are presented on Figures 5 and 6. These results were attributed to the highest resistance of the polyurethane topcoat paint to the UV radiation, rain and temperature changes due to the strong interaction between the reactive components of the polymer and the chemically stable pigment (TiO_2) added to the effective anticorrosive protection offered by the primer.

At this point, it is noteworthy to remark that besides knowing the behavior of painting systems when they are intact, it is important to evaluate how they performed when mechanical damage occurs. For that purpose, some of the samples were scribed in an X-shape before being exposed to the natural atmosphere.

The main characteristic of duplex systems is to get and maintain good adhesion to the metallic-coated steel surface during its weathering period. As it is shown in Figure 7, independent of the metallic substrate the polyurethane coating presented the largest adhesion loss during the weathering. Due to the previously mentioned behavior of Epoxy and Alkyd paint systems from the 4th year of weathering, is important to mention that in the case of both Alkyd systems the adhesion test considered mainly the primer and in the case of the Epoxy-based samples the evaluation was interrupted as a consequence of the observed chalking degree.

3.2. Electrochemical Tests. During atmospheric corrosion, in general, the metal is not immersed in large quantities of electrolyte but in contact with thin layers or monolayers of moisture, due to that the corrosion process develops as localized corrosion cells. In that situation, the measurement of the corrosion potential as well as of the resistive and capacitive parameters governing the electrochemical behavior of the metal/coating interface is not always possible during the atmospheric corrosion [51, 52].

According to Zhang and Lyon [52], the cathodic process for metals like steel, zinc, and copper coated with thin ($<100\,\mu$m) water films reveals a diffusional limiting current whose value depends on the water film thickness. For thinner thicknesses, like in most of the atmospheric corrosion cases, the main cathodic process is controlled by activation. In the case of zinc, due to its high electronegativity, the cathodic process is not sensitive to the water film thickness present on

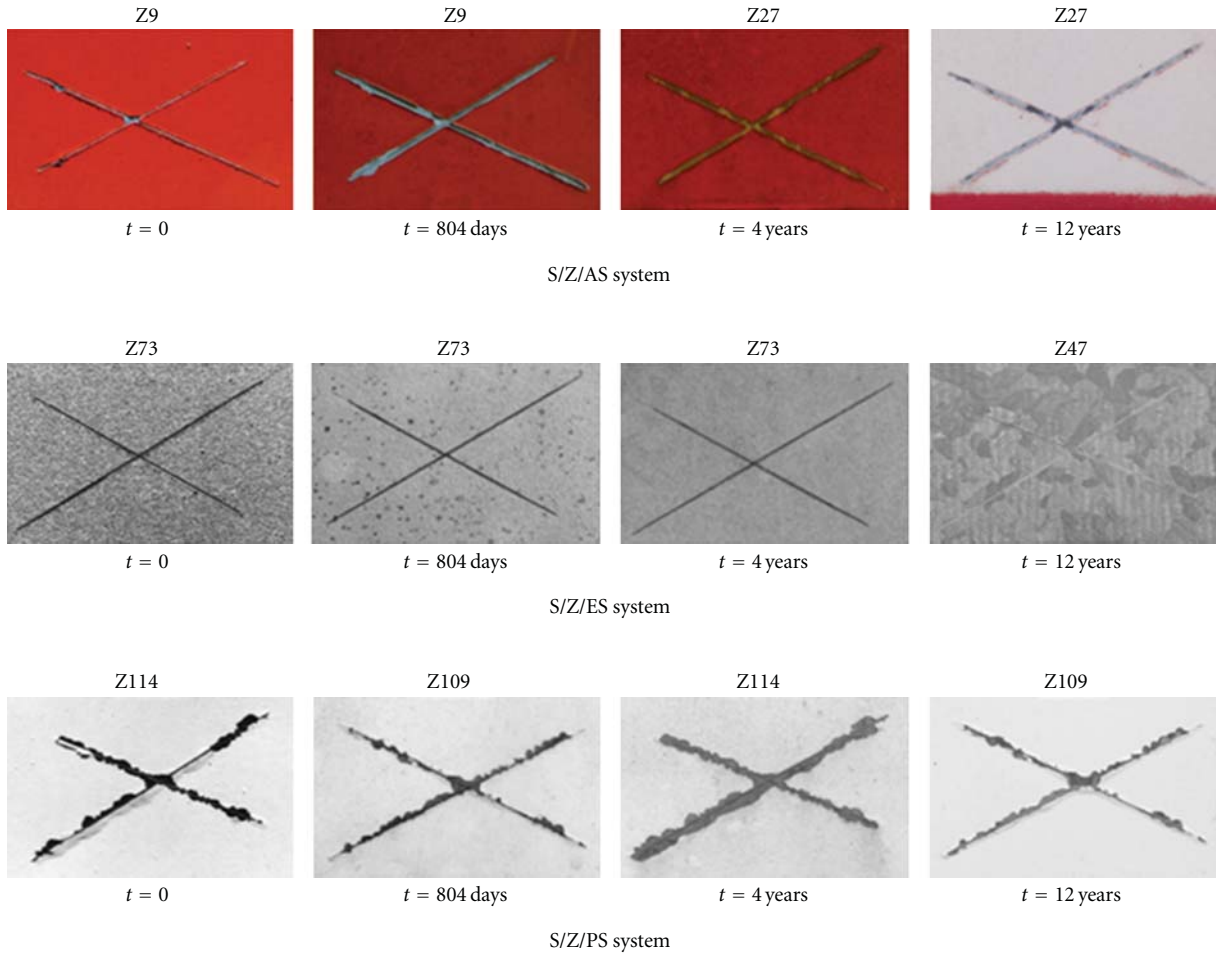

Figure 5: Photographs showing the evolution of S/Z/painting systems as a function of the exposure time.

the surface. On the other hand, as it was mentioned earlier, the protective capacity of the corrosion products formed during the atmospheric exposure depends on a variety of properties, which are also dependent on the composition and metallurgical history of the metal as well as on the atmospheric variables [1, 5, 53].

3.2.1. Corrosion Potential and Impedance Results for Bare S/Z and S/ZA Sheets. The measured corrosion potential values (E_{corr}) point out the metal susceptibility to be corroded. In general, when a value for a given medium is nobler (positive), it will result more resistant to corrosion. As it is possible to see in Figure 8, the corrosion potential evolution for the bare coating materials (Z and ZA) along the 12 years of exposure was quite similar. In this case, the surface of both the bare S/Z and the S/ZA sheets remained active up to the end of the test exposure with potential values ranging between −1.04 V/SCE and −1.00 V/SCE, which are characteristics of these metals under free corrosion processes. [54]. The continuous electrochemical reactivity was attributed to the rain runoff effect on the corrosion products, which avoided the formation of an oxide, hydroxide, and/or passive protective layer on the bare surfaces.

These data are in accordance not only with the visual inspection but also with the results obtained elsewhere [55] by optic and electronic microscopy techniques, which put in evidence a developed corrosion process. The surface had hollows and corrosion products characterized as oxides and basic carbonates. On the other hand, the 55%Al-Zn alloy had a big cathodic area where the metals exposed to the atmosphere will corrode by coupling with the oxygen cathodic reduction reaction:

$$O_2 + 2H_2O + 4e^- \longrightarrow 4OH^- \quad (1)$$

although when the level of contamination with acid products is high, the hydrogen evolution gets importance as cathodic reaction:

$$2H^+ + 2e^- \longrightarrow H_2 \quad (2)$$

regardless of which reaction prevails, the pH on the cathodic region increases. From a certain level of acidity, it is possible that the SO_2 of a polluted atmosphere acts as an oxidant able to impart a great acceleration to the cathodic process.

The impedance spectra of the coating Zn (Figure 9) may be interpreted in terms of the corrosion products film

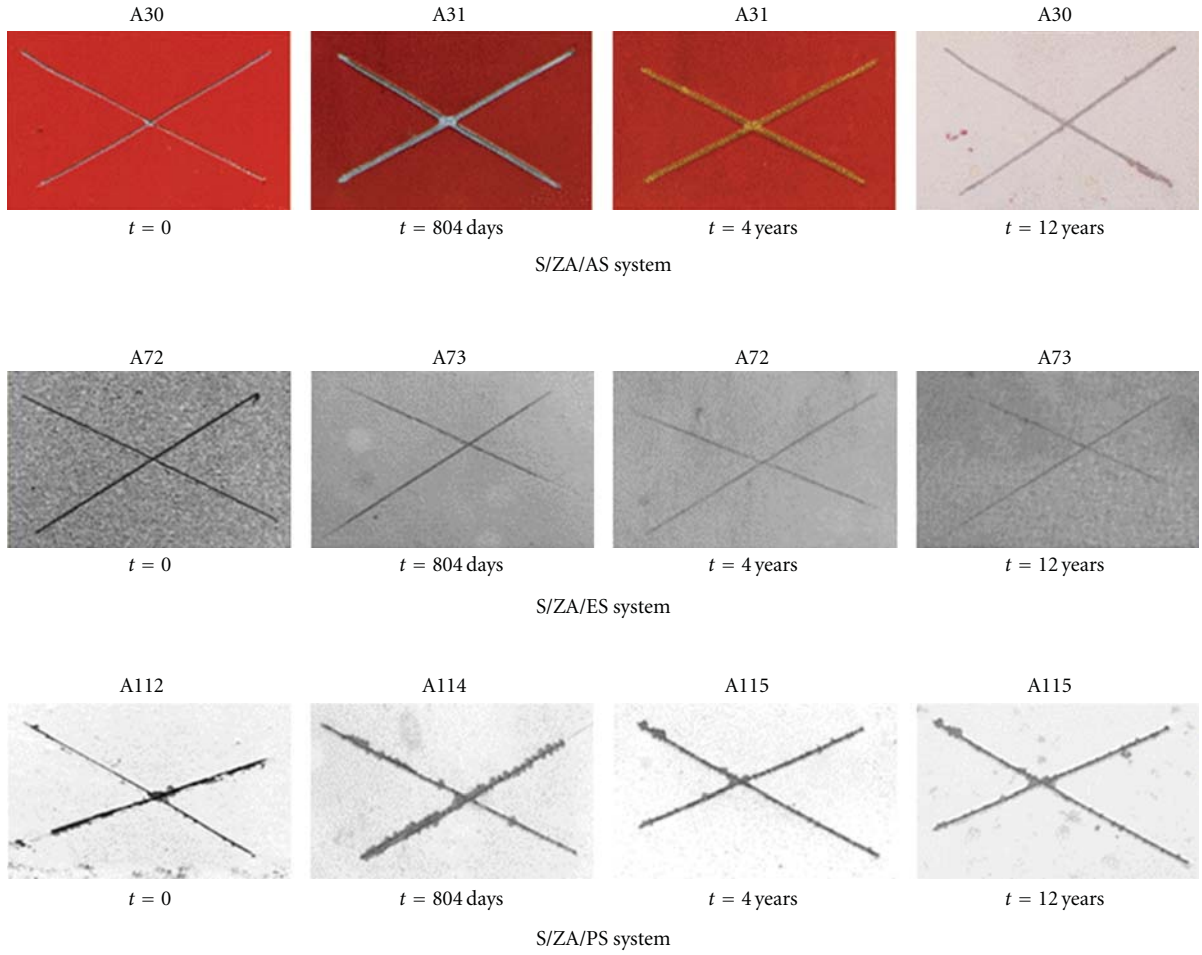

Figure 6: Photographs showing the evolution of S/ZA/painting systems as a function of the exposure time.

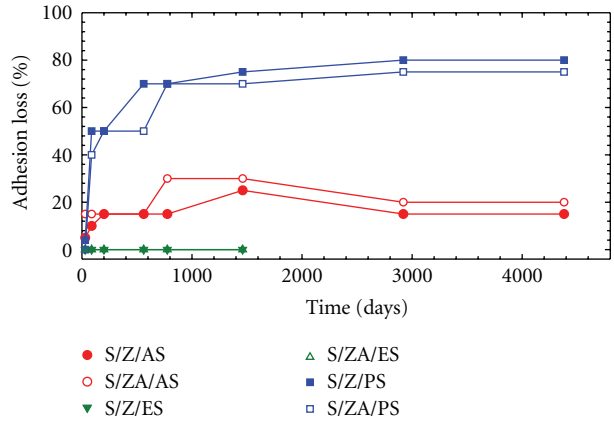

Figure 7: Plots showing the time dependence of the adhesion loss suffered by the painted S/Z and S/ZA sheets.

structure that is usually formed on the surface. The first time constant (R_1C_1) may be linked with the compact inner layer of ZnO and the second one (R_2C_2) with the external and porous layer of $Zn_4CO_3(OH)_6 \cdot H_2O$ [55, 56]. This surface film seems to inhibit further metal dissolution, although the environmental conditions determine the extent of corrosion progress due to a competition between film formation and film removal reactions. It was found that data of zinc corrosion measurements correlate with the air pollution levels given as a function of the SO_2 and Cl^- concentrations [57].

For similar exposure conditions, the influence of the coating composition on the bare sheet impedance values is shown in Figure 10. In it can be seen that the charge transfer

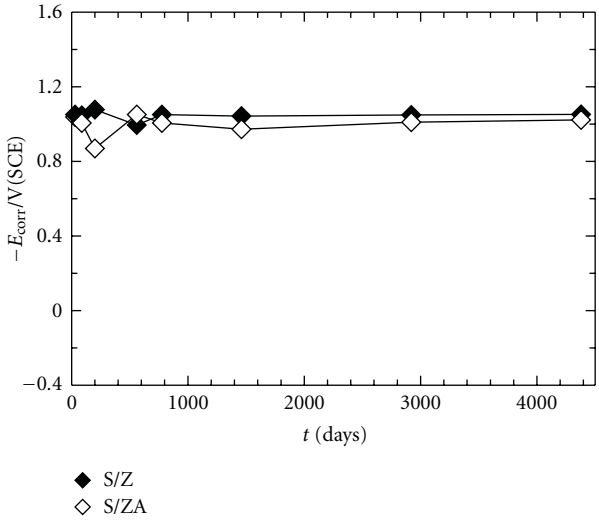

Figure 8: Plots showing the time dependence of the E_{corr} values of bare S/Z and S/ZA sheets as a function of the exposure time.

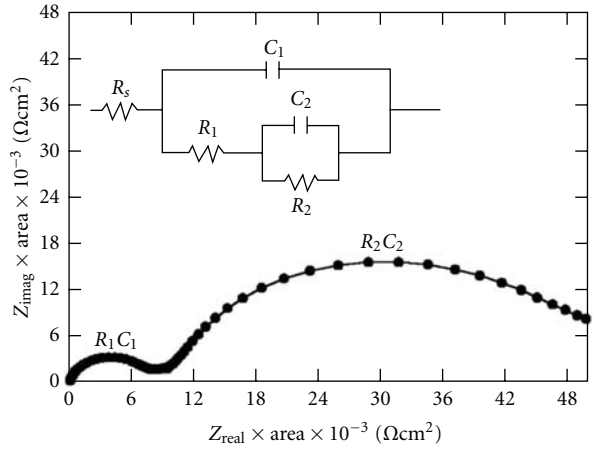

Figure 9: Equivalent circuit model used for fitting the tested bare S/Z and S/ZA sheets.

resistance (R_1) values shown by the 55%Al-Zn alloy was slightly higher than that of the zinc layer but the resistive contribution (R_2) of the external and porous layer to the system total impedance was very similar. These results are in accordance with the electrochemical activation demonstrated by both metallic surfaces.

3.2.2. Corrosion Potential and Impedance Results for Painted S/Z and S/ZA Sheets. Rest or corrosion potential (E_{corr}) measurements for painted metals and their time dependence have been questioned with regard to their use as a technique for evaluating the anticorrosive resistance of organic coatings [58]. However, its changes as a function of the exposure time to aqueous media have been successfully used as a simple tool to study the corrosion protection afforded by organic coatings [59–62]. Depending upon the microstructure of the paint coating, especially its polymerization degree, a certain period elapses until electrolyte penetration channels are established through which the underlying metal comes into contact with the medium. So, it is not surprising that, when a compact structure and high crosslinking level are accompanied by an also high film thickness, a few days of testing is not enough time for the electrolyte to enter in contact with the base metal of coated specimens, form the electrochemical double layer, and enable the measurement of a corrosion potential.

Figure 11 shows the corrosion potential (E_{corr}) values measured for each coated steel sheet exposed to the natural atmosphere of La Plata station. As can be seen, the E_{corr} values measured almost from the beginning and up to the end of the test for S/Z/AS, S/ZA/AS, S/Z/ES, and S/ZA/ES were quite similar to those obtained for the bare S/Z and S/ZA sheets (between −0.9 and −1.1 V/SCE). This means that, at least from the thermodynamic point of view, the protective properties offered by the alkyd- and epoxy-based painting systems were not sufficiently effective as to avoid the onset of the underlying zinc or 55%Al-Zn corrosion. On the other hand, the polyurethane-based painting system offered

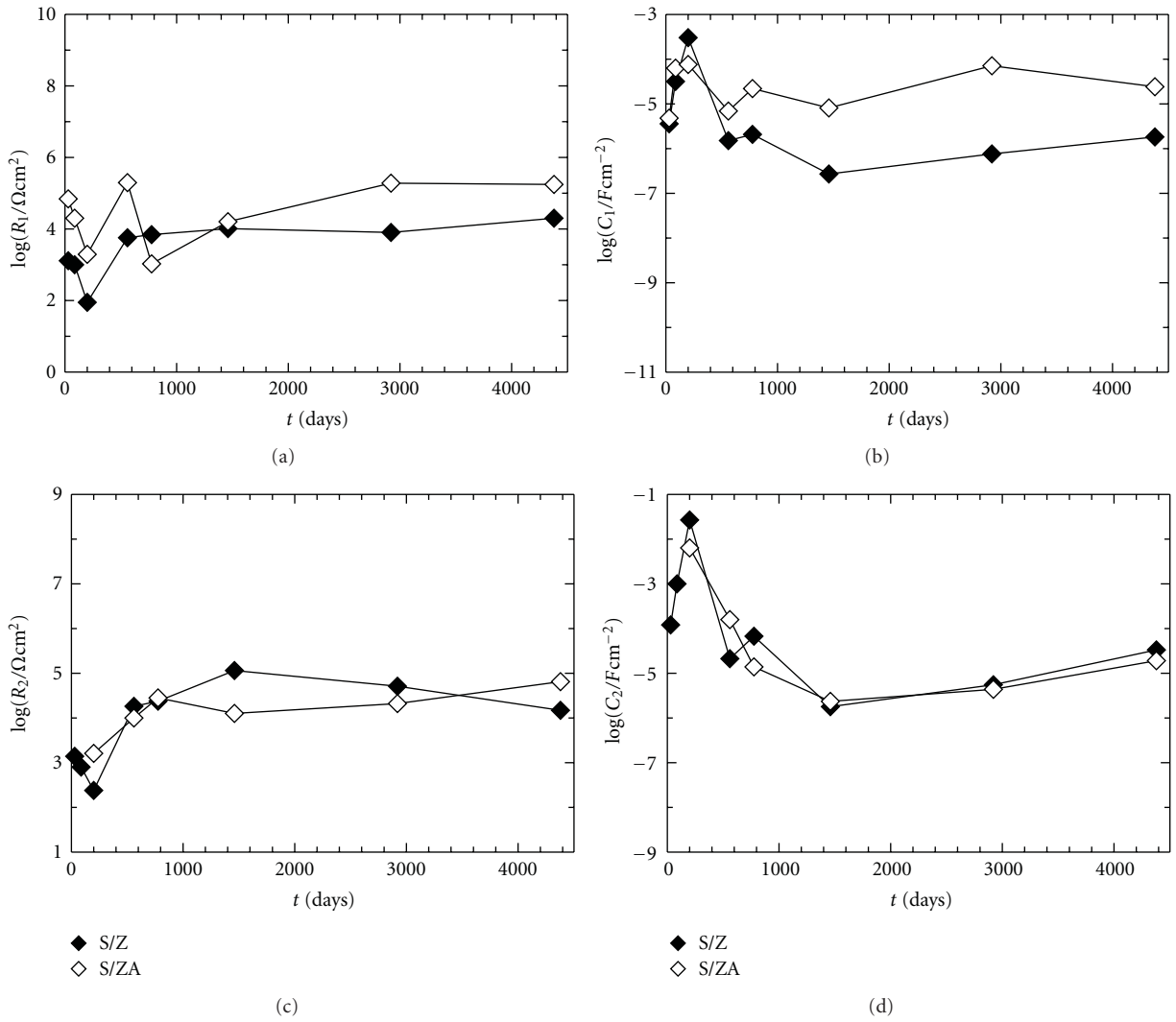

Figure 10: Evolution of log R_1, log C_1, log R_2, and log C_2 parameters of the tested bare S/Z and S/ZA sheets.

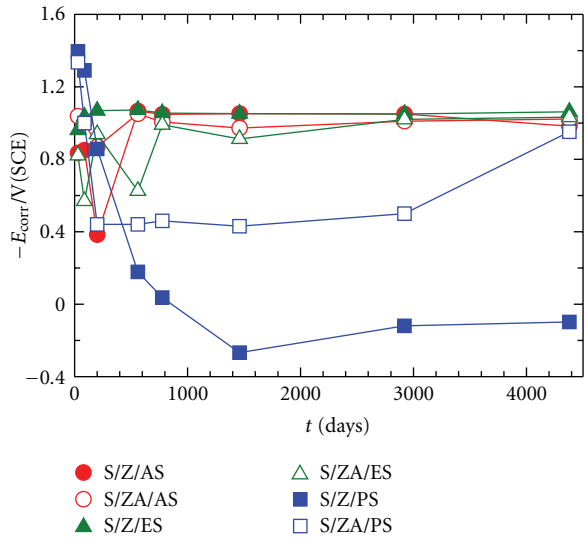

Figure 11: Plots showing the time dependence of the E_{corr} values of painted S/Z and S/ZA sheets as a function of the exposure time.

much more promising protective properties, particularly when applied on S/Z sheets, since the S/Z/PS system potential values remained in an electrochemically passive zone. A similar performance was supplied by the S/ZA/PS up to almost reaching the 12 years of exposure where together with the measurement of an $E_{corr} \approx -1.00$ V/SCE, the first sign of a localized corrosion was detected by EIS.

Since the main difference among the S/Z/painting systems and S/ZA/painting systems was the applied paint formulation used in each case, it is assumed that the magnitude of the E_{corr} displacements may be particularly associated with both the relative easiness with which the climatic variables affect the paint film structure and, hence, its protective properties. However, and it will be discussed in the next paragraph, except in the case of the epoxy-based painting system, the other two were able to protect relatively (AS) and effectively (PS) the metallic substrate from the corrosive atmosphere. This conclusion arises from the fact that the corrosion potential values measured for the S/Z/PS and S/ZA/PS panels were mostly nobler than the corresponding to bare S/Z or S/ZA sheets subjected to the same experimental conditions. This effective protection was mainly attributed to the PS barrier painting system, which could resist the strong aggressive action coming from the atmospheric conditions.

The impedance modulus ($|Z|$) of replicated samples as a function of their exposure time to the natural atmosphere of La Plata station illustrates Figure 12. A fast and simple qualitative analysis of this figure allows to infer that both the shape of all the experimental diagrams was fairly similar and it is possible to presume the presence of at least two time constants, one at low frequencies and another at high frequencies.

As seen in Figure 12, all the tested systems showed changes more or less significant of their ($|Z|$) and phase angle (Theta) during the weathering period. The fluctuating impedance values can be attributed to the dynamic behavior of the painting system structure frequently subjected to wet/dry cycles and/or other climatic changes as well as of the metal/paint interface through which the corrosion products gathered at the bottom and/or within the coating defects enhanced the coating barrier protection and, therefore, contribute to an increase in the impedance of the protective system at medium and low frequencies; however, as the time elapses, new defects appear at the weaker (less protective areas) paint layer allowing the inducing corrosion species permeation, and, consequently, the development of new electrochemically active zones.

The fact that the initial substrate attack is localized could be ascribed to the presence of very small defects in the paint layer, which act as an electrical shunt. As the exposure time goes on, the equilibrium between the development rate of the corrosion products and their diffusion rate towards the outdoor medium may be reached and, consequently, the total impedance fluctuations become small.

(1) *Equivalent Circuit Models.* The painting system as well as the S/Z or S/ZA substrates deterioration takes place from processes having a complex nature. Consequently, to interpret and explain in electrochemical terms the time dependence of the acquired impedance data, it has been necessary to propose appropriate equivalent circuit models.

Impedance spectra provide useful information concerning the evolution of both the protective features of the organic coating and the kinetics of the underlying metallic substrate corrosion process as a function of the exposure time to experimental or real service conditions. Thus, the dynamic character of the painting system barrier properties, the anticorrosive action of specific pigments, the corrosion products formation, and also changes in the disbonded area are accounted for the time dependence of the coated steel/medium impedance spectra. In general, an explanation of why and how such changes take place can be given by associating them to the resistive and capacitive parameters derived from fitting impedance data with nonlinear least squares algorithms involving the transfer function of the equivalent circuit model shown in Figure 13, [63–67]. They represent the parallel and/or series connection of some resistors and capacitors, simulating a heterogeneous arrangement of electrolytically conducting paths, where R represents the electrolyte resistance between the reference and working (coated steel) electrodes, R_c (resistance to the ionic flux) describes paths (pores, low crosslinking) of lower resistance to the electrolyte diffusion short-circuiting the paint film, and C_c is the dielectric capacitance representing the intact part of the same paint film [68]. Once the permeating and corrosion-inducing chemicals (water, oxygen and ionic species) reach electrochemically active areas of the substrate, particularly at the bottom of the paint film defects, the metallic corrosion become to be measurable so that its associated parameters, the electrochemical double-layer capacitance, C_{dl}, and the charge transfer resistance, R_t, can be estimated. It is important to remark that the values of these parameters vary direct (C_{dl}) and inversely (R_t) with the size of the corroding area.

On the other hand, distortions observed in these resistive-capacitive contributions indicate a deviation from the theoretical models in terms of a time constants distribution due to either lateral penetration of the electrolyte at the steel/paint interface (usually started at the base of intrinsic or artificial coating defects), underlying metallic substrate surface heterogeneity (topological, chemical composition, surface energy), and/or diffusion processes that could take place along the test [69, 70]. Since all these factors make the impedance/frequency relationship nonlinear, they are taken into consideration by replacing one or more capacitive components (C_i) of the equivalent circuit transfer function by the corresponding constant phase element Q_i (CPE), whose impedance dispersion relation is given by $Z = (j\omega)^{-n}/Y_0$ and n = CPE power = $\alpha/(\pi/2)$ [32, 71].

Difficulties in providing an accurate physical description of the occurred processes are sometimes found. In such cases, a standard deviation value ($\chi^2 < 5 \times 10^{-4}$) between experimental and fitted impedance data may be used as final criterion to define the most probable circuit.

According to the impedance data dispersion, the fitting process was performed using either the dielectric capacitance C_i or the phase constant element Q_i; however, the C_i

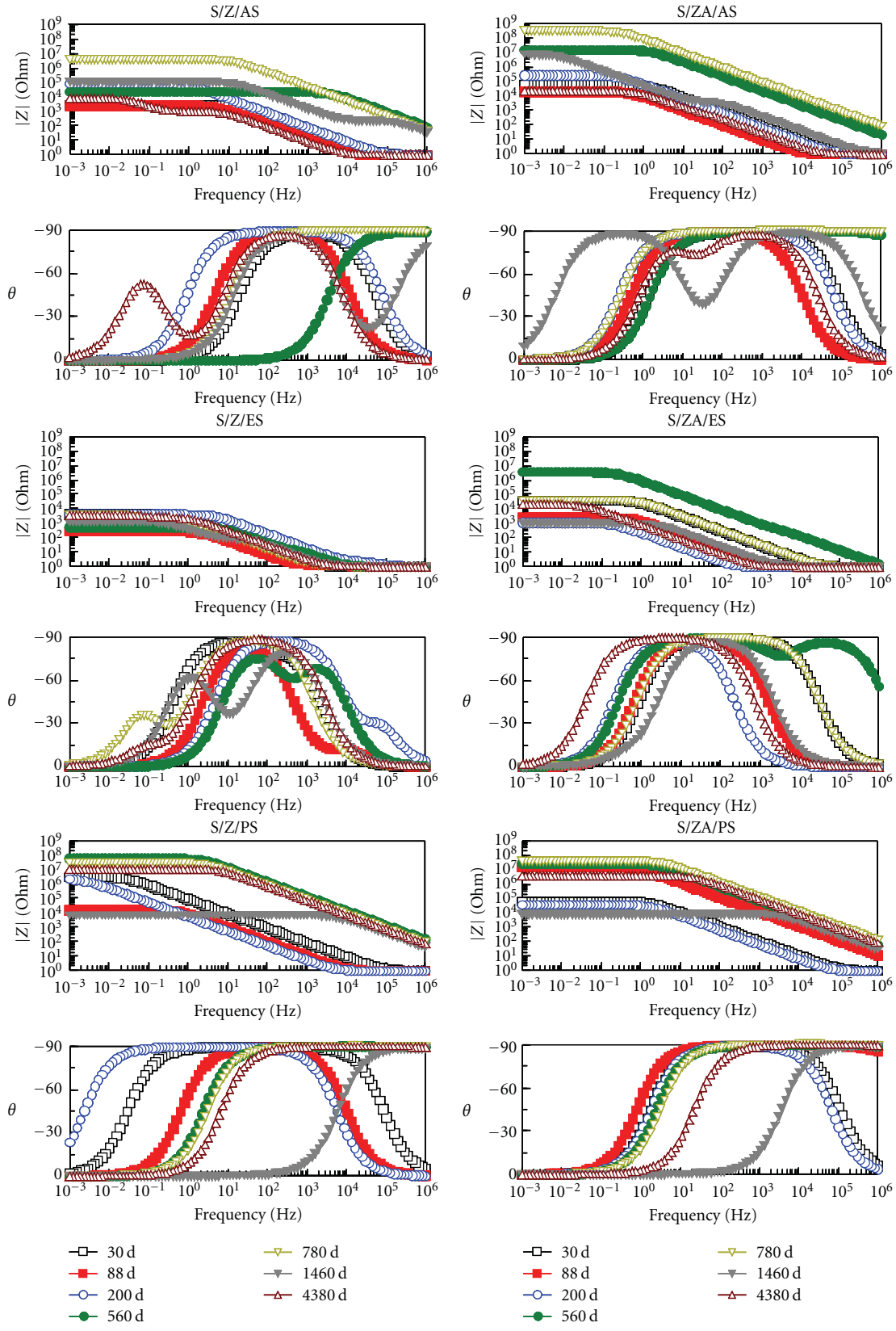

Figure 12: Bode plots showing the time dependence of the duplex systems impedance during their exposure to the natural atmosphere of La Plata station for 12 years.

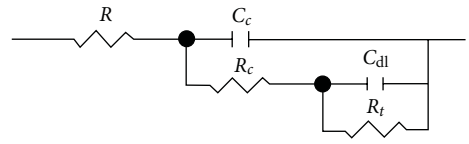

Figure 13: Equivalent circuit model used for fitting the tested duplex systems.

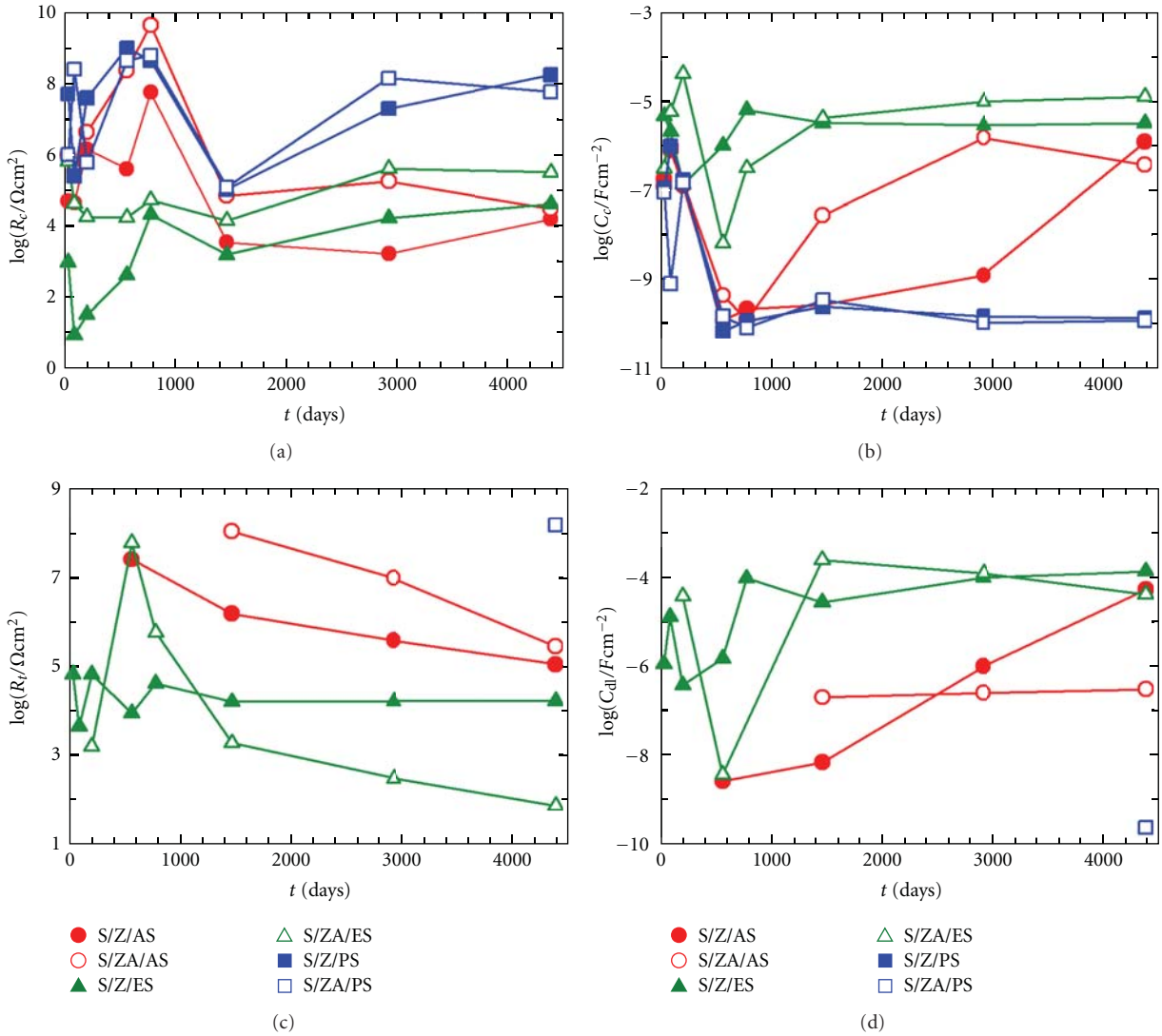

Figure 14: Evolution of R_c, C_c, R_t, and C_{dl} parameters of the duplex systems impedance during their exposure to the natural atmosphere of La Plata station for 12 years.

parameter was used in the following plots to facilitate the results visualization and interpretation.

(2) *Time Dependence of the Impedance Resistive and Capacitive Components.* The values of the resistive and capacitive components of the impedance corresponding to all the painted samples exposed to the natural atmosphere of La Plata station for 12 years are shown in Figure 14. As seen, the S/Z/PS and S/ZA/PS samples offered an excellent anticorrosive performance up to the end of the exposure. This behavior could be attributed to its excellent barrier effect due to the structurally homogeneous and strong paint film ($R_c \approx 10^7$–$10^8\,\Omega\text{cm}^2$, $C_c \approx 10^{-10}$–$10^{-9}\,\text{Fcm}^{-2}$), which was able to counteract the significant adhesion loss suffered by this painting system during weathering and slowed down the development of the alloy coating corrosion process up to the end of the exposure.

For the other two sample types, a rather highly fluctuating R_c values (two or more orders of magnitude) were found within the first 1400 days of exposure but then, and

up to the end of the test, they remained changing between 10^6–$10^4\,\Omega\text{cm}^2$; on the other hand, its coupled dielectric capacitance (C_c) followed the same unstable trend at the beginning of the test but then, due to the deterioration degree reached by the AS and ES painting systems as a consequence of the adverse climatic conditions, led to C_c values ($\approx 10^{-6}$–$10^{-5}\,\text{Fcm}^{-2}$), that is, close to the bare S/Z and S/ZA sheets.

On the other hand, the same Figure shows great differences in the electrochemical response (R_tC_{dl}) of the different systems. In the case of the polyurethane systems, the corrosion process was either absent (S/Z/PS) or at least its development was delayed up to the end of exposure (S/ZA/PS). On the contrary, for the rest of the considered duplex systems after variable induction periods, the metallic coating degradation was detected. The worst corrosion protection was afforded by the Epoxy-based painting system since the corrosion process was detected by EIS at 30 (S/Z/ES) and 200 (S/ZA/ES) days. This behavior would be ascribed to the different electrochemical reactivity of the Z and ZA coatings. In the case of the Alkyd system, the induction period was of 600 and 1400 days for S/Z/As and S/ZA/AS, respectively. Again, the better performance of the last system could be accredited to a relatively good, although too short for practice purposes, barrier effect offered by the paint film added to the lower electrochemical reactivity of the S/ZA sheet.

4. Conclusions

At the end of this work, it is possible to summarize some conclusions valid for the studied materials.

All the laboratory and field tests involved in this work were useful to understand the behavior of the studied duplex systems subjected to natural weathering at La Plata Station. The good correlation between visual inspection and electrochemical tests allowed explaining some troubles observed in practice and, on this base, contribute to solve them to maintain its useful life as long as possible.

An almost constant corrosion rate of bare zinc and zinc-aluminum layers acting as galvanic coating of steel sheets was found during the long-term exposure to the natural atmosphere of the La Plata station. Both materials were able to cathodically protect the steel substrate for 12 years.

Regarding the comparative study among the three painting systems applied on S/Z or S/ZA sheets, different R_cC_c and R_tC_{dl} evolutions were obtained depending mainly on the paint. The best protective performance offered by the Polyurethane-based painting system was explained in principle taking in account its better barrier properties. The experimental results coming from the alkyd- and epoxy-based painting systems were not satisfactory due to their low resistance to the atmospheric conditions existing at La Plata station.

Despite the interface degradation (loss of adhesion) shown by all the painting systems, the corrosion process did not progress from the cross cut towards the underlying metallic substrate.

Acknowledgments

The authors thank the Comisión de Investigaciones Científicas de la Provincia de Buenos Aires (CICPBA), the Consejo Nacional de Investigaciones Científicas y Técnicas (CONICET), and the Universidad Nacional de La Plata for the financial support to carry out the present paper.

References

[1] M. Stratmann, K. Bohnenkamp, and W. J. Engell, "An electrochemical study of phase-transitions in rust layers," *Corrosion Science*, vol. 23, no. 9, pp. 969–985, 1983.

[2] L. Ferretti, E. Traverso, and G. Ventura, "Marine corrosion of mild steel in a thermically altered natural environment," *Anti-Corrosion Methods and Materials*, vol. 23, no. 5, pp. 3–5, 1976.

[3] C. E. Bird and F. J. Strauss, "Effect of wet storage staining on subsequent atmospheric corrosion of galvanized iron sheets," *Materials Performance*, vol. 15, no. 11, p. 27, 1976.

[4] F. E. Goodwin, "Mechanism of corrosion of Zinc and Zinc -5% Aluminum steel sheet coatings," in *Zinc-Based Steel Coatings Systems: Metallurgy and Performance*, G. Krauss, Ed., pp. 183–193, The Minerals, Metals & Materials Society, Warrendale, Pa, USA, 1990.

[5] M. Pourbaix, "Une méthode éléctrochimique rapide de predetermination de la corrosion atmospherique," Tech. Rep. 1, CEBELCOR, 1969.

[6] Y. Suzuki, Y. Hisamatsu, and N. Masuko, "Nature of atmospheric rust on iron," *Journal of the Electrochemical Society*, vol. 127, no. 10, pp. 2210–2214, 1980.

[7] *ASM Handbook*, vol. 13 of *Corrosion: Materials*, ASM International, 1992.

[8] J. C. Zoccola, H. E. Townsend, A. R. Borzillo, and J. B. Horton, "Atmospheric factors affecting the corrosion of engineering metals," in *Proceedings of the American Society for Testing and Materials (STP '78)*, vol. 646, pp. 165–184, 1978.

[9] F. C. Porter, *Zinc Handbook: Properties, Processing and Use in Design*, Marcel Dekker, New York, NY, USA, 1991.

[10] J. F. H. van Eijnsbergen, *Duplex Systems*, vol. 7, Elsevier, Amsterdam, The Netherlands, 1994.

[11] K. L. Mittal, "Stresses and adhesion of thin metallic coatings on oxide substrates," in *Adhesion Measurements of Film and Coatings*, K. L. Mittal, Ed., pp. 1–13, VSP, Utrecht, The Netherlands, 1995.

[12] *Steel Structure Painting Manual. Systems and Specifications*, vol. 2, Steel Structures Painting Council, Pittsburgh, Pa, USA, 7th edition, 1995.

[13] J. F. Malone, "Painting hot dip galvanized steel," *Materials Performance*, vol. 31, no. 5, pp. 39–42, 1992.

[14] C. H. Hare, "Corrosion and the preparation of metals for painting," in *Unit 26 Federation Series on Coatings Technology*, Federation of Societies for Coatings Technology, Philadelphia, Pa, USA, 1978.

[15] K. W. Allen, *Strength and Structures. Aspect of Adhesion*, vol. 1, University Press of London, London, UK, 1965.

[16] T. R. Bullet and A. T. S. Rudram, "The coating and the substrate," *Journal of the Oil and Colour Chemists' Association*, vol. 44, pp. 787–807, 1961.

[17] C. H. Hare, *Good Painting Practice. Steel Structure Painting Manual*, Steel Structures Painting Council, Pittsburgh, Pa, USA, 3rd edition, 1995.

[18] R. Barnhart, D. Mericle, Ch. Mobley, T. Hocking, J. H. Bogran, and E. McDaniel, "Why surface preparation is important?"

Journal of Protective Coatings and Linings, vol. 14, no. 9, pp. 61–64, 1997.

[19] H. Leidheiser Jr., "Corrosion of painted metals—a review," *Corrosion*, vol. 38, no. 7, pp. 374–383, 1982.

[20] I. Sekine, M. Yuasa, N. Hirose, and T. Tanaki, "Degradation evaluation of corrosion protective coatings by electrochemical, physicochemical and physical measurements," *Progress in Organic Coatings*, vol. 45, no. 1, pp. 1–13, 2002.

[21] G. Rocchini, "The importance of choosing the correct electrochemical technique for evaluating corrosion rates," *Corrosion Prevention and Control*, vol. 48, no. 4, pp. 125–134, 2001.

[22] S. Maeda, "Surface chemistry of galvanized steel sheets relevant to adhesion performance," *Progress in Organic Coatings*, vol. 28, no. 4, pp. 227–238, 1996.

[23] R. L. Howard, I. M. Zin, J. D. Scantlebury, and S. B. Lyon, "Inhibition of cut edge corrosion of coil-coated architectural cladding," *Progress in Organic Coatings*, vol. 37, no. 1, pp. 83–90, 1999.

[24] R. L. Howard, S. B. Lyon, and J. D. Scantlebury, "Accelerated tests for the prediction of cut-edge corrosion of coil-coated architectural cladding. Part I: cyclic cabinet salt spray," *Progress in Organic Coatings*, vol. 37, no. 1, pp. 91–98, 1999.

[25] R. L. Howard, S. B. Lyon, and J. D. Scantlebury, "Accelerated tests for prediction of cut edge corrosion of coil-coated architectural cladding. Part II: cyclic immersion," *Progress in Organic Coatings*, vol. 37, no. 1, pp. 99–105, 1999.

[26] S. Feliu, V. Barranco, and S. Feliu, "Contradictory results of the UVCON and saline immersion tests regarding the evaluation of some inhibitor/lacquer combinations on galvanised coatings," *Progress in Organic Coatings*, vol. 50, no. 3, pp. 199–206, 2004.

[27] A. R. di Sarli and R. A. Armas, "An assessment of the anticorrosive properties of epoxy paints. Correlation between impedance measurements and the salt-spray cabinet test," *Corrosion Prevention & Control*, vol. 36, no. 5, pp. 127–131, 1989.

[28] P. R. Seré, J. D. Culcasi, C. I. Elsner, and A. R. Di Sarli, "Study of the corrosion process at the galvanized steel/organic coating interface," in *Proceedings of the SCANNING '98*, vol. 20, no. 3, pp. 274–275, Baltimore, Md, USA, 1998.

[29] B. M. Rosales, A. R. di Sarli, F. Fragata et al., "PATINA network—performance of coil coating in natural atmospheres of Ibero-America," *Revista de Metalurgia*, vol. Extra, pp. 201–205, 2003.

[30] B. M. Rosales, A. R. di Sarli, O. de Rincón, A. Rincón, C. I. Elsner, and B. Marchisio, "An evaluation of coil coating formulations in marine environments," *Progress in Organic Coatings*, vol. 50, no. 2, pp. 105–114, 2004.

[31] B. Del Amo, L. Véleva, C. I. Elsner, and A. R. di Sarli, "Performance of coated steel systems exposed to different media: part I. Painted galvanized steel," *Progress in Organic Coatings*, vol. 50, no. 3, pp. 179–192, 2004.

[32] B. A. Boukamp, *Report CT88/265/128, CT89/214/128*, University of Twente, Amsterdam, The Netherlands, 1989.

[33] E. V. Schmid, *Exterior Durability of Organic Coatings*, FMJ International Publications, Redhill, UK, 1988.

[34] S. C. Chung, A. S. Lin, J. R. Chang, and H. C. Shih, "EXAFS study of atmospheric corrosion products on zinc at the initial stage," *Corrosion Science*, vol. 42, no. 9, pp. 1599–1610, 2000.

[35] Q. Qu, C. Yan, Y. Wan, and C. Cao, "Effects of NaCl and SO_2 on the initial atmospheric corrosion of zinc," *Corrosion Science*, vol. 44, no. 12, pp. 2789–2803, 2002.

[36] J. Morales, S. Martín-Krijer, F. Díaz, J. Hernández-Borges, and S. González, "Atmospheric corrosion in subtropical areas: influences of time of wetness and deficiency of the ISO 9223 norm," *Corrosion Science*, vol. 47, no. 8, pp. 2005–2019, 2005.

[37] V. Kucera and E. Mattsson, *Corrosion Mechanisms*, Marcel Dekker, New York, NY, USA, 1987.

[38] T. E. Graedel, "Corrosion mechanisms for zinc exposed to the atmosphere," *Journal of the Electrochemical Society*, vol. 136, no. 4, pp. 193C–203C, 1989.

[39] X. G. Zhang, *Corrosion and Electrochemistry of Zinc*, Plenum Press, New York, NY, USA, 1996.

[40] F. Mansfeld, *Corrosion Mechanisms*, Marcel Dekker, New York, NY, USA, 1987.

[41] H. E. Townsend, L. Allegra, R. J. Dutton, and S. A. Kriner, "Hot-dip coated sheet steels—a review," *Materials Performance*, vol. 25, no. 8, pp. 36–46, 1986.

[42] H. E. Townsend and A. R. Borzillo, "Twenty-year atmospheric corrosion tests of hot-dip coated sheet steel," *Materials Performance*, vol. 26, no. 7, pp. 37–41, 1987.

[43] J. W. Spence, F. H. Haynie, F. W. Lipfert, S. D. Cramer, and L. G. McDonald, "Atmospheric corrosion model for galvanized steel structures," *Corrosion*, vol. 48, no. 12, pp. 1009–1019, 1992.

[44] I. W. Odnevall Wallinder, P. Verbiest, W. He, and C. Leygraf, "Effects of exposure direction and inclination of the runoff rates of zinc and copper roofs," *Corrosion Science*, vol. 42, no. 8, pp. 1471–1487, 2000.

[45] S. Bertling, I. Odnevall, C. Leygraf, and D. Berggren, "Environmental effects of zinc runoff from roofing materials- A new multidisciplinary approach," in *Outdoor Atmospheric Corrosion, ASTM STP 1421*, H. E. Townsend, Ed., pp. 200–215, American Society for Testing and Materials International, West Conshohocken, Pa, USA, 2002.

[46] W. He, I. Odnevall, and C. Leygraf, "Runoff rates of zinc—a four-year field and laboratory study," in *Outdoor Atmospheric Corrosion, ASTM STP 1421*, H. E. Townsend, Ed., pp. 216–229, American Society for Testing and Materials International, West Conshohocken, Pa, USA, 2002.

[47] J. H. Sullivan and D. A. Worsley, "Zinc runoff from galvanised steel materials exposed in industrial/marine environment," *British Corrosion Journal*, vol. 39, no. 4, pp. 282–288, 2002.

[48] S. Matthes, S. Cramer, S. Bullard, B. Covino, and G. Holcomb, "Atmospheric corrosion and precipitation runoff from zinc and zinc alloy surfaces," in *Proceedings of the 58th Annual Conference Corrosion*, NACE, 2003, Paper 03598.

[49] S. Jouen, B. Hannoyer, A. Barbier, J. Kasperek, and M. Jean, "A comparison of runoff rates between Cu, Ni, Sn and Zn in the first steps of exposition in a French industrial atmosphere," *Materials Chemistry and Physics*, vol. 85, no. 1, pp. 73–78, 2004.

[50] D. Reiss, B. Rihm, C. Thöni, and M. Faller, "Mapping stock at risk and release of zinc and copper in Switzerland-dose response functions for runoff rates derived from corrosion rate data," *Water, Air, and Soil Pollution*, vol. 159, no. 1, pp. 101–113, 2004.

[51] R. M. Kain and E. A. Baker, *ASTM STP 947*, ASTM, Philadelphia, Pa, USA, 1986.

[52] S. H. Zhang and S. B. Lyon, "The electrochemistry of iron, zinc and copper in thin layer electrolytes," *Corrosion Science*, vol. 35, no. 1–4, pp. 713–718, 1993.

[53] A. Meneses Garcia, J. Rodarte Corro, O. Vidal Gutierrez, and E. Gonzalez Guzman, "The Mexican National Cancer Institute: case report," *Revista del Instituto Nacional de Cancerologia*, vol. 36, no. 4, pp. 1179–1182, 1990.

[54] M. Pourbaix, *Atlas of Electrochemical Equilibria in Aqueous Solutions*, NACE, Houston, Tex, USA, 1974.

[55] E. A. Sacco, J. D. Culcasi, C. I. Elsner, and A. R. di Sarli, "Evaluation of the protective performance of several duplex systems exposed to industrial atmosphere," *Latin American Applied Research*, vol. 32, no. 4, pp. 307–311, 2002.
[56] J. M. Costa and M. Vilarrasa, "Effect of air pollution on atmospheric corrosion of zinc," *British Corrosion Journal*, vol. 28, no. 2, pp. 117–120, 1993.
[57] M. W. Kendig, A. T. Allen, and F. Mansfeld, "Optimized collection of ac impedance data," *Journal of the Electrochemical Society*, vol. 131, no. 4, pp. 935–936, 1984.
[58] J. Wolstenholme, "Electrochemical methods of assessing the corrosion of painted metals-a review," *Corrosion Science*, vol. 13, no. 7, pp. 521–530, 1973.
[59] R. A. Armas, C. Gervasi, A. R. di Sarli, S. G. Real, and J. R. Vilche, "Zinc-rich paints on steels in artificial seawater by electrochemical impedance spectroscopy," *Corrosion*, vol. 48, no. 5, pp. 379–383, 1992.
[60] J. E. O. Mayne, "The mechanism of the inhibition of the corrosion of iron and steel by means of paint," *Official Digest*, vol. 24, pp. 127–136, 1952.
[61] L. Meszáros and S. A. Lindquist, "Study of the performance of zinc-rich paints coatings," in *Proceedings of the 115th Event of the European Federation of Corrosion (EUROCORR '82)*, pp. 147–156, Budapest, Hungary, October 1982, Section 11.
[62] M. Morcillo, R. Barajas, S. Feliu, and J. M. Bastidas, "A SEM study on the galvanic protection of zinc-rich paints," *Journal of Materials Science*, vol. 25, no. 5, pp. 2441–2446, 1990.
[63] B. del Amo, L. Véleva, A. R. di Sarli, and C. I. Elsner, "Performance of coated steel systems exposed to different media: part I. Painted galvanized steel," *Progress in Organic Coatings*, vol. 50, no. 3, pp. 179–192, 2004.
[64] O. Ferraz, E. Cavalcanti, and A. R. di Sarli, "The characterization of protective properties for some naval steel/polimeric coating/3% NaCl solution systems by EIS and visual assessment," *Corrosion Science*, vol. 37, no. 8, pp. 1267–1280, 1995.
[65] P. R. Seré, D. M. Santágata, C. I. Elsner, and A. R. di Sarli, "The influence of the method of application of the paint on the corrosion of the substrate as assessed by ASTM and electrochemical method," *Surface Coatings International*, vol. 81, no. 3, pp. 128–134, 1998.
[66] D. M. Santágata, P. R. Seré, C. I. Elsner, and A. R. di Sarli, "Evaluation of the surface treatment effect on the corrosion performance of paint coated carbon steel," *Progress in Organic Coatings*, vol. 33, no. 1, pp. 44–54, 1998.
[67] P. R. Seré, A. R. Armas, C. I. Elsner, and A. R. di Sarli, "The surface condition effect on adhesion and corrosion resistance of carbon steel/chlorinated rubber/artificial sea water systems," *Corrosion Science*, vol. 38, no. 6, pp. 853–866, 1996.
[68] H. Leidheiser Jr. and M. W. Kendig, "Mechanism of corrosion of polybutadiene-coated steel in aerated sodium chloride," *Corrosion*, vol. 32, no. 2, pp. 69–75, 1976.
[69] T. Szauer and A. Brandt, "Impedance measurements on zinc-rich paints," *Journal of the Oil and Colour Chemists' Association*, vol. 67, pp. 13–17, 1984.
[70] D. J. Frydrych, G. C. Farrington, and H. E. Townsend, "The barrier properties of thin carbonaceous films formed by ion beam assisted deposition," in *Corrosion Protection by Organic Coatings*, M. W. Kendig and H. Leidheiser Jr., Eds., vol. 87-2, p. 240, The Electrochemical Society, Pennington, NJ, USA, 1987.
[71] E. P. M. van Westing, G. M. Ferrari, F. M. Geenen, and J. H. W. van de Wit, "In situ determination of the loss of adhesion of barrier epoxy coatings using electrochemical impedance spectroscopy," *Progress in Organic Coatings*, vol. 23, no. 1, pp. 89–103, 1993.

Hindawi Publishing Corporation
International Journal of Corrosion
Volume 2012, Article ID 318279, 11 pages
doi:10.1155/2012/318279

Research Article

Six-Year Evaluation of Thermal-Sprayed Coating of Zn/Al in Tropical Marine Environments

Orlando Salas, Oladis Troconis de Rincón, Daniela Rojas, Adriana Tosaya, Nathalie Romero, Miguel Sánchez, and William Campos

Centro de Estudios de Corrosión, Facultad de Ingeniería, Universidad del Zulia, Maracaibo, Zulia, Venezuela

Correspondence should be addressed to Oladis Troconis de Rincón, oladis1@yahoo.com

Received 27 May 2011; Revised 12 August 2011; Accepted 10 September 2011

Academic Editor: Blanca M. Rosales

The main objective of this research was to evaluate the performance of thermal-sprayed coating of Zn/Al (double layer) after six years of exposure, with and without the use of sealant (wash primer) in tropical marine environments of very high aggressiveness: La Voz Station (located at the Peninsula de Paraguaná/Falcón State) and Lake Maracaibo Crossing Station (located at Zulia State), in Venezuela. To that effect, carbon steel coupons (100 mm × 150 mm × 2 mm) were sprayed by flame process. The coupons were characterized by means of initial weight, thickness, metallographic, adherence, and roughness, being evaluated monthly by visual inspection during six years. After removal, the coupons were evaluated by microscopic analysis to determine the morphology of attack, microstructure, penetration of contaminants, composition, and morphology of corrosion products. The results showed that after six years, the double-layer system represents an excellent choice for corrosion protection of steel by combining the galvanic protection of zinc with the erosion resistance of aluminum. However, due to the erosion-corrosion effect, a sealant such as wash primer can be used in order to extend its service life.

1. Introduction

Worldwide, many organizations have made numerous efforts in terms of studies and research looking for new coating systems to improve the durability of structures exposed to marine and coastal marine environments, providing protection to the steel during its service life and producing a minimal impact on the environment. In marine and coastal marine environments, where a number of factors are present such as high-chloride concentrations, strong winds, changing conditions of relative humidity and temperature (especially in tropical climates like Venezuela), organic coatings do not perform properly. In this regard, thermal-sprayed coatings appear as an alternative to protect steel structures in those environments. In the United States, Europe, and Japan [1, 2], these coatings are gaining importance for their promising low environmental impact, corrosion resistance, cost benefits, durability, and other advantages over other conventional paint systems.

In 1974, the American Welding Society [3] performed a study that was considered a pioneer in thermal sprayed coating where it reported that these coatings with Zn and Al, with and without sealer, exposed in marine and industrial environments, provided protection against corrosion for 19 years. Moreover, in 1987, the Laque Center for Corrosion Technology, INC. [4] reported that the degree of protection of the coatings, after 34 years of continuous exposure in a moderately aggressive marine atmosphere, varies considerably with alloy content, type of material applied, and method of application. They also highlighted that the best thermal sprayed system is given by the coating of Zn/Al, double layer, and Zn/Al alloy (with a higher content of aluminum).

In tropical marine environments, for example, Venezuela, little is known about the application and performance of this coating technology. Venezuela's environment is completely different from the above-mentioned places given the high incidence of winds, high temperatures, and relative humidity during all the year. Only the PATINA Network [5] is known to have studied the effect of these environments on coating systems. In it, the behavior under corrosion of a wide variety of conventional and new generation coatings in the atmospheres of the Ibero-American region

Table 1: Characterization of coating system [10].

Coating	Thickness (μm)	Adhesion (MPa)	Porosity (%)		Anchor profile (μm)
Zn/Al by flame process	215.9–469.9	2.90	23 (Zn)	8 (Al)	37.85 ± 4.01

was evaluated. The performance of metal-based sacrificial coatings (aluminum, zinc and their alloys, among them thermal sprayed aluminum and Zn/15Al with vinyl sealer and wash primer) was also evaluated. The Zn/15Al with sealer gave the best performance in the atmosphere at La Voz. Recent research [6–13] in Venezuela (at Centro de Estudios de Corrosión, Faculty of Engineering, Universidad del Zulia) on thermal sprayed coatings with different materials (Zn, Al, Zn/85Al, and Zn/Al Double Layer) applied by two processes (flame and electric arc) with and without the use of different sealants (wash primer 1, wash primer 2, phenolic, and polyurethane), indicates that thermal sprayed coatings applied with only zinc or aluminum do not provide adequate protection in the exposure environments evaluated. However, the Zn/Al double-layer system has performed excellently in comparison with other thermal-sprayed systems. This coating system represents one of the best options for countering these aggressive environments. This paper presents the results after six years of evaluation.

2. Experimental Procedure

2.1. Preparing the Coupons [6–10]

2.1.1. Preparing the Surface. The company applying the thermal spray coating (flame) used its own steel coupons (100 mm × 150 mm × 2 mm) and its own criteria for preparing the surface; it did not supply the latter information. Because of this, indirect measurements of the anchor profile left on the substrate were made by using optical microscopy at 200x magnification, in transversal sections in some of the coupons, sweeping and measuring the distance between the peaks and valleys left on the substrate, with an average value of the measurements being reported.

2.1.2. Coatings and Application Methods. Two systems were evaluated: (1) a dual system (Zn/Al) formed by a first coat of thermal sprayed Zn as a primer and a second coat of thermal sprayed aluminum as a top coat, applied by the flame process without sealer; (2) the same coating but with the application of two additional layers of wash primer sealer.

In each of the test stations, 5 coupons per coating were installed. Each year, one coupon per coating was removed for evaluation in the laboratory to complete the total exposure period of six years, presented in this paper.

2.2. Characterization of Coatings [6–10]. Before being set up in the test stations, the coupons were swabbed with acetone to remove any oil and grease, then, cleaned with distilled water and dried immediately with an air pistol. After cleaning, they were characterized with respect to thickness, microscopic analysis, porosity, and adhesion.

2.2.1. Thickness. This measurement was carried out in accordance with Standard ASTM D 1186 [14], using a nondestructive instrument ("constant pressure probe DFT", "gauge (type II)") that measures the dry-film thickness of nonmagnetic coatings on ferrous metallic substrates. Due to the variability of thicknesses (nonuniform thicknesses) in this type of coating even on the same coupon, it was decided to use a template with the same dimensions (100 mm × 150 mm) with ten evenly distributed orifices and located at 2 cm away from the edges so that the measurements would be always taken on the same spot.

2.2.2. Metallographic Analysis and Porosity. An optical microscope with magnifications of 200x and 400x was used to analyze microstructure and porosity as well as to verify the thickness of these coatings. Samples were prepared by means of 2.5 cm × 2.5 cm cuts and then encapsulated in Bakelite with a cupping machine. It was then surfaced with emery paper and burnished with alumina to a specular aluminum finish. Specifically, Standard ASTM E 2109-01 [15] was used to determine the percentage of porosity in the thermal sprayed coatings with an image analysis program.

2.2.3. Adhesion. Adhesion tests were run by the "Pulloff test" method of tensile strength according to ISO Standard 4624 [16]/ASTM4541 [17], using an adhesion tester.

2.2.4. Incisions. In order to evaluate the galvanic effect of the coatings, a horizontal incision of approximately 6 cm was made into each coupon to reach the metal base in the lower part; a 2 cm space was left between the incision and the lateral and lower borders for observation.

Table 1 shows a summary of the initial characterization of the coupons.

2.3. Evaluating the Coatings [6–10]

2.3.1. Visual Inspection. The coating systems were examined and photographed monthly, collecting data on registration forms. The presence or absence of corrosion products detected during these inspections indicated whether they were coating corrosion products or substrate corrosion products, both on the general surface of the coupon as well as on the edges and incisions.

2.3.2. Analysis under the Scanning Electron Microscope. After the coupons were taken out from the test stations, cuts were made in the places of interest, using a diamond-point cutter, for subsequent encapsulation in conducting Bakelite to enable the execution of the elementary chemical analyses. The chemical analyses and the morphology of the transversal area of the coatings were carried out using the Energy Dispersion Spectroscopy (EDS) technique on a PHILLIPS Model XL 30 Scanning Electron Microscope.

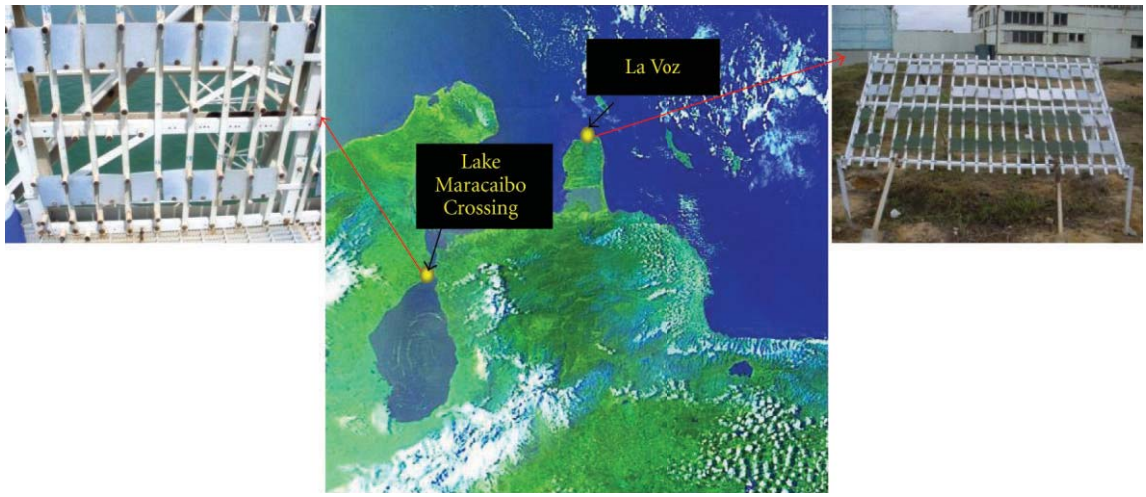

Figure 1: Geographic location of the Lake Maracaibo Crossing Station and La Voz Station.

2.3.3. Analysis by X-Ray Diffraction (XRD). This analysis was carried out to identify compounds and oxides formed after exposure, using a BRUKER AXS equipment of eight radiation sources of copper. Each sputtering lasted 45 minutes.

2.4. Test Stations. Two very aggressive tropical marine environments with high wind impingement were selected.

2.4.1. Lake Maracaibo Crossing Station (LMC). This station is located at the crossing with Lake Maracaibo, Venezuela, at 117 m above lake level (Figure 1). Besides being a marine atmosphere, it is characterized by strong winds, as well as changing conditions of high humidity and high temperatures. The station is also surrounded by two industrial complexes, both of which release sulfur dioxide into the atmosphere from fossil combustion processes.

2.4.2. La Voz Station. It is Located on the Peninsula of Paraguaná, Falcón State (Figure 1), in the direction of the prevailing winds, 21 nautical km away from the refinery at Aruba, and 300 m from the Caribbean. This atmosphere is classified as a special atmosphere in accordance with the MICAT Project (Latin American Map of Atmospheric Corrosion), because of its high aggressivity and strong prevailing winds, reaching corrosion rates of 921 μm/year for steel and 27 μm/year for zinc [18].

2.4.3. Chemical Pollutant Levels and Meteorological Variables. Chemical pollutant levels were measured according to ISO 9225 [19]. For the measurement of meteorological variables (relative humidity, temperature, time of wetness, wind speed, and rainfall), the data belonging to the station nearby was used [10]. Corrosivity of atmospheres was determined using ISO 9223 [20].

2.4.4. Location of Coupons on the Test Bank. The test bank at La Voz Station is placed at an angle of 45° to avoid the accumulation of water on the coupons and they are located facing the prevailing winds. At the Lake Maracaibo Crossing Station, the test bank is fastened to the railing of a tower at a height of 117 m above sea level, with the coupons in vertical position and facing east. The incidence of the prevailing winds at this station is particularly on the right edge of the test coupons.

3. Results and Discussion

3.1. Characterization of Environments. The results of the characterization of the environments under study are shown in Tables 2 and 3; notice their high aggressiveness (high–very high) where it is evident a more corrosive environment in La Voz Station (C_5/C_4) in relation to the Lake Maracaibo Crossing Station (C_4).

3.2. Behavior of the Thermal-Sprayed Systems in La Voz Station

3.2.1. Double-Layer System without Sealer. During the first twelve months of evaluation, the double-layer system Zn/Al without sealing (Figure 2(a)) had an excellent performance, presenting corrosion only at the coating in the bottom border. It must be pointed out that the area of the coupons hit by the prevailing winds, where the erosive effect is manifested, is different for each station. In the case of LMC station, winds impinge on the right edge whereas impingement is frontal in La Voz station.

However, for the second period of evaluation (24 months) [8], it was reported that these are susceptible to present border flaws, as after 14 months of evaluation, one of the valued samples evidenced detachment of the coating in the lower-left corner (Figure 3). This type of flaw in the border of the probe was possibly caused by an inadequate application of the coating due to the geometry of the probe (90° degrees angle/Figure 3(c1)), as being a critical and difficult area to cover; however, this can be corrected by guaranteeing a good thickness in that area or diminishing the angle of the

Table 2: Meteorological data during four and six years of exposure in La Voz Station and Lake Maracaibo Crossing Station (LMC), respectively.

Station	Time (years)	Temperature (°C)	Relative humidity (%)	Precipitation (mm)	Wind speed (m/s)
La Voz	1	28.3	82.4	834.6	5.6
	2	28.6	80.4	758.4	6.0
	3	28.7	82.5	538.4	7.3
	4	28.4	82.4	482.6	7.0
LMC	1	28.1	81.2	794.6	6.4
	2	27.8	83.4	1036.3	6.6
	3	28.0	80.3	544.3	6.5
	4	27.0	83.6	656.3	6.6
	5	26.7	80.4	698.4	6.6
	6	26.7	82.6	197.6	6.4

Source: For the LMC Station, the first 3 years correspond to meteorological data supplied by the "Air Base Rafael Urdaneta" (BARU), Zulia State, located at 30 km from the station. The rest of data for that station for the following three years was provided by a pilot station installed in situ at 110 m of height in the tower of the mentioned station.

Table 3: Average levels of air chemical agents during four and six years of exposure in La Voz Station and LMC Stations, respectively.

Station	Time (years)	Sulphur compounds mg/(m^2·d)	Chloride mg/(m^2·d)	Time of Wetness fraction	Corrosion category according to ISO 9223
La Voz	1	27.2	284.23	0.79	P_1S_2 T_5/C_5
	2	16.3	178.13	0.70	P_1S_2 T_5/C_5
	3	9.0	320.76	0.58	P_0S_3 T_5/C_5
	4	12.2	178.63	0.59	P_1S_2 T_5/C_5
LMC	1	16.4	125.3	0.48	P_1S_2 T_4/C_4
	2	17.8	89.49	0.46	P_1S_2 T_4/C_4
	3	13.1	100.44	0.52	P_1S_2 T_4/C_4
	4	45.0	80.72	0.71	P_2S_2 T_5/C_5
	5	—	—	0.62	—
	6	—	—	0.63	—

edge to reduce the drag coefficient, as the ones applied for the process of electric arch (Figure 3(c2)).

After 36 months of an excellent performance, the system started to diminish its protection capacity as it was affected by the erosive effect (Figures 2(c) and 2(d)), specially the border effect (lower-left corner); a worn area was noticed as well as some coating oxidation products; there were also deposits of salts and dust and even some substrate corrosion spots. In relation to the incision, an excellent galvanic protection was observed covered by the corrosion products from the coating, mixed with dust.

3.2.2. Double Layer System Sealed with Wash Primer. After 4 years of exposure, this system (Figure 4), contrary to the one without sealer, presented an excellent appearance, with some corrosion spots of the aluminum spread over the exposed surface and dust deposits in the low border. At the incision, the coating provided an excellent galvanic protection. It was totally covered by the corrosion products of the coating and dust, without signs of damages to the steel base.

According to the observations done, it can be said that the use of the sealer wash primer improves significantly the performance of this system (aluminum as finishing), as it offers an additional barrier to the erosive effect of the environment as well as it enhances its esthetic appearance. The reason for this improvement is the chemical composition of the sealant. This chemical analysis was carried out in another research [9] at the Centro de Estudios de Corrosión, Faculty of Engineering, Universidad del Zulia, on samples of thermal sprayed aluminum sealed with the same wash primer (wash primer 1) used in this evaluation and other sealer (wash primer 2), of another manufacturer, obtaining different performances.

Table 4 shows the chemical analysis for EDS that was made on the surface of a thermal sprayed sample with aluminum, sealed with wash primer 1 and its comparison with wash primer 2, on which some localized corrosion in the pores of the coatings was observed.

It was determined [9] that the improvement of this system is due to the chemical composition of this sealer (wash primer 1) as it presents, titanium (4,84%), a high chromium percentage (11,54%) and aluminum phosphates that are formed on the surface which increase the resistance of the passive aluminum film to the erosive effect. It should be noted that the performance of this system was better than each of the separate coatings (Al and Zn) [6–11].

(a) (b) (c) (d)

Figure 2: Thermal-sprayed coating of Zn/Al by the flame process (470 μm). (a) 12 months of exposure. (b) 24 months of exposure. (c) 36 months of exposure. (d) 48 months of exposure.

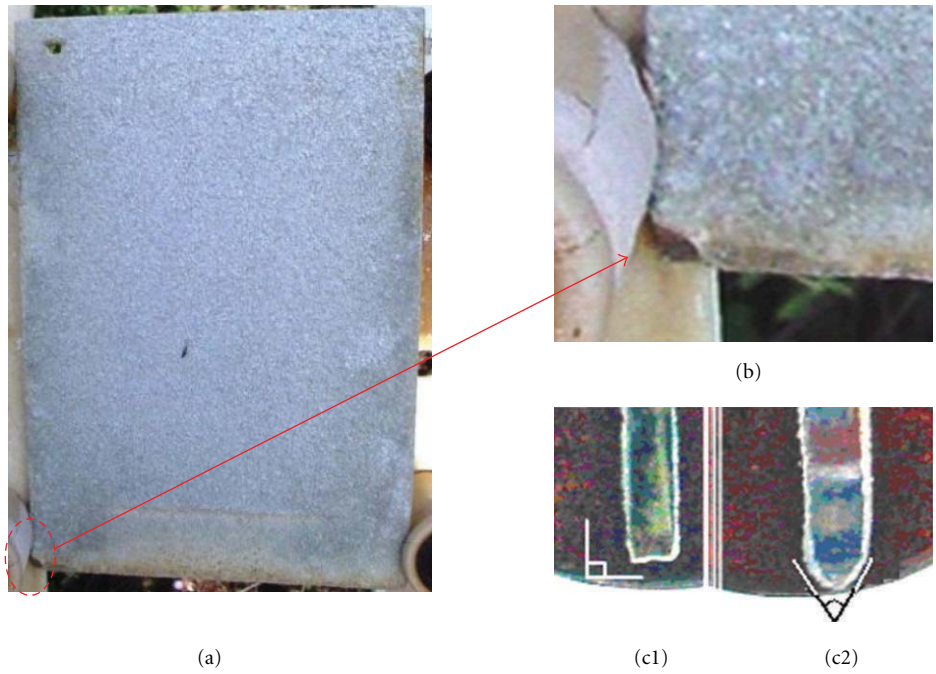

(a) (b) (c1) (c2)

Figure 3: (a) Thermal-sprayed coating of Zn/Al, Thickness = 445 μm. (b) Details of the edge flaw in the lower border. (c) Transversal cutting: details of the edge of the sample applied by the flame process (90° angle (c1) and acute (c2)), sample applied by electrical arch.

3.3. Behavior of the Thermal-Sprayed Systems in the Lake Maracaibo Crossing Station

3.3.1. Double-Layer System without Sealing. The environment in LMC Station is less aggressive (C_4) than in La Voz Station (C_5), which means that flaws will appear after a longer time of exposure. The thermal sprayed system with Zn/Al double layer without sealing, up to 36 months of evaluation, presented a good performance, without signs of corrosion at the surface substrate of the probe and with a good galvanic effect; it showed only a slight accumulation of environmental dust (Figure 5).

At 71 months of exposure, this coating began to surrender to the erosive attack, so some zinc corrosion products were noticed on the right edge (Figure 6), near the area of the border. This area, as it has been established in previous researches [6–9], is critical because coupons coated by the flame process presented an edge with a 90° angle which implies that the coating did not acquire the appropriate thickness as it was difficult to apply the product in that area; this opens the possibility for the aluminum fail to provide the necessary protection against the erosive effect and, therefore, to expose zinc, a material highly affected by the erosive action of the environment. The last inspection completed in this

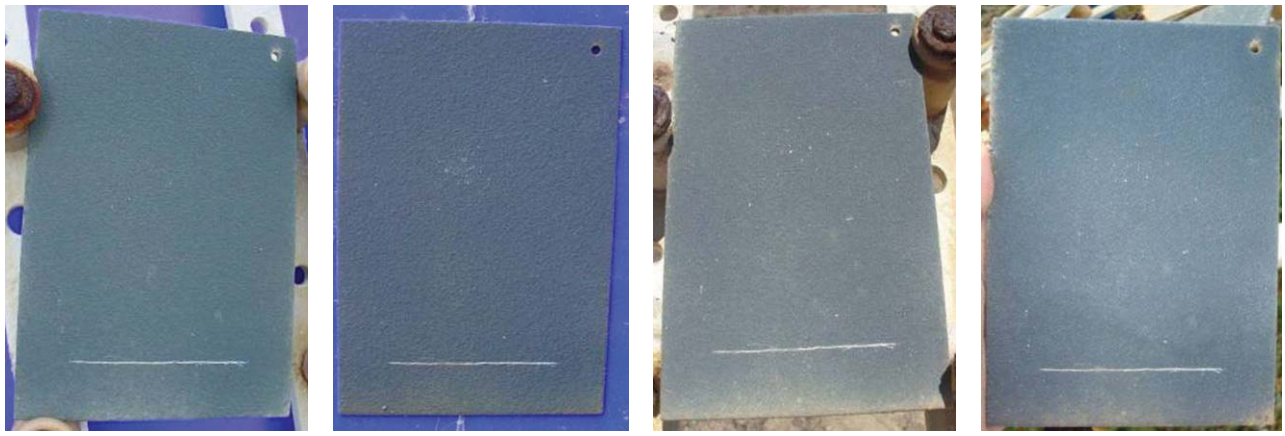

(a) (b) (c) (d)

Figure 4: Thermal-sprayed coating of Zn/Al by flame process, sealed with wash primer (445 μm). (a) 12 months of exposure. (b) 24 months of exposure. (c) 36 months of exposure. (d) 48 months of exposure.

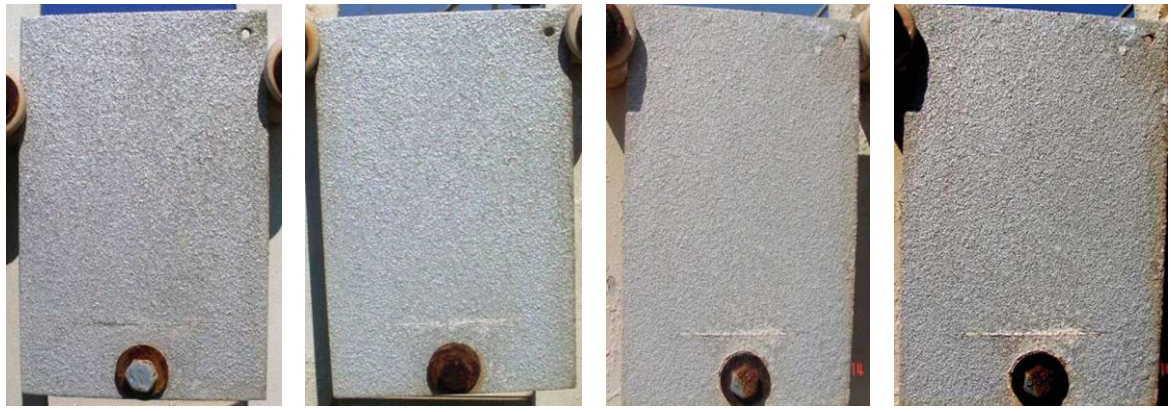

(a) (b) (c) (d)

Figure 5: Thermal-sprayed coating of Zn/Al by flame process (318 μm) (a) 12 months of exposure. (b) 24 months of exposure. (c) 36 months of exposure. (d) 41 months of exposure.

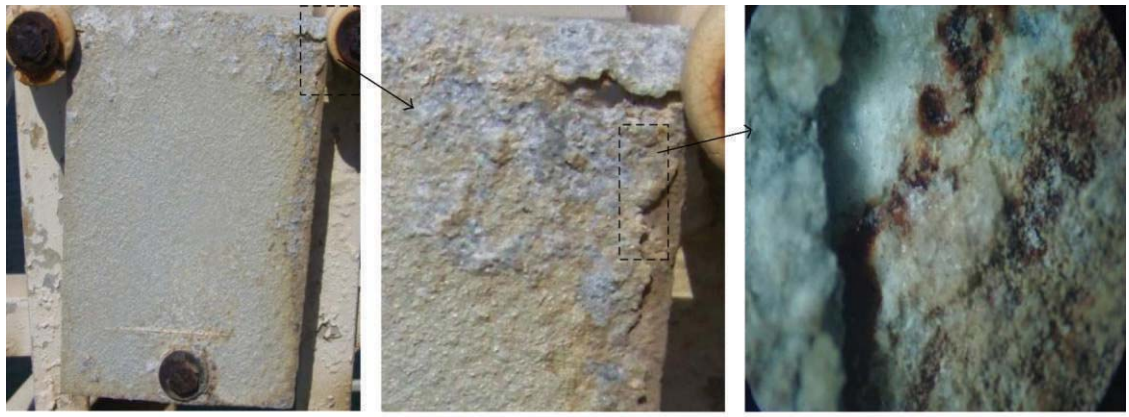

(a) (b) (c)

Figure 6: Thermal-sprayed coating of Zn/Al by flame process (318 μm). (a) 71 months of exposure. (b) Delamination detail of the coating in the right edge. Notice the formation of corrosion products of Zn (white color) and the substrate corrosion (brown color). (c) A magnifying stereoscopic view 45x.

Table 4: Elemental analysis: wash primer sealer manufacturer 1 and 2.

Chemical analysis (Weight %)	
Wash primer 1	Wash primer 2
Al = 23.31	Na = 6.49
P = 13.52	Al = 30.36
Cl = 3.24	Si = 15.63
Ca = 1.45	P = 18.59
Ti = 4.84	Cl = 12.38
Cr = 11.54	K = 2.46
Fe = 9.66	Ca = 1.66
Zn = 32.42	Cr = 1.69
—	Fe = 6.21
—	Zn = 4.53

environment was almost after six years of exposure; some substrate corrosion was observed as the coating at the right border was slightly starting to delaminate.

3.3.2. Double-Layer System Sealed with Wash Primer. After 71 months of exposure, the probe was practically intact, with an excellent appearance and galvanic effect (Figure 7). Of all the systems evaluated in the project, this one has had the best performance, only a slight accumulation of environmental dust, a product of the last months of drought.

At La Voz Station, and just as previously explained, wash primer 1 drastically improved the resistance of the coating, as it helped it to face these very aggressive environments from the corrosion-erosion point of view.

Through the evaluation of this project, from the 5 studied samples of this system in this environment, only one presented an edge flaw at the lower-left corner after 13 months of exposition (Figure 8), the crack advanced to a longitude of 3.5 cm.

In spite of this, and similarly to the results of the previous station, the performance of the system was better than the one of the other systems of Zn and Al separately (Figure 9) [6–11].

3.3.3. Analysis by Scanning Electron Microscope (SEM). During the different phases of the project, some cuttings were made in areas which presented good or problem conditions (e.g., with flaws at the edges) to analyze through SEM the integrity of the coating, its microstructure changes, the penetration of polluting agents, the morphology of corrosion products, and their corrosion mechanisms. One of the analyses is presented below, specifically, the one done in a sample after 36 months of exposure (Figure 10) at the LMC Station; the area analyzed is localized at the right edge; it was chosen so that the integrity of the coating in the proximities of the edge of incidence could be verified.

The elemental analysis in zone 1 shows an attack to the zinc layer (corrosion products/light gray color). In this area, two things can be observed: first, a high concentration of pollutants (Table 5); and, second, a group of imperfections or interconnected pores that form a kind of channels, through

Table 5: Chemical analysis for thermal-sprayed Zn/Al, double layer, without sealer.

Chemical analysis (weight %)			
Area 1	Area 2	Area 3	Area 4
Al = 10.42	Al = 3.09	Mn = 0.46	Al = 98.85
S = 6.79	S = 3.18	Fe = 90.67	Fe = 0.58
Cl = 8.74	Cl = 3.46	Zn = 8.72	Zn = 0.57
Fe = 0.50	Zn = 90.52	Ga = 0.15	—
Zn = 73.23	Ga = 0.26		—
Ga = 0.33			—

Table 6: Chemical analysis of the right edge.

Chemical analysis (weight %)
Al = 13.03
Si = 6.37
Cl = 0.76
K = 0.44
Ca = 1.08
Fe = 1.42
Zn = 76.89

which pollutants easily ingress toward the internal layers of the coating. On the other hand, in zone 2, there are high concentrations of chlorides and sulphur compounds. The high zinc content of the area suggests the presence of corrosion products of zinc. As observed in Figure 10, these zinc corrosion products are over the aluminum layer, as they are deposited on their discontinuities. Zone 3 is located in the interface area of steel/zinc (the furthest zone), as seen in Table 5, without the presence of pollutants for that time of exposition. However, in Figure 10, some microcracks and discontinuities of the zinc layer can be detected in the proximities of the zone; through them, aggressive agents could possibly ingress when reaching the level of the interface aluminum/zinc. Finally, in zone 4, the aluminum remains intact (Table 5), as expected; this element has remained in excellent conditions up to now.

The microscopic analysis revealed important aspects such as (a) differences in the thickness of the layers, which gave as a result a considerable aluminum thickness (200 μm approximately), clearly higher than zinc (100 μm); (b) interconnected porosity: there were appreciated some areas with interconnected pores through which aggressive agents entered through the zinc covered zone; (c) changes in zinc microstructure and penetration of polluting agents.

In relation to the analysis done on the right edge of the coupon (Figure 11), contrary to the observed in the border, there are two not-well-defined layers of zinc and aluminum. The chemical analysis (Table 6) shows that there is a low percentage of aluminum in the area, but it is rich in zinc. This inequality, and just as it was observed in the visual inspection, is responsible for the border flaws in these areas. Also, as it has been previously explained, it would be different if there was a uniform layer with a sufficient quantity of

(a) (b) (c) (d) (e)

Figure 7: Thermal-sprayed coating of Zn/Al, sealed with wash primer 1 (345 μm). (a) 12 months of exposure. (b) 24 months of exposure. (c) 36 months of exposure. (d) 41 months of exposure. (e) 71 months of exposure.

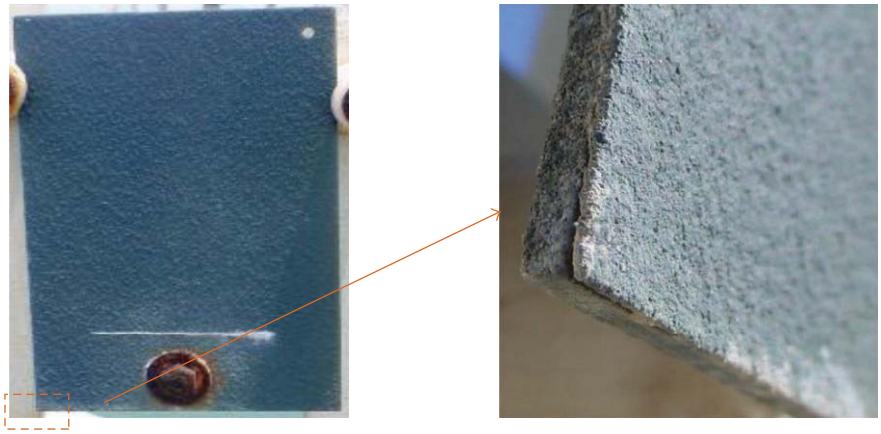

Figure 8: Thermal-sprayed coating of Zn/Al/wash primer 1 (325 μm). Notice the flaw at the edge on the left corner.

aluminum. Furthermore, the chemical analysis of the area reveals the presence of silicon, chlorine, and calcium (Table 6), suggesting deposits of environmental dust.

3.4. Analysis by X-Rays Diffraction (XRD). The XRD assays were carried out for the unsealed and sealed systems with wash primer (Figures 12 and 13). In relation to the double-layer system without sealing (Figure 12), Bayerite was found as a main component (α-$Al(OH)_3$), results that coincide with the ones reported by Pombo et al. [21], who affirm that if aluminum is thermal-sprayed by the flame process, the formation of this oxide will prevail (formed on the mouthpiece of the pistol) in the surface of the test probe. Additionally, the presence of SiO_2 was detected as a result of the accumulation of environmental dust during the period of exposure in the LMC station.

The obtained spectrum for the double-layer system sealed with wash primer 1 (Figure 13) showed phosphates formation as a product of the reaction of the coating with the sealer. It is important to highlight that the wash primer is a type of coating that is commercially used as a promoter of adherence, made up of two components: a component A which is a resin of polyvinyl butyral with pigment of Zn chromate; and a component B that is an alcoholic solution of phosphoric acid. When the latter is applied on zinc or aluminum, it reacts with them and forms a fine film of crystals of the respective phosphates, with the purpose of sealing the pores left by the application process. It is necessary to highlight that the formed phosphates contribute with a higher resistance to erosion and to the ingress of polluting agents from the environment; in contrast to the unsealed systems, it offers an additional protective barrier to the surface of the probe.

Titanium was also detected in wash primer 1 (Table 4), which is present as TiO_2 in paintings and sealers with the purpose of adding solids to confer them a better capacity to seal the pores. This element was not detected in the wash primer 2, which may be the reason why the wash primer 1 had a much better performance.

4. Conclusions

(1) Thermal-sprayed coatings with Zn/Al (double layer) sealed with wash primer extend the service life of this system, besides improving the physical appearance of the test coupon.

(2) Along the six years of studies, it was found that La Voz Station is a more aggressive area than Lake Maracaibo Crossing Station.

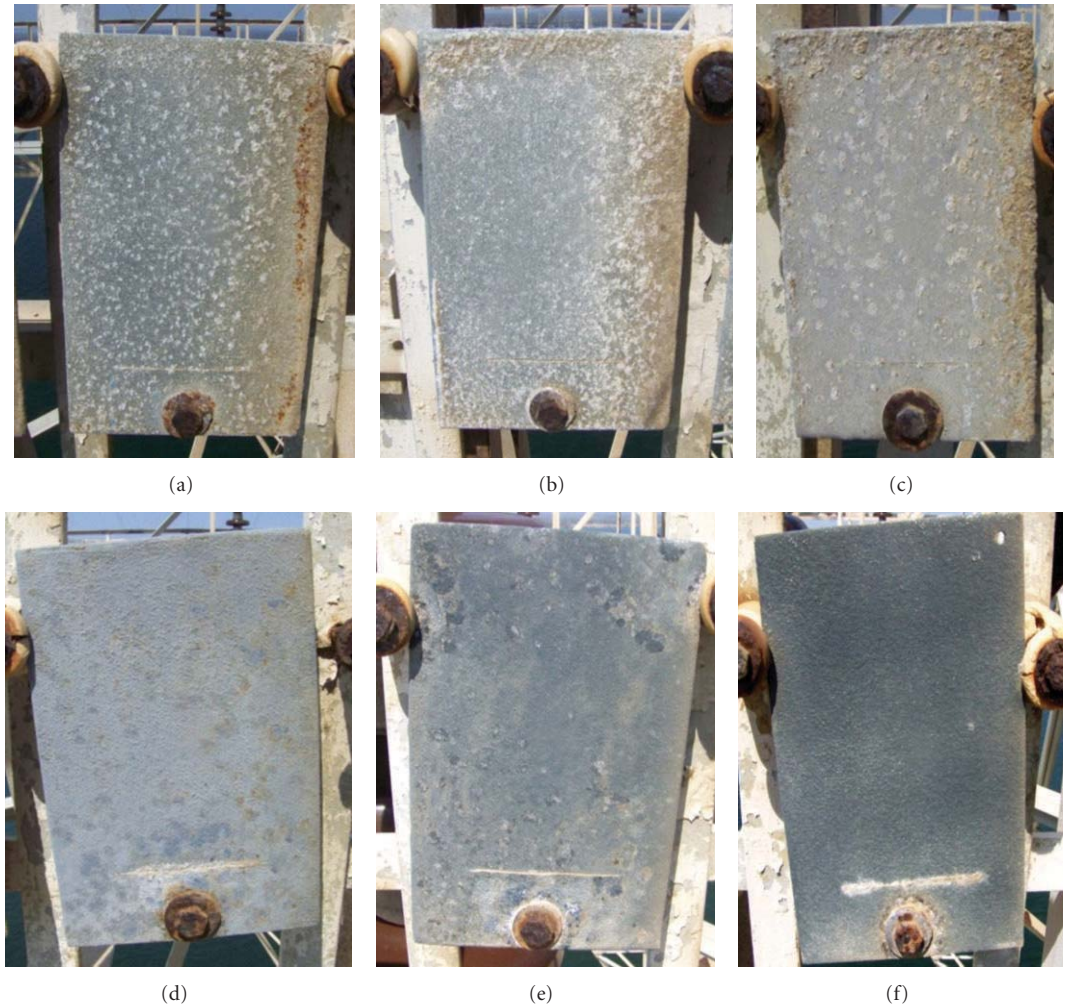

Figure 9: Comparison of different sealed systems used at the LMC Station, after 41 months of exposure (a) Thermal sprayed coating of zinc by flame process (wire), sealed with wash primer 1 (173 μm). (b) Thermal sprayed coating of zinc by the electric arch process, sealed with wash primer 1 (264 μm). (c) Thermal sprayed coating of zinc by electric arch process, sealed with phenolic (261 μm) (66 months of exposure). (d) Thermal sprayed coating of aluminum by electric arch process with phenolic (261 μm). (e) Thermal sprayed coating of aluminum by electric arch process, sealed with wash primer 1 (251 μm). (f) Thermal sprayed coating of Zn/Al by the flame process, sealed with wash primer 1 (345 μm).

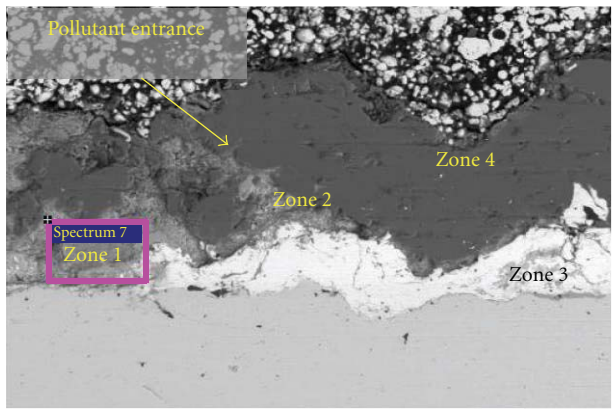

Figure 10: Thermal-sprayed Zn/Al double-layer, without sealer (thickness = 345 μm). View in the SEM. Area near the incidence edge.

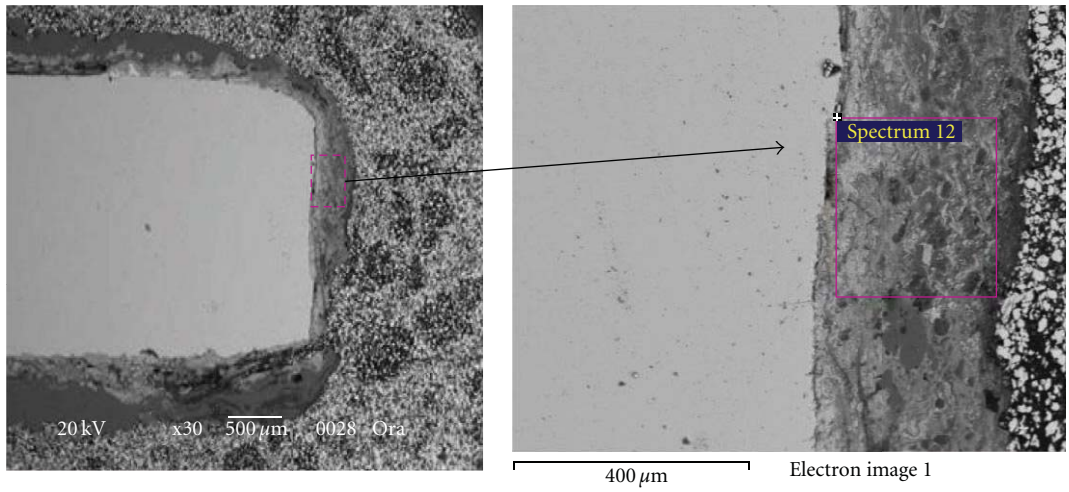

Figure 11: Thermal-sprayed Zn/Al double layer, without sealer. Thickness = 345.44 μm. View in the SEM. Right edge.

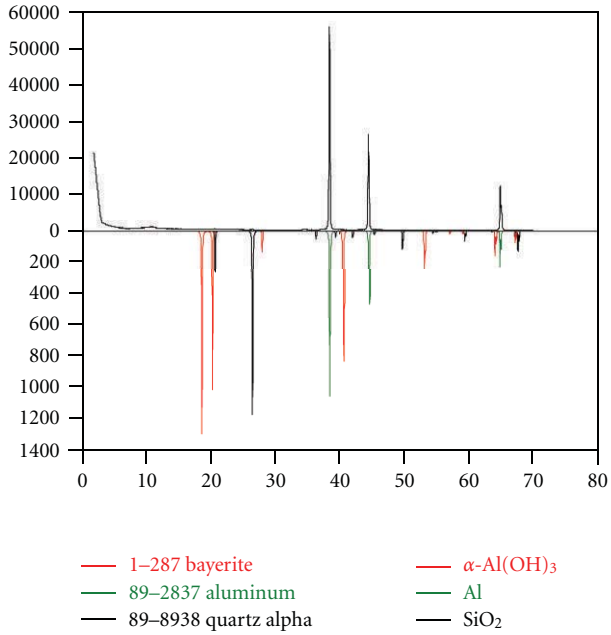

Figure 12: Spectrum of the double-layer system without sealer.

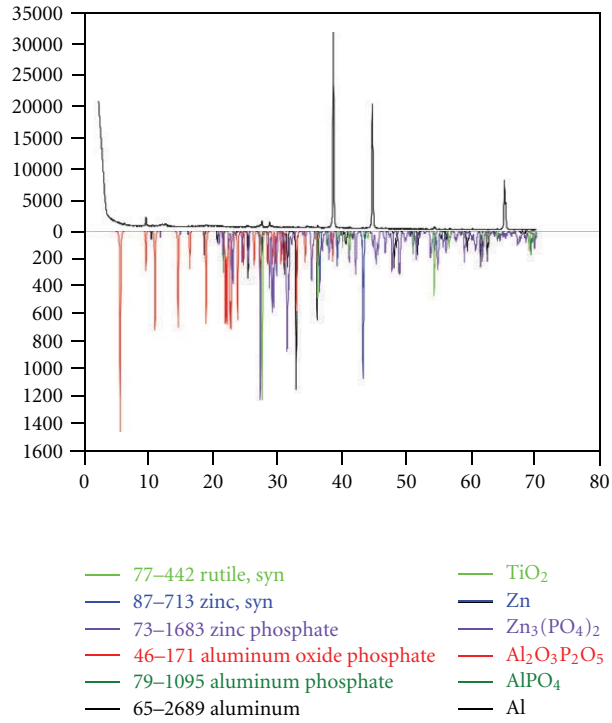

Figure 13: Spectrum of the double-layer system with sealer.

(3) The best performance in the sealed systems is due to the reaction of the wash primer with the Al (external layer of coating) of the test coupons, forming phosphates that contribute to a higher resistance to the polluting agents and erosive effects of the exposure environments; this resistance increases in the case of the wash primer 1, with the presence of TiO_2.

(4) The double-layer system with sealer represents a good protection option against the corrosion in marine and coastal marine environments with a high incidence of winds.

Acknowledgment

Thanks are due to CONDES (Consejo de Desarrollo Cientifico y Humanistico), from the Universidad del Zulia, for the economical support.

References

[1] S. Kuroda, J. Kawakita, M. Komatsu, T. Aoyaggi, and H. Saitoh, "Characterization of thermal sprayed Zn and Al coatings after 18 years' exposure in marine environment," Advancing the

Science & Applying the Technology. ASM International USA. pp 343–352, 2003.

[2] R. A. Kogler, D. Brydl, and C. Highsmith, "Recent FHWA experience with metallized coatings for steel bridges," *Materials Performance*, vol. 38, no. 4, pp. 43–45, 1999.

[3] American Welding Society. Corrosion Tests of Flame-Sprayed Coated Steel 19 Year Report, 1974, http://www.intmetl.com/19_year_report.htm.

[4] R. Kain, *Marine Atmospheric Corrosion Museum Report on the Performance of Thermal Spray Coatings on Steel*, American Society for Testing and Materials, Philadelphia, Pa, USA, 1987.

[5] M. Morcillo, M. Almeida, F. Fragata, and Z. Panossian, Corrosión y Protección de Metales en las Atmósferas de Ibero América. Parte II. Protección Anticorrosiva de Metales en las Atmósferas de Ibero América (Red Temática Patina, XV.D /CYTED) Madrid, España, 2002.

[6] O. Salas, *Comportamiento de los Recubrimientos por Termorociado de Aluminio y Cinc en Ambientes Marinos y Costeros Marinos*, Trabajo Especial de Grado Magíster Scientarium. Facultad de Ingeniería. Centro de Estudios de Corrosión. Universidad del Zulia, Maracaibo, Venezuela, 2005.

[7] A. Uzcátegui and A. Valdivieso, *Efecto del Ambiente Tropical en el comportamiento de Recubrimiento Termo-Rociados de Zn, Al, y Zn/Al*, Tesis de Grado. Facultad de Ingeniería. Centro de Estudios de Corrosión. Universidad del Zulia, Maracaibo, Venezuela, 2006.

[8] J. Godoy and N. Sualce, *Corrosión- Erosión de Recubrimientos Termorociados de cinc, aluminio, Cinc/Aluminio en Ambientes Marinos Tropicales*, Tesis de Grado. Facultad de Ingeniería. Centro de Estudios de Corrosión. Universidad del Zulia, Maracaibo, Venezuela, 2006.

[9] J. Atencio and L. Hernández, *Desempeño de Recubrimientos Termo-Rociados en Zinc y/o Aluminio en Ambientes Marinos y Tropicales*, Tesis de Grado. Facultad de Ingeniería. Centro de Estudios de Corrosión. Universidad del Zulia, Maracaibo, Venezuela, 2008.

[10] D. Rojas and A. Tosaya, *Resistencia a la Corrosión de Recubrimientos Termorociados de Zn y/o Al en Ambientes Marinos Tropicales*, Trabajo especial de grado. Facultad de Ingeniería. Centro de Estudios de Corrosión. Universidad del Zulia, Maracaibo, Venezuela, 2009.

[11] O. Salas, O. De Rincón, N. Romero et al., "Behavior of thermal-sprayed Al, Zn, and Zn/Al coatings in tropical marine environments," *Materials Performance*, vol. 47, no. 11, pp. 42–46, 2008.

[12] S. Orlando, T. De Rincón Oladis, R. Álvaro, S. Miguel, and L. Maldonado, "Long-term performance of thermal sprayed coatings in tropical marine environments," in *Proceedings of the International Corrosion Conference Series (NACE '07)*, March 2007.

[13] S. Orlando, T. De Rincón Oladis, R. Álvaro et al., "Thermal sprayed Zn/Al double layer: a protection alternative against steel corrosion in tropical marine atmospheres," in *Proceedings of the International Corrosion Conference Series (NACE '08)*, 2008.

[14] ASTM D 1186, *Standard Test Method for Nondestructive Measurement of Dry Film Thickness of Nonmagnetic Coatings Applied to a Ferrous Base*, ASTM International, West Conshohocken, Pa, USA, 2002.

[15] ASTM E 2109, *Test Methods for Determining Area Porcentage Porosity in Thermal Sprayed Coatings*, ASTM International, West Conshohocken, Pa, USA, 2001.

[16] ISO 4624, *Paints and Varnishes—Pull-Off Test for Adhesion*, ISO, Geneva, Switzerland, 2002.

[17] ASTM D 4541, *Pull-Off Adhesion Testing of Paint, Varnish and other Coatings and Films*, ASTM International, West Conshohocken, Pa, USA, 2002.

[18] M. Morcillo, E. Almeida, B. Rosales, J. Uruchurtu, and M. Marrocos, Corrosión y Protección de los Metales en la Atmósfera de Iberoamérica. Parte I. Mapas de Iberoamerica de Corrosividad atmosferica (Proyecto MICAT, XV. 1 /CYTED), Madrid, España, 1998.

[19] ISO 9225, *Corrosion of Metals, and Alloys—Corrosivity of Atmospheres—Measurement of Pollution*, ISO, Geneva, Switzerland, 1992.

[20] ISO 9223, *Corrosion of Metals, and Alloys—Corrosivity of Atmospheres—Classification*, ISO, Geneva, Switzerland, 1992.

[21] R. R. M. H. Pombo, R. S. C. Paredes, S. H. Wido, and A. Calixto, "Comparison of aluminum coatings deposited by flame spray and by electric arc spray," *Surface and Coatings Technology*, vol. 202, no. 1, pp. 172–179, 2007.

Hindawi Publishing Corporation
International Journal of Corrosion
Volume 2012, Article ID 496321, 16 pages
doi:10.1155/2012/496321

Review Article

Effects of Air Pollution on Materials and Cultural Heritage: ICP Materials Celebrates 25 Years of Research

Johan Tidblad,[1] Vladimir Kucera,[1] Martin Ferm,[2] Katerina Kreislova,[3] Stefan Brüggerhoff,[4] Stefan Doytchinov,[5] Augusto Screpanti,[5] Terje Grøntoft,[6] Tim Yates,[7] Daniel de la Fuente,[8] Ott Roots,[9] Tiziana Lombardo,[10] Stefan Simon,[11] Markus Faller,[12] Lech Kwiatkowski,[13] Joanna Kobus,[13] Costas Varotsos,[14] Chris Tzanis,[14] Linda Krage,[15] Manfred Schreiner,[16] Michael Melcher,[16] Ivan Grancharov,[17] and Nadya Karmanova[18]

[1] *Swerea KIMAB AB, Drottning Kristinas väg 48, 11428 Stockholm, Sweden*
[2] *IVL Swedish Environmental Research Institute, P.O. Box 5302, 400 14 Gothenburg, Sweden*
[3] *SVUOM Ltd., U Mestanského Pivovaru 934 /4, 17000 PRAHA 7, Czech Republic*
[4] *Deutsches Bergbau-Museum Bochum, Herner Straße 45, 44787 Bochum, Germany*
[5] *ENEA, C. R. Casaccia via Anguillarese 301, S. Maria di Galeria 00123, Rome, Italy*
[6] *Norwegian Institute for Air Research (NILU), Instituttveien 18, P.O. Box 100, 2027 Kjeller, Norway*
[7] *Building Research Establishment (BRE Ltd.), Bucknalls Lane, Watford WD25 9XX, UK*
[8] *CENIM (CSIC), Avenida Gregorio del Amo 8, 28040 Madrid, Spain*
[9] *Estonian Environmental Research Centre, Estonian Environmental Research Institute, Marja street 4D, 10617 Tallinn, Estonia*
[10] *Laboratoire Interuniversitaire des Systèmes Atmosphériques (LISA), UMR-CNRS 7583, Université Paris Est Créteil 61, avenue du Général de Gaulle, 94010 Créteil Cedex, France*
[11] *Rathgen-Forschungslabor, Staatliche Museen zu Berlin, Schlossstraße 1a, 14059 Berlin, Germany*
[12] *EMPA, Ueberlandstraße 129, 8600 Duebendorf, Switzerland*
[13] *Institute of Precision Mechanics, Duchnicka 3, 01-796 Warsaw, Poland*
[14] *Climate Research Group, Division of Environmental Physics and Meteorology, Faculty of Physics, University of Athens, University Campus Bldg. Phys. V, 15784 Athens, Greece*
[15] *Department of Silicate Material Technology, Faculty of Materials Science and Applied Chemistry, Riga Technical University, Azenes Street 14/24, 1048 Riga, Latvia*
[16] *Institute of Science and Technology in Art, Academy of Fine Arts, Schillerplatz 3, 1010 Vienna, Austria*
[17] *University of Chemical Technology and Metallurgy, Bul. Kl. Ohridski 8, 1756 Sofia, Bulgaria*
[18] *International Cooperation Section, JSC "SRI Atmosphere", 7, Karbyshev Street, St. Petersburg 194021, Russia*

Correspondence should be addressed to Johan Tidblad, johan.tidblad@swerea.se

Received 19 July 2011; Accepted 9 September 2011

Academic Editor: Blanca M. Rosales

An overview is given of all results from the International Co-operative Programme on Effects on Materials including Historic and Cultural Monuments (ICP Materials), which was launched in 1985. Since then, about twenty different materials have been exposed repeatedly in a network of test sites consisting of more than twenty sites with an extensive environmental characterisation and more than sixty official reports have been issued. Recent results on trends in corrosion, soiling, and pollution show that corrosion of carbon steel, zinc, and limestone is today substantially lower than 25 years ago, but while corrosion of carbon steel has decreased until today, corrosion of zinc and limestone has remained more or less constant since the turn of the century. Unique data are given on measured HNO_3 concentrations from 2002-2003, 2005-2006, and 2008-2009, and the relative average decrease was about the same from 2002-2003 to 2005-2006 as it was from 2005-2006 to 2008-2009.

1. Introduction

ICP Materials or "the International Co-operative Programme on Effects on Materials including Historic and Cultural Monuments" was launched in 1985 and had its first Task Force Meeting in March 10-11, 1986, Watford, United Kingdom. Since then, more than sixty reports in the official report series have been issued [1–66].

The history of ICP Materials [67] begins, however, with the history of the Convention on Long-range Transboundary Air Pollution (CLRTAP, LRTAP Convention or simply "the Convention"). In 1979, the Member States of the United Nations Economic Commission for Europe (UNECE) adopted the Convention as a response to acid rain, brought on by contamination of the air, killing forests and lakes even in remote places far from industrial facilities [68]. The Convention has been extended by eight protocols that identify specific measures to be taken by their 51 Parties to cut their emissions of air pollutants [69]. Worth mentioning in this context are the 1985 Protocol on the Reduction of Sulphur Emissions or their Transboundary Fluxes by at least 30 per cent, the 1994 Protocol on Further Reduction of Sulphur Emissions, and the 1999 Protocol to Abate Acidification, Eutrophication and Ground-level Ozone. The last of these is also named the "Gothenburg Protocol" or the "multipollutants/multi-effects protocol".

Already in 1980, Vladimir Kucera was approached by UNECE with a request to provide a short summary of the state of knowledge concerning the effects of sulphur compounds on materials. The reason for selecting Sweden was most likely due to Sweden's well-received case study for the United Nations conference on the human environment published in 1971 [70]. This led to the development of a proposal in 1983 for an international exposure program where Sweden declared its willingness to be lead country. A decision to launch the program was made by the Executive Body of the Convention during its third session in Helsinki, July 1985. Later the same year an unofficial planning meeting took place in Stockholm, December 1985 with participation from research subcentres from the countries Czechoslovakia, Norway, Federal Republic of Germany, and United Kingdom.

The first phase of ICP Materials (1987–1995) was marked by a focus on development of dose-response functions where long-term data on corrosion and pollution is required. During this time, SO_2 concentrations were still relatively high but decreasing, so it was in 1996 realised that a new exposure programme was needed, the multipollutant exposure (1997–2001). The aim of this program was to quantify not only the effect of SO_2, but also other important "new" pollutants such as HNO_3 and particulate matter. In connection with this, an EU proposal was submitted by the group with the aim of strengthening the multipollutant exposure. This proposal was, however, rejected but was successfully resubmitted and in 2002 the 40-month MULTI-ASSESS project could start with the first extensive measurements of HNO_3 and PM in the program [71].

In 1996, there was also a turning point with the first ICP Materials workshop "Economic Evaluation of Air Pollution Damage to Materials," January 23–25, 1996, Stockholm, Sweden. This emphasis on the use of results for policy purposes was further strengthened with the launch of a subcentre for the assessment of stock of materials at risk and cultural heritage in 2005, together with the close cooperation with the 2004–2007 EU 6FP CULT-STRAT project on management strategies that resulted in a textbook on the effects of air pollution on materials and cultural heritage [72], and even more with the significant involvement of ICP Materials in the revision of the Gothenburg protocol, 2011.

The aim of the present paper is first to present a complete overview of all results that are available from the ICP Materials programme, including references to original data and publications. During the last 25 years, there are many individual results that are more or less well known, and even though these results have been published to varying degrees they are now for the first time presented in one single paper. The second aim is to give new results on trends in corrosion, soiling, and pollution. The exposure of materials for trend analysis has been one of the key activities of ICP Materials from the beginning in 1987, with the addition of limestone for corrosion and modern glass for soiling as new trend materials in 2005, in addition to the original trend materials: carbon steel and limestone. Regarding pollution, the focus in this paper will be on N pollutants, especially HNO_3, where unique data from the period 2002–2009 are presented.

2. Exposure of Materials (1987–2009)

A wide range of materials has been exposed over the years and an overview of the performed corrosion exposures for the period 1987–2009 for individual materials/materials groups are given in Figure 1. Note that modern glass is not included in the figure since it is a material exposed for evaluation of soiling (see Section 6.3). The main exposure with the widest range of materials was the original 8-year exposure (1987–1995). This was later complemented in the multipollutant 4-year exposure (1997–2001). Since 2000, only so-called trend exposures, that is, repeated one-year exposures with the aim of establishing trends in corrosion and pollution, have been performed for selected indicator materials. The individual materials are described in more detail in the following with references to original publications and data sources.

Recently, soiling is also included as an important effect on materials next to corrosion, and since 2005 modern glass has been exposed in sheltered position as a trend material for evaluation of soiling effects.

2.1. Carbon Steel. The subcentre responsible for evaluation of carbon steel was SVUOM, Czech Republic. Several materials, including carbon steel, were in addition to the unsheltered exposure also exposed under shelter, but not in all exposures. One-year data of unalloyed carbon steel

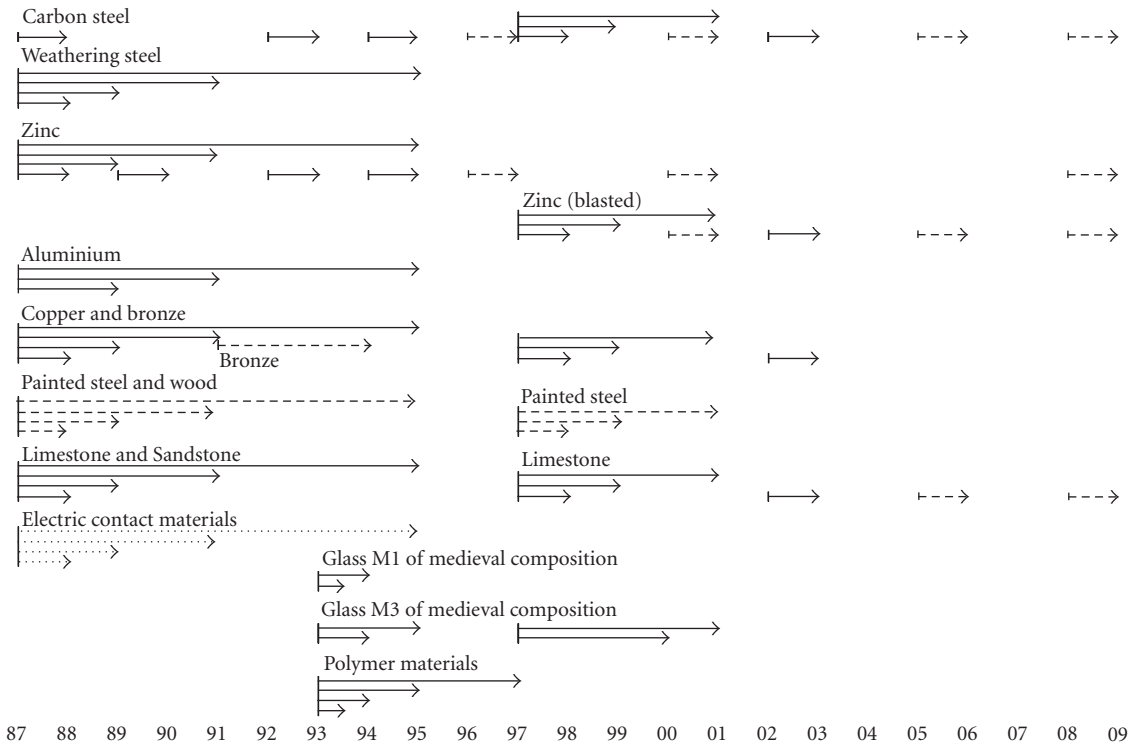

Figure 1: Overview of performed corrosion exposures within ICP Materials (solid arrows: unsheltered and sheltered exposure; dashed arrows: unsheltered exposure; dotted arrows: sheltered exposure inside an aluminium box).

(C < 0.2%, P < 0.07%, S < 0.05%, Cu < 0.07%) exposed in unsheltered position are available for the exposure years 1987-1988, 1992-1993, and 1994-1995 [29], 1996-1997 [46], 1997-1998 [41], 2000-2001 [46], 2002-2003 [73], 2005-2006 [52], and 2008-2009 [61]. One-year data for sheltered position are available for 1987-1988, 1992-1993, and 1994-1995 [29], 1997-1998 [41], and 2002-2003 [73]. Carbon steel was not exposed for longer periods than one year in the original exposure (1987–1995) but were in addition exposed both in unsheltered and sheltered positions in the multipollutant exposure, 1997–1999 and 1997–2001 [41], see Figure 1.

2.2. Weathering Steel. The subcentre responsible for evaluation of weathering steel was SVUOM, Czech Republic. Weathering steel (C < 0.12%, Mn 0.3–0.8%, Si 0.25–0.7%, P 0.07–0.15%, S < 0.04%, Cr 0.5–1.2%, Ni 0.3–0.6%, Cu 0.3–0.55%, Al < 0.01%) was exposed in unsheltered as well as sheltered position in the original exposure for the periods 1987-1988, 1987–1989, 1987–1991, and 1987–1995 [22], and an analysis of the results was later presented at the International workshop on atmospheric corrosion and weathering steels, Cartagena, 2004 [74].

2.3. Zinc. Two variants of zinc samples have been exposed, one "traditional" suitable for corrosivity classification and one that was blasted as a surface preparation prior to exposure resulting in slightly higher corrosion rates.

The subcentre responsible for evaluation of traditional zinc was SVUOM, Czech Republic. Zinc (>98.5%) was exposed in the original exposure for the periods 1987-1988, 1987–1989, 1987–1991, and 1987–1995, both in unsheltered and sheltered positions [22]. Additional data for one-year exposures are available for unsheltered position for the years 1989-1990, 1992-1993, and 1994-1995 [29], 1996-1997, and 2000-2001 [46], and 2008-2009 [61], and for sheltered position for the years 1987-1988, 1992-1993, and 1994-1995 [29], see Figure 1.

The subcentre responsible for evaluation of blasted zinc was EMPA, Switzerland. The first exposures were the multipollutant exposures in 1997-1998, 1997–1999, and 1997–2001 where samples were exposed in unsheltered as well as sheltered positions [42]. After that, blasted zinc has replaced traditional zinc as a trend material with exposures in 2000-2001 [42], 2002-2003 [73], 2005-2006 [53], and 2008-2009 [61]. In the year 2002-2003, sheltered samples were exposed as well [73].

2.4. Aluminium. The subcentre responsible for evaluation of aluminium was SVUOM, Czech Republic. Aluminium (>99.5%) was exposed in the original exposure program for the periods 1987-1988, 1987–1989, 1987–1991, and 1987–1995, both in unsheltered and sheltered positions. However, results are only available after 2, 4, and 8 years of exposure since the corrosion attack after 1 year of exposure could not be evaluated [22].

2.5. Copper, Cast Bronze, and Pretreated Bronzes. The subcentre responsible for evaluation of copper, bronze, and pretreated bronzes was the Bavarian State Department of Historical Monuments, Germany. Copper was of quality SF Cu, DIN 1787 (Cu 99%, P 0.015–0.04%) and cast bronze Cu Sn6Pb7Zn5, ISO/R 1338 (Cu 81%, Sn 5.8%, Pb 6.7%, Zn 4.5%, Ni 1.6% + trace elements). Both copper and cast bronze were exposed in unsheltered as well as sheltered positions in the original exposure program for the periods 1987-1988, 1987–1989, 1987–1991, and 1987–1995 [23] and later also in the multipollutant exposure program for 1997-1998, 1997–1999, and 1997–2001, and last in 2002-2003 [73].

In addition, recycled 1- and 2-year bronze specimens from the original exposure were grinded and then exposed in unsheltered position as untreated, waxed, patinated, and patinated/waxed for the period 1991–1994 [31].

2.6. Painted Steel and Wood. The subcentre responsible for evaluation of paint coatings was NILU, Norway. Four coatings were exposed, two painted on wood and two on steel: coil coated steel with alkyd melamine, steel panel with silicon alkyd, wood panel with alkyd, and wood panel with primer and acrylate. All these were exposed in unsheltered, but not sheltered, position in the original exposure program for the periods 1987-1988, 1987–1989, 1987–1991, and 1987–1995 [25]. One of these, the steel with silicon alkyd was then later also exposed in the multipollutant exposure program for 1997-1998, 1997–1999, and 1997–2001 [45].

2.7. Sandstone and Limestone. The subcentre responsible for evaluation of stone materials was BRE, UK. Portland limestone and white Mansfield dolomitic sandstone were exposed in unsheltered as well as sheltered positions in the original exposure program for the periods 1987-1988, 1987–1989, 1987–1991, and 1987–1995 [24].

In subsequent exposures limestone only was exposed. It was included in the multipollutant exposure in unsheltered and sheltered positions for 1997-1998, 1997–1999, and 1997–2001 [44] and also in 2002-2003 [73]. It is now classified as one of the indicator materials and was exposed in subsequent trend exposure in unsheltered position in 2005-2006 [54] and 2008-2009 [61].

2.8. Electric Contact Materials. The subcentre responsible for evaluation of electric contact materials was the former Swedish Corrosion Institute, now Swerea KIMAB. Nickel, copper, silver, and tin as well as Eurocard connectors of three different qualities were exposed in sheltered positions inside an aluminium box in the original exposure program for the periods 1987-1988, 1987–1989, 1987–1991, and 1987–1995 [26]. Several publications resulted from the evaluation including but not limited to [75–79].

2.9. Glass of Medieval Composition. The subcentre responsible for evaluation of glass of composition representative for medieval stained glass windows was the Institute of Sciences and Technology in Art, Academy of Fine Arts, Austria. Glass of two compositions were exposed, the more sensitive M1 (SiO_2 48%, K_2O 25.5%, CaO 15%, MgO 3%, Al_2O_3 1.5%, P_2O_5 4%, and Na_2O 3%) and M3 (SiO_2 60%, K_2O 15%, CaO 25%). Glass M1 was exposed for half a year (1993-1994) and one year (1993-1994) in both unsheltered and sheltered positions and in the same program glass M3 was exposed in unsheltered and sheltered positions for one (1993-1994) and two years (1993–1995) [27].

In the multipollutant exposure, only M3 was exposed for the periods 1997–2000 and 1997–2001 (3 and 4 years). However, by partly exposing samples already exposed for one and two years in the previous exposure (1993–1995) for the period 1997–2001 the final reports for sheltered [47] and unsheltered [48] exposure were able to contain results after 3, 4, 5, and 6 years of exposure. Several publications, Ph.D. and Diploma Theses resulted from these systematic investigations [80–87].

2.10. Polymer Materials. The subcentre responsible for evaluation of electric contact materials was the former Swedish Corrosion Institute, now Swerea KIMAB. Polyamide and polyethylene were exposed in unsheltered and sheltered positions for 0.5 (1993-1994), 1 (1993-1994), 2 (1993–1995), and 4 (1993–1997) years [28]. An analysis of the results was later presented at the 1st European Weathering Symposium, 2004 [88].

2.11. Modern Glass. The sub-center responsible for the evaluation of soiling on glass was LISA, France. Silica-soda-lime float glass (70 to 72% of SiO_2, about 14% of Na_2O, and about 10% of CaO, and other oxides) currently used as windows glass, as well as in building facades, was exposed in sheltered position inside an aluminium box for 1 year (2005-2006 and 2008-2009).

3. Network of Test Sites

A complete list of sites used for the previously described exposures is given in Table 1. The first thirty-nine sites (1–39) were used in the original exposure (1987–1995). When the multipollutant exposure (1997–2001) was started eight, new sites were added (40–49) but at the same time several sites were removed that were part in the original exposure. One of the criteria for keeping sites was that they should be measuring ozone, which during this time changed status from optional to mandatory (see below). Subsequent individual additions/removals of test sites have been made in connection with trend exposures as specified in Table 1.

4. Measurements of Environmental Data

Environmental data has been the back-bone of the program, and the extensive environmental characterisation is perhaps what most distinguishes this corrosion program from other. In fact, some of the reported environmental data (see HNO_3 below) is unique, even from the perspective of environmental research.

NILU, Norway has been responsible for the reporting of environmental data and data for individual years have

Table 1: List of ICP Materials test sites showing number, name, country site type, and years with available data 1987–2009.

Name	Country	Site type[a]	Available data
(1) Prague-Letnany	Czech Republic	Urban	1987–2009
(2) Kasperske Hory	Czech Republic	Rural	1987–1995
(3) Kopisty	Czech Republic	Industrial	1987–2009
(4) Espoo	Finland	Urban	1987–1995
(5) Ähtäri	Finland	Rural	1987–2003
(6) Helsinki-Vallila	Finland	Industrial	1987–1995
(7) Waldhof-Langenbrügge	Germany	Rural	1987–2003
(8) Aschaffenburg	Germany	Urban	1987–1995
(9) Langenfeld-Reusrath	Germany	Rural	1987–2003
(10) Bottrop	Germany	Industrial	1987–2009
(11) Essen-Leithe	Germany	Rural	1987–1995
(12) Garmisch-Partenkirchen	Germany	Rural	1987–1995
(13) Rome	Italy	Urban	1987–2009
(14) Casaccia	Italy	Rural	1987–2009
(15) Milan	Italy	Urban	1987–2009
(16) Venice	Italy	Urban	1987–2009
(17) Vlaardingen	Netherlands	Industrial	1987–1995
(18) Eibergen	Netherlands	Rural	1987–1995
(19) Vredepeel	Netherlands	Rural	1987–1995
(20) Wijnandsrade	Netherlands	Rural	1987–1995
(21) Oslo	Norway	Urban	1987–2009
(22) Borregard	Norway	Industrial	1987–1995
(23) Birkenes	Norway	Rural	1987–2009
(24) Stockholm South	Sweden	Urban	1987–2009
(25) Stockholm Centre	Sweden	Urban	1987–1995
(26) Aspvreten	Sweden	Rural	1987–2009
(27) Lincoln Cathedral	United Kingdom	Urban	1987–2009
(28) Wells Cathedral	United Kingdom	Urban	1987–1995
(29) Clatteringshaws Loch	United Kingdom	Rural	1987–1988
(30) Stoke Orchard	United Kingdom	Industrial	1987–1993
(31) Madrid	Spain	Urban	1987–2009
(32) Bilbao	Spain	Industrial	1987–1995
(33) Toledo	Spain	Rural	1987–2009
(34) Moscow	Russian Federation	Urban	1987–2003
(35) Lahemaa	Estonia	Rural	1987–2009
(36) Lisbon	Portugal	Urban	1987–2003
(37) Dorset	Canada	Rural	1987–2006
(38) Research Triangle Park	USA	Rural	1987–1995
(39) Steubenville	USA	Industrial	1987–1995
(40) Paris	France	Urban	1997–2009
(41) Berlin	Germany	Urban	1997–2009
43) Tel Aviv	Israel	Urban	1997–2001
(44) Svanvik	Norway	Rural	1997–2009
(45) Chaumont	Switzerland	Rural	1997–2009
(46) London	United Kingdom	Urban	1997–2003
(47) Los Angeles	USA	Urban	1997–2001
(49) Antwerpen	Belgium	Urban	1997–2003
(50) Katowice	Poland	Industrial	2000–2009
(51) Athens	Greece	Urban	2005–2009
(52) Riga	Latvia	Urban	2005–2009

Table 1: Continued.

Name	Country	Site type[a]	Available data
(53) Vienna	Austria	Urban	2008-2009
(54) Sofia	Bulgaria	Urban	2008-2009

[a]The characterisation of test sites as rural/urban/industrial is in some cases a difficult decision and is not an indication of the corrosivity of the test site.

been reported for 1987–1989 [3], 1989-1990 [9], 1990-1991 [10], 1991-1992 [16], 1992-1993 [17], 1993-1994 [20], 1987–1995 [21], 1995–1998 [33], 1998-1999 [39], 1997–2001 [40], 2002-2003 [49], 2005-2006 [51], and 2008-2009 [66]. Table 2 gives an overview of the reported environmental data for the period 1987–2009.

Temperature and relative humidity have always been included as a representation of the climatic conditions. Time of wetness was included from the beginning but has not been reported since 1995, with the reason being that this parameter is not given from meteorological institutions but needs to be calculated from highly time-resolved data of temperature and relative humidity, which is not always practical. Also the additional information contained in this variable, compared to what is already included in annual averages of temperature and relative humidity, is very limited. Sunshine data was also included from the beginning but has not been reported since 2005. This is a parameter that is especially important for polymeric materials and paint coatings, which were not exposed in the 2005-2006 and 2005-2006 trend exposures.

The gaseous pollutants SO_2 and NO_2 were included from the beginning as mandatory parameters, and in connection with the multipollutant exposure more emphasis was also put on O_3. A special campaign was launched in connection with the MULTI-ASSESS project in 2002-2003 [71], and since then HNO_3 and particulate matter has been included as mandatory parameters.

5. Dose-Response Functions

One of the main aims of ICP Materials from the beginning has been to "perform a quantitative evaluation of the effects of multipollutants such as S and N compounds, O_3 and particles, as well as climate parameters, on the atmospheric corrosion and soiling of important materials, including materials used in objects of cultural heritage". This has been done by developing dose-response functions. Of all the functions that have been developed through the years, some have been selected as suitable for mapping effects on materials. These are given in the UN ECE Manual on Methodologies and Criteria for Modelling and Mapping Critical Loads and Levels; and Air Pollution Effects, Risks and Trends [89]. As described in the manual, two sets of functions have been developed. One for the SO_2 dominating situation [90], based on data from the original exposure (1987–1995) and one for the multipollutant situation [91], based on data from the multipollutant exposure (1997–2001). The dose-response functions given in the mapping manual are valid for unsheltered conditions, see Table 3.

6. Trends in Pollution, Corrosion, and Soiling

6.1. Trends in Pollution and Corrosion (1987–2009). The average absolute pollutant levels have changed during the period 1987–2009 not only because of changing pollutant concentrations, but also because of ICP Materials test site selection. Figure 2 shows average relative SO_2, NO_2, and O_3 concentrations at ICP Materials sites, corrected for site selection. The average trends are quite different for the gases. O_3 increased during the 1990s but has been relatively constant after this period. NO_2 has decreased and continues to decrease over the entire period, while the decrease in SO_2 ceased during 2000 to 2006 with a slight decrease in the most recent exposure in 2008-2009. Corrosion of materials has decreased during the same period, mainly due to the decreasing SO_2 concentration, but to varying degrees depending on the material. Figure 3 shows the surface recession of limestone for the exposure periods 1987-1988, 1997-1998, 2002-2003, 2005-2006, and 2008-2009.

Compared to the first exposure, the values today are obviously lower, but there is significant year to year variation and there is no obvious decrease since 1998. The same is true for zinc (Figure 4). In Figure 4, it is an obvious difference between traditional and blasted zinc, with use of the latter resulting in corrosion values on average almost twice that of traditional zinc. Therefore, blasted zinc values are shown in a different scale (Figure 4, right) in order to make a complete visual impression of the relative zinc trends. For carbon steel, however, the decrease in corrosion is in principle following an exponential decay with corrosion halving its value each 12th year in industrial/urban areas and each 16th year in rural areas (Figure 5).

6.2. Recent Trends in N Pollutants (HNO_3, NO_2, and Particulate NO_3^-). Nitric acid and particulate nitrate are the most stable forms when the primary pollutants nitric oxide and nitrogen dioxide are transformed in the atmosphere. There are very few reported measurements of HNO_3 and particulate NO_3^- in urban air in Europe and elsewhere. Nitric acid is a strong acid and its salts are very hygroscopic. It can, therefore, lead to increased atmospheric corrosion [92]. In the EU project MULTI-ASSESS [71], a diffusive sampler was validated for HNO_3 and a surrogate surface for particulate deposition was chosen for air quality measurements in connection with corrosion studies [72]. Nitric acid is rapidly adsorbed on most surfaces and, therefore, has a very high dry deposition velocity. Nanoparticles and coarse particles, but not accumulation mode particles, also deposit fast to surfaces. Nanoparticles generally represent a negligible fraction of the total airborne particle mass.

Table 2: Reported environmental data from ICP Materials test 1987–2009: X: mandatory; (X): optional; —: not reported.

Parameter	Symbol	Unit	1987–1995	1995–2001	2002-2003	2005–2009
Temperature	T	°C	X	X	X	X
Relative humidity	Rh	%	X	X	X	X
Time of wetness	Tow	h	X	—	—	—
Sunshine	Sun	h	X	—	—	—
Sunshine[a]	Sun	MJ m^{-2}	X	X	X	—
SO_2 concentration	SO_2	$\mu g\ m^{-3}$	X	X	X	X
NO_2 concentration	NO_2	$\mu g\ m^{-3}$	X	X	X	X
O_3 concentration	O_3	$\mu g\ m^{-3}$	(X)	(X)	X	X
HNO_3 concentration	HNO_3	$\mu g\ m^{-3}$	—	(X)[b]	(X)	X
Precipitation: amount	Prec	mm	X	X	X	X
(i) conductivity	Cond	$\mu S\ cm^{-1}$	X	X	X	(X)
(ii) pH	pH	—	X	X	X	X
(iii) SO_4^{2-}, NO_3^-, Cl^-	varies	$mg\ L^{-1}$	X	X	X	X
(iv) $HN4^+$, Na^+, Ca^{2+}, Mg^{2+}, K^+	varies	$mg\ L^{-1}$	(X)	(X)	(X)	(X)
Particulate matter	PM	$\mu g\ cm^{-2}\ month^{-1}$	—	(X)[b]	(X)	X

[a]Calculated from sunshine hours and latitude.
[b]Only data at a few test sites reported.

Table 3: Materials for which dose-response functions are given for the SO_2 dominating situation (top) and the multipollutant situation (bottom) in the UNECE Mapping Manual and the required environmental data.

Material	T	Rh	SO_2	O_3	HNO_3	PM10	Prec	pH	Cl^-
Weathering steel	X	X	X						
Zinc	X	X	X				X	X	
Aluminium	X	X	X				X		X
Copper	X	X	X	X			X	X	
Bronze	X	X	X				X	X	X
Limestone	X		X				X	X	
Sandstone	X		X				X	X	
Coil-coated steel with alkyd melamine	X	X	X				X		
Steel panel with alkyd	X	X	X				X		
Carbon steel (multipollutant)	X	X	X			X	X	X	
Zinc (multipollutant)	X	X	X		X				
Bronze (multipollutant)	X	X	X			X	X	X	
Limestone (multipollutant)		X	X		X	X	X	X	

Therefore, deposited particulate nitrate are mainly associated with coarse particles. Coarse particles are often alkaline and can also contain sodium chloride. These properties make them a sink for nitric acid. The reaction can either take place in the atmosphere or on already deposited particles.

Nitrogen oxides are mainly emitted as nitric oxide, but a small fraction is also emitted as nitrogen dioxide. The directly emitted nitrogen dioxide fraction from vehicles has increased during the last decades partly due to modern diesel engines. Nitric oxide forms nitrogen dioxide by reaction with ozone (R1):

$$NO + O_3 \longrightarrow NO_2 + O_2 \quad (R1)$$

$$NO2 + OH \xrightarrow{M} HNO_3 \quad (R2)$$

$$NO_2 + O_3 \longrightarrow NO_3 + O_2$$

$$NO_3 + NO_2 \longleftrightarrow N_2O_5 \quad (R3)$$

$$N_2O_5 + H_2O \longrightarrow 2HNO_3$$

$$2NO_2 + H_2O \longrightarrow HONO + HNO_3 \quad (R4)$$

The main reaction for oxidizing NO_2 to HNO_3 is the daytime gas-phase oxidation with OH radicals (R2). NO_2 can also be oxidized during nighttime by ozone through a series of reactions involving nitrate radicals and dinitrogen pentoxide (R3). Further, NO_2 adsorbed on a wet surface can recombine giving nitrous acid, HONO, and HNO_3 (R4).

HNO_3 was measured with diffusive samplers [93] and nitrate on deposited particles with a surrogate surface [94].

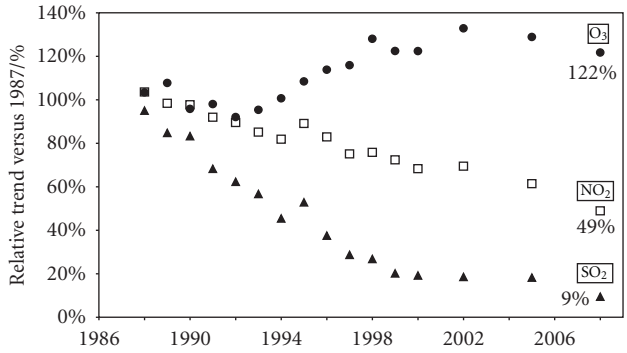

Figure 2: Average SO_2, NO_2 and O_3 trends relative to the year 1987 at ICP Materials test sites.

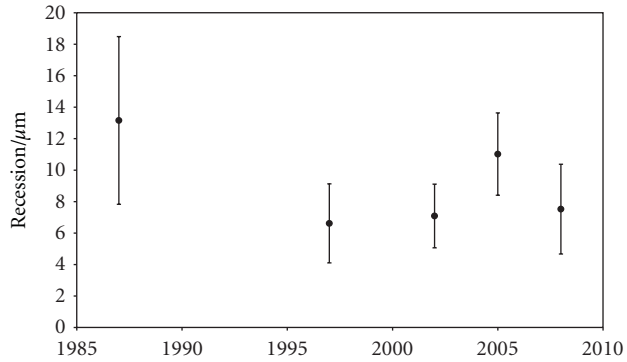

Figure 3: Averages and ranges (standard deviations) of limestone surface recession at ICP Materials test sites (one year exposures).

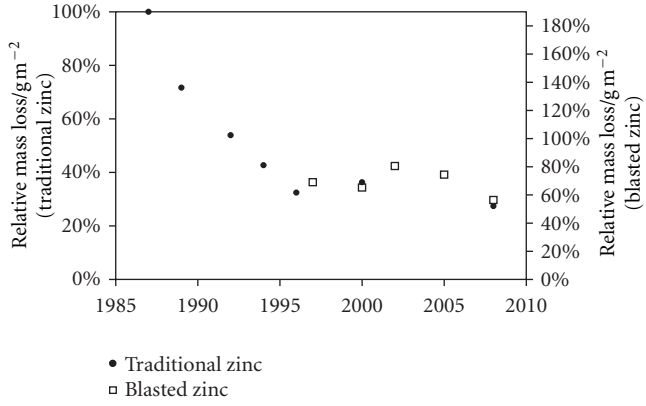

Figure 4: Average relative zinc corrosion at ICP Materials test sites. Values for both traditional and blasted zinc have been normalised to the 1987-1988 value for traditional zinc before averaging.

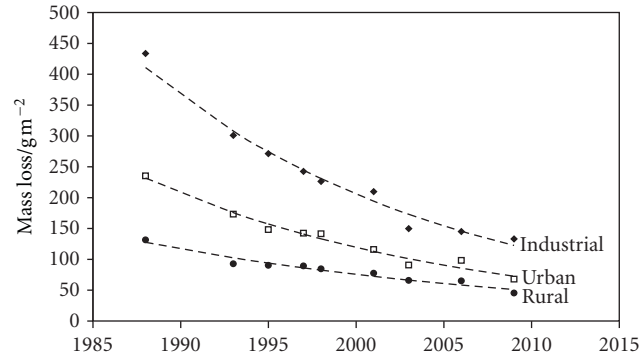

Figure 5: Carbon steel corrosion for industrial, urban, and rural ICP Materials test sites.

The exposure time was generally 2 months and each campaign lasted one year for the periods 2002-2003, 2005-2006, and 2008-2009. Two precursors to HNO_3, namely, NO_2 and O_3, were in the 2002-2003 exposure measured with diffusive samplers, or with other methods depending on exposure time and site. Most sites in ICP Materials used chemiluminescent and UV-instruments, respectively, to measure NO_2 and O_3. Monthly averages are available from these measurements. Some sites used, however, the same diffusive samplers as in 2002-2003.

Since only 17 stations (12 urban and 5 rural) did nitric acid measurements in all three campaigns, the nitric acid concentrations are compared between two campaigns at a time, in order to use all data and to see if there is a trend or random changes, as presented in Figure 6. The results are well correlated between the campaigns except for a few odd sites, which were excluded in the linear regression lines. The decrease in nitric acid concentrations seems to be substantial, on the average about 20% per three-year period, which would correspond to about 50% for a 10-year period, should the decrease continue at the same rate.

The concentrations of the precursors NO_2 and O_3 were also lower during the campaign 2008-2009 compared to 2002-2003, see Figure 7. As can be seen from the figure, the annual average concentration of these precursors has also decreased during this period (see also Figure 2 presented above). Since particulate nitrate requires a counter ion, it is not likely that the deposited particulate nitrate formation rate is proportional to the nitric acid concentration in air. A small decrease in particulate nitrate deposition was, however, observed between the first and latest campaigns.

To illustrate the correlation between HNO_3 concentration and its precursors, the concentrations were plotted against the latitude of the sites. Figure 8 shows that the HNO_3 concentration decreases from south to north, while the precursors' concentrations are not well correlated with latitude. This suggests that the photochemical formation of nitric acid (R2) is the most important. This is also supported by Figure 9, which shows the average seasonal variation of the HNO_3 concentration. Nitric acid and ozone both show a seasonal trend with maximum during the brightest time of the year and minima during the darkest.

At four places in the network, a rural site is quite close to a corresponding urban site. At these sites (Toledo-Madrid, Birkenes-Oslo, Aspvreten-Stockholm, and Casaccia-Rome) the HNO_3 concentrations are much higher at the urban sites than the rural except for Casaccia-Rome where they are quite similar. The NO_2 concentrations were always much lower at the nearby rural sites.

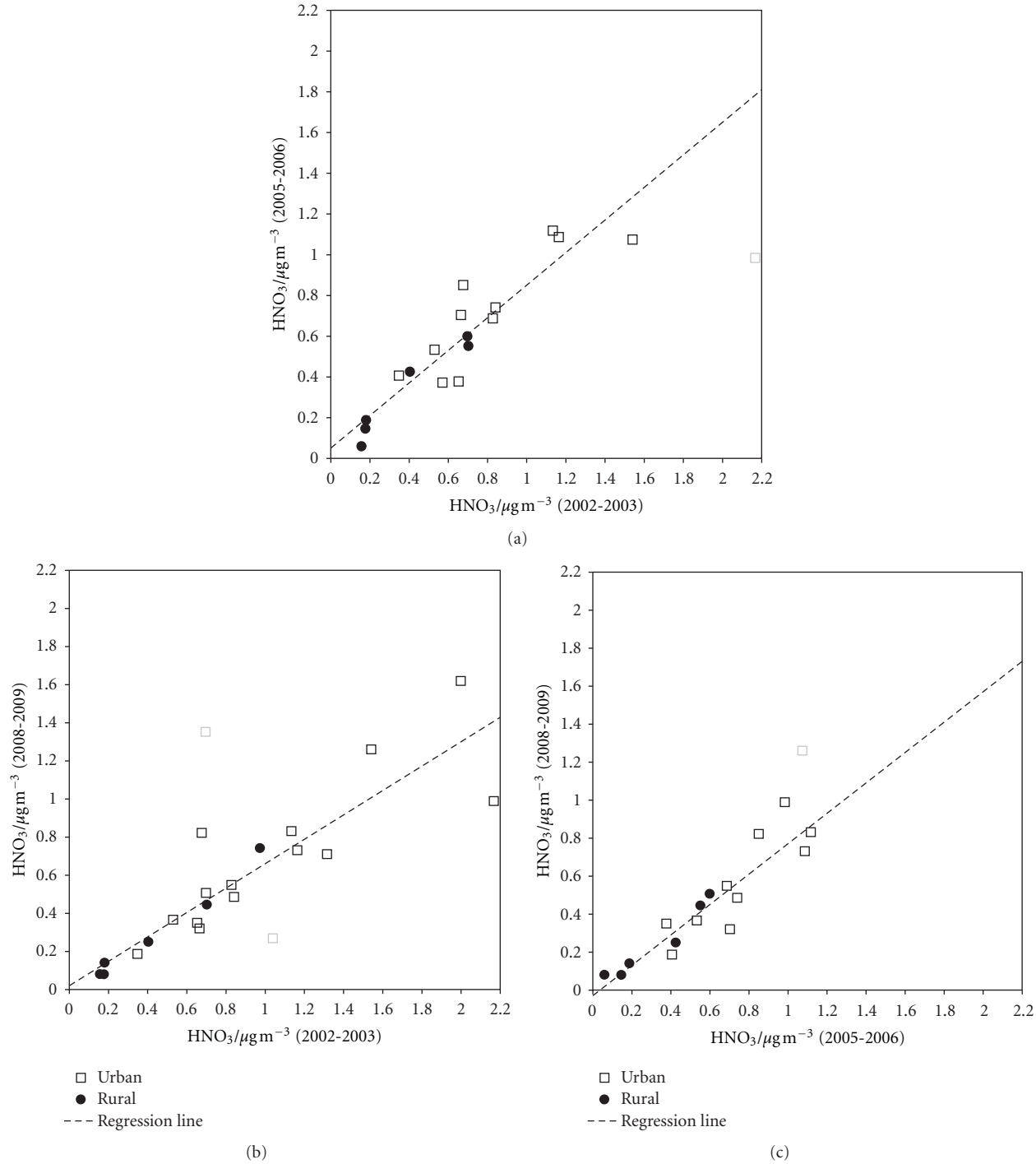

Figure 6: Annual average HNO_3 concentration at ICP Materials test sites for the three one-year campaigns 2002-2003, 2005-2006, and 2008-2009. The grey squares have been excluded when calculating the linear regression lines $y = 0.80x + 0.05$ (2005-2006 *versus* 2002-2003), $y = 0.80x - 0.03$ (2008-2009 *versus* 2005-2006), $y = 0.64x + 0.02$ (2008-2009 *versus* 2002-2003).

6.3. Recent Trends in Soiling of Modern Glass. Due to the increasing importance of particulate matter, modern glass was officially included as a trend material for soiling of materials in the 2005-2006 exposure, so this means that only two exposure periods are available. Dose-response functions are currently being evaluated [58, 95], but the final functions will not be available until end 2013 and will include results also after four years of exposure (2008–2012). Figure 10 shows soiling of modern glass measured by the haze parameter, which is the ratio between the diffuse and direct transmitted light. Taking into account the accuracy of the measurements, it is not possible to say that soiling, on

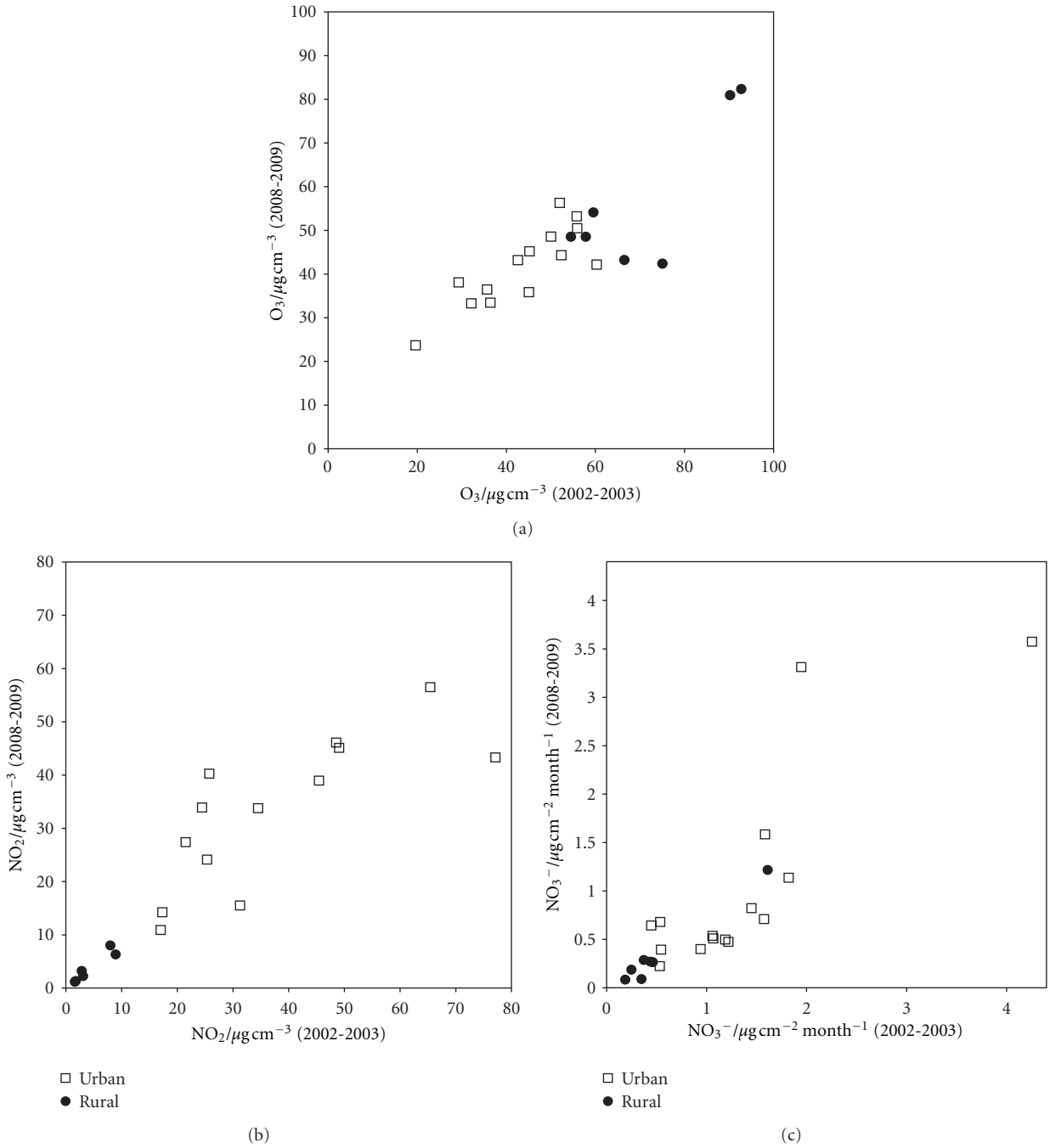

Figure 7: Annual average O_3 concentration, NO_2 concentration, and NO_3^- deposition at ICP Materials test sites for the two one-year campaigns 2002-2003, and 2008-2009.

average, has increased or decreased when comparing the two exposure periods 2005-2006 and 2008-2009.

7. Use of Results for Policy Purposes

The last main aim of ICP Materials is to "use the results for mapping areas with increased risk of corrosion and soiling, and for calculation of cost of damage caused by deterioration of materials". This was put high on the agenda in 2005 when Italy was selected as responsible for a new subcentre on the assessment of stock of materials at risk and cultural heritage, and Sweden and Italy started to share the position as chairs of ICP Materials.

The main results from ICP Materials in this area are the case studies on assessment of stock at risk and mapping areas of increased corrosion risk in Madrid [56, 96] and Italy [59, 62], and recent reviews of available data on stock of materials at risk [60] and economic evaluations [64]. Also

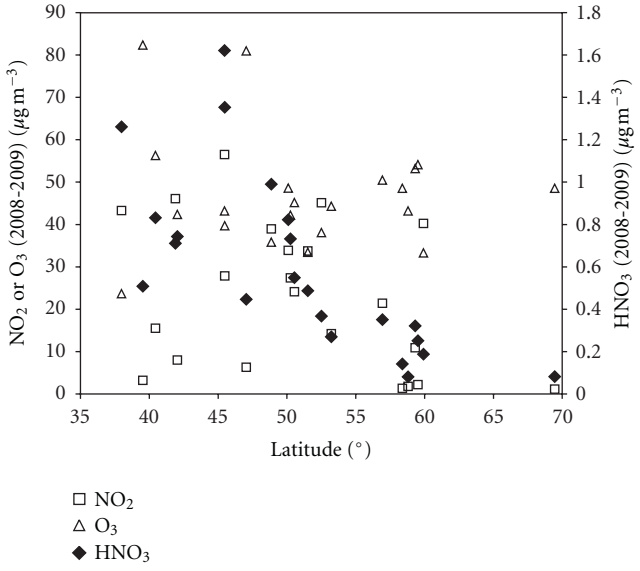

Figure 8: The concentration of nitric acid during 2008/09 and two of its precursors as a function of latitude.

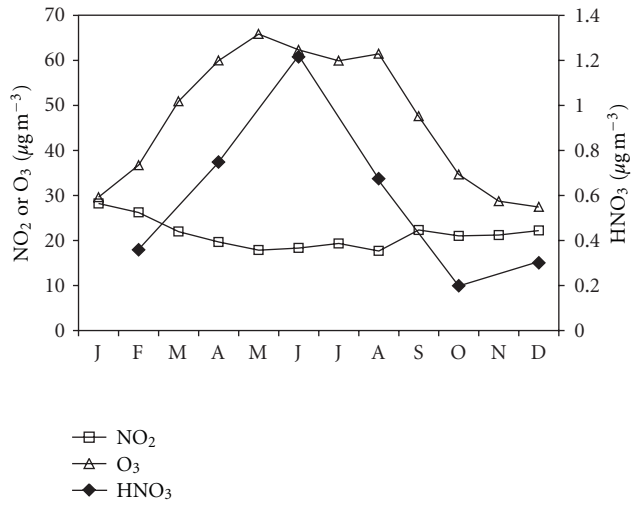

Figure 9: Seasonal cycle of nitric acid and two of its precursors during 2008/09.

there was a close link between ICP Materials and the CULTSTRAT project, which resulted in a book on effects of air pollution on cultural heritage, which included significant parts from the ICP Materials project, including stock at risk studies and discussion on the use of results for policy purposes [72].

At least two separate ways are possible in order to use the results for policy purposes, as outlined in the recent report on economic assessment [64]. The first, and most preferable if all data are available, is to perform a complete evaluation of cost savings (as part of a cost-benefit analysis) for materials and cultural heritage due to reductions in air pollution based on assessment of stock of materials at risk, data on maintenance practices, and costs and mapped

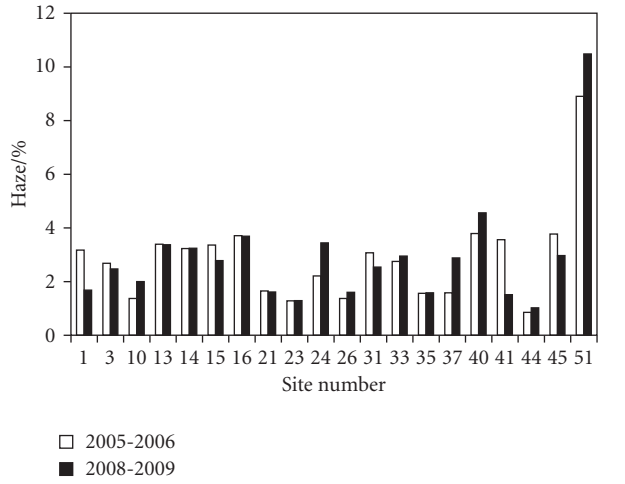

Figure 10: Soiling of modern glass at ICP Materials test sites (see Table 1).

areas of corrosion risk. The other approach is to use the concept of tolerable corrosion/soiling and pollution levels for indicator materials. The last approach is currently used in the evaluation of results from the working group on effect in connection with the current revision of the Gothenburg protocol [97].

Figure 11 shows a selected map [59] of calculated corrosion values for limestone. As is evident from the figure, the scale on which the original data is presented has a large impact on the results. If the scale is too coarse to capture the variation in urban areas, where cultural heritage is located, then the calculated corrosion attack can be significantly underestimated.

8. Plans for Future Exposures

A new trend exposure will start in the fall of 2011. Besides the usual trend exposures of carbon steel, zinc, limestone and modern glass, which are now part of the on-going three-year cycle of trend exposures, additional exposures will start including 4-year samples of these materials (2011–2015) as well as corresponding exposures for weathering steel, copper, and possibly aluminium. In addition, a new test site will be launched in St Petersburg. The incorporation of countries in Eastern Europe, Caucasus, and Central Asia (EECCA countries), that is, Armenia, Azerbaijan, Belarus, Georgia, Kazakhstan, Kyrgyzstan, Moldova, Russian Federation, Tajikistan, Turkmenistan, Ukraine, and Uzbekistan, is a high priority of the Convention.

9. Conclusions

An overview of available results from ICP Materials has been presented. Since the main focus of the programme has been to use the results for development of the policy process within the Convention on Long-range Transboundary Air Pollution, there are still significant parts of the results that

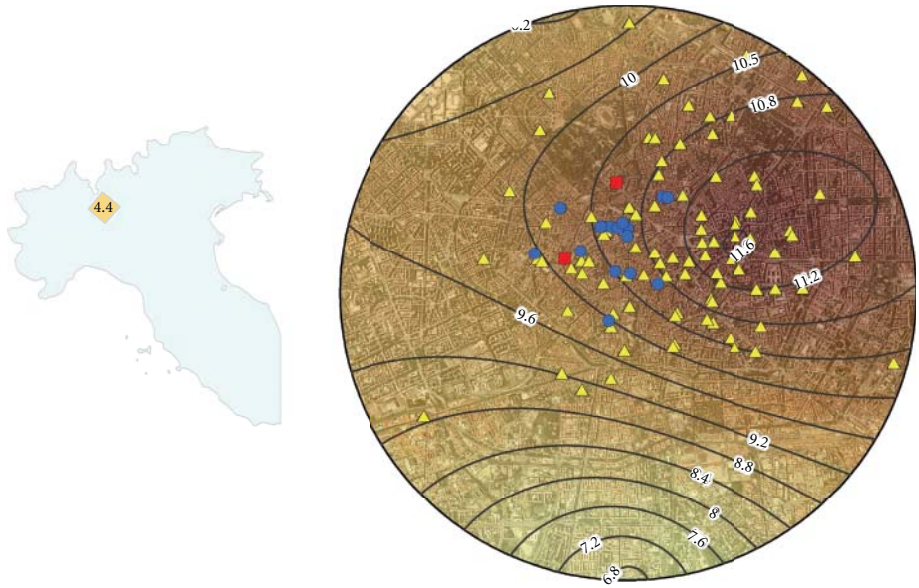

Figure 11: Calculated surface recession of limestone in μm (one-year exposure), based on the dose-response function for the SO_2 dominating situation, for the Milan city centre, reported either as one single value based on the EMEP 50 km × 50 km grid cell (left, 4.4 μm) or as a map of the city centre based on local data (right, 6.8 to 11.6 μm). Coloured symbols (blue, red, and yellow) in the map to the right indicate different types of cultural heritage [59].

have not been published outside the official UNECE ICP Materials report series.

Results on recent trends in corrosion, soiling, and pollution have been presented for the indicator materials carbon steel, zinc limestone, modern glass, and for the gaseous pollutants SO_2, NO_2, O_3, and HNO_3.

(i) Carbon steel corrosion has since the beginning of exposures (1987) decreased exponentially at industrial, urban, and rural sites so that the corrosion has been halved about each 12th year for industrial/urban sites and each 16th year for rural sites.

(ii) Zinc and limestone corrosion have decrease substantially compared to the levels in 1987, but since the turn of the century there is no obvious average trend in the ICP Materials network of test sites.

(iii) Modern glass as an indicator for soiling has only been exposed for two periods so far, 2005-2006 and 2008-2009, and when comparing the results from these periods, there is no average difference in the results. However, more exposures are needed before long-term trends can be established.

(iv) Nitric acid concentrations were measured in 2002-2003, 2005-2006, and 2008-2009. When comparing these three periods, the relative decrease was about the same from 2002-2003 to 2005-2006 as it was from 2005-2006 to 2008-2009, corresponding to about 50% for a 10-year period, should the decrease continue at the same rate. However, only three exposure periods are not sufficient to rule out that this apparent trend is not instead part of a natural year-to-year variation.

Acknowledgments

Coauthors to this paper are those who are currently active in the work of ICP Materials. However, during the years many researchers and organisations have come and left and the work would not have been possible without them. Since the list would otherwise most likely be incomplete, only previously involved organisations are listed here: (i) Technical Research Centre of Finland (VTT), (ii) Bavarian State Department of Historical Monuments, Germany, (iii) TNO Division of Technology for Society Department of Environmental Chemistry, the Netherlands, (iv) Institute of Physical Chemistry, Russian Academy of Sciences, Russian Federation, (v) Institute of Technology, Laboratory of Mineralogy and Petrology, Portugal, (vi) National Research Council of Canada and the Ministries of the Environment of Canada and of Ontario, (vii) United States Environmental Protection Agency, (viii) Israel Antiquities Authority, Conservation Department, and (ix) Department of Chemistry, University of Antwerp, Belgium. This compilation work was financed by the Swedish Environmental Protection Agency. However, ICP Materials has been and is financed by numerous sources and these can be found in the original papers referenced in this publication.

References

[1] C. Leygraf and V. Kucera, "UNECE international co-operative programme on effects on materials, including historic and cultural monuments," Tech. Rep. 1, Swedish Corrosion Institute, Stockholm, Sweden, 1988.

[2] C. Leygraf and V. Kucera, "UNECE international co-operative programme on effects on materials, including historic and

cultural monuments," Report no. 2 Description of test sites, Swedish Corrosion Institute, Stockholm, Sweden, 1993.

[3] J. F. Henriksen, K. Arnesen, A. Rode et al., "UNECE international co-operative programme on effects on materials, including historic and cultural monuments," Report no. 3 Environmental data report, September 1987 to August 1989, Norwegian Institute for Air Research (NILU), Lillestrøm, Norway, 1991.

[4] A.T. Coote, T. J. S. Yates, S. Chakrabarti, D. J. Bigland, J. P. Ridal, and R. N. Butlin, "UNECE international co-operative programme on effects on materials, including historic and cultural monuments," Report no. 4 Evaluation of decay to stone tablets: part 1. After exposure for 1 year and 2 years, Building Research Establishment (BRE), Watford, UK, 1991.

[5] B. Stöckle, G. Pöhlmann, M. Mach, and R. Snethlage, "UNECE international co-operative programme on effects on materials, including historic and cultural monuments," Report no. 5 Corrosion attack on copper and cast bronze. Evaluation after 1 and 2 years of exposu, Bavarian State Conservation Office, Münich, Germany, 1991.

[6] P. Holler, D. Knotkova, A. Bouskova et al., "UNECE international co-operative programme on effects on materials, including historic and cultural monuments," Report no. 6. Corrosion attack on steel, zinc and aluminium. Evaluation after 1 and 2 years of exposure, National Research Institute for the Protection of Materials, Prague, Czech Republic, 1991.

[7] J. F. Henriksen, A. Bartonova, O. Anda, and A. Rode, "UNECE international co-operative programme on effects on materials, including historic and cultural monuments," Report no. 7 Results for evaluation of decay to paint systems for wood, steel and galvanized steel after 1 and 2 years of exposure, Norwegian Institute for Air Research (NILU), Lillestrøm, Norway, 1992.

[8] J. Tidblad, C. Leygraf, and V. Kucera, "UNECE international co-operative programme on effects on materials, including historic and cultural monuments," Report no. 8 Corrosion attack on electric contact materials. Evaluation after 1 and 2 years of exposure, Swedish Corrosion Institute, Stockholm, Sweden, 1991.

[9] J. F. Henriksen, A. Bartonova, K. Arnesen, and A. Rode, "UNECE international co-operative programme on effects on materials, including historic and cultural monuments," Report no. 9 Environmental data report. September 1989 to August 1990, Norwegian Institute for Air Research (NILU), Lillestrøm, Norway, 1992.

[10] J. F. Henriksen, A. Bartonova, K. Arnesen, and A. Rode, "UNECE international co-operative programme on effects on materials, including historic and cultural monuments," Report no. 10 Environmental data report. September 1990 to August 1991, Norwegian Institute for Air Research (NILU), Lillestrøm, Norway, 1992.

[11] B. Stöckle, A. Reisener, and R. Snethlage, "UNECE international co-operative programme on effects on materials, including historic and cultural monuments," Report no. 11 Corrosion attack on copper and cast bronze. Evaluation after 4 years of exposure, Bavarian State Conservation Office, Münich, Germany, 1993.

[12] D. Knotkova, K. Kreislova, P. Holler, and J. Vlckova, "UNECE international co-operative programme on effects on materials, including historic and cultural monuments," Report no. 12 Corrosion attack on weathering steel, zinc and aluminium. Evaluation after 4 years of exposure, National Research Institute for the Protection of Materials, Prague, Czech Republic, 1993.

[13] A. T. Coote, T. J. S. Yates, S. Chakrabarti, M. J. Murray, and R. N. Butlin, "UNECE international co-operative programme on effects on materials, including historic and cultural monuments," Report no. 13 Evaluation of decay to stone tablets: part 2. After exposure for 4 years, Building Research Establishment (BRE), Watford, UK, 1993.

[14] J. F. Henriksen, K. Arnesen, O. Anda, and A. Rode, "UNECE international co-operative programme on effects on materials, including historic and cultural monuments," Report no. 14 Evaluation of decay to paint systems for wood, steel and galvanized steel after 4 years of exposure, Norwegian Institute for Air Research (NILU), Lillestrøm, Norway, 1993.

[15] J. Tidblad, C. Leygraf, and V. Kucera, "UNECE international co-operative programme on effects on materials, including historic and cultural monuments," Report no. 15 Corrosion attack on electric contact materials. Evaluation after 4 years of exposure, Swedish Corrosion Institute, Stockholm, Sweden, 1993.

[16] J. F. Henriksen, K. Arnesen, and A. Rode, "UNECE international co-operative programme on effects on materials, including historic and cultural monuments," Report no. 16 Environmental data report. September 1991 to August 1992, Norwegian Institute for Air Research (NILU), Lillestrøm, Norway, 1993.

[17] J. F. Henriksen, K. Arnesen, A. Rode et al., "UNECE international co-operative programme on effects on materials, including historic and cultural monuments," Report no. 17 Environmental data report. September 1992 to August 1993, Norwegian Institute for Air Research (NILU), Lillestrøm, Norway, 1993.

[18] V. Kucera, J. Tidblad, J. F. Henriksen, A. Bartonova, and A. A. Mikhailov, "UNECE international co-operative programme on effects on materials, including historic and cultural monuments," Report no. 18 Statistical analysis of 4 year materials exposure and acceptable deterioration and pollution levels, Swedish Corrosion Institute, Stockholm, Sweden, 1995.

[19] D. Knotkova, K. Kreislova, and P. Boschek, "UNECE international co-operative programme on effects on materials, including historic and cultural monuments," Report no. 19 Trends of corrosivity based on corrosion rates and pollution data, part 1, National Research Institute for the Protection of Materials, Prague, Czech Republic, 1995.

[20] J. F. Henriksen, K. Arnesen, and A. Rode, "UNECE international co-operative programme on effects on materials, including historic and cultural monuments," Report no. 20 Environmental data report. September 1993 to August 1994, Norwegian Institute for Air Research (NILU), Lillestrøm, Norway, 1996.

[21] J. F. Henriksen, A. Dahlback, K. Arnesen Rode, U. Elvedal, and A Rode, "UNECE international co-operative programme on effects on materials, including historic and cultural monuments," Report no. 21 Environmental data report. September 1993 to August 1994, Norwegian Institute for Air Research (NILU), Lillestrøm, Norway, 1997.

[22] D. Knotkova, K. Kreislova, P. Boschek, and J. Vlckova, "UNECE international co-operative programme on effects on materials, including historic and cultural monuments," Report no. 22 Corrosion attack on weathering steel, zinc and aluminium, Evaluation after 8 years of exposure, SVUOM Praha a. s., Prague, Czech Republic, 1998.

[23] B. Stöckle, A. Krätschmer, M. Mach, and R. Snethlage, "UNECE international co-operative programme on effects on materials, including historic and cultural monuments," Report

no. 23 Corrosion attack on copper and cast bronze. Evaluation after 8 years of exposure, Bavarian State Conservation Office, Münich, Germany, 1998.

[24] R. N. Butlin, T. Yates, G. J. Ashall, and S. Massey, "UNECE international co-operative programme on effects on materials, including historic and cultural monuments," Report no. 24 Evaluation of decay to stone tablets: part 3. After exposure for 8 years, Building Research Establishment (BRE), Watford, UK, 1998.

[25] J. F. Henriksen, O. Anda, A. Bartonova, K. Arnesen, and U. Elvedal, "UNECE international co-operative programme on effects on materials, including historic and cultural monuments," Report no. 25 Evaluation of decay to paint systems for wood, steel and galvanized steel after 8 years of exposure, Norwegian Institute for Air Research (NILU), Kjeller, Norway, 1998.

[26] J. Tidblad and V. Kucera, "UNECE international co-operative programme on effects on materials, including historic and cultural monuments," Report no. 26 Corrosion attack on electric contact materials. Evaluation after 8 years of exposure, Swedish Corrosion Institute, Stockholm, Sweden, 1998.

[27] G. Woisetschläger and M. Schreiner, "UNECE international co-operative programme on effects on materials, including historic and cultural monuments," Report no. 27 Evaluation of decay to glass samples after 1 and 2 years of exposure, Institute of Chemistry, Academy of Fine Arts, Vienna, Austria, 1998.

[28] J. Tidblad, B. Dolezel, D. Persson, and V. Kucera, "UNECE international co-operative programme on effects on materials, including historic and cultural monuments," Report no. 28 Evaluation of decay to polymer samples after 4 years of exposure, Swedish Corrosion Institute, 1998.

[29] K. Kreislova, D. Knotkova, and P. Boschek, "UNECE international co-operative programme on effects on materials, including historic and cultural monuments," Report no. 29 Trends of corrosivity based on corrosion rates and pollution data. Part 2, SVUOM Praha a. s., Prague, Czech Republic, 1998.

[30] J. Tidblad, V. Kucera, and A. A. Mikhailov, "UNECE international co-operative programme on effects on materials, including historic and cultural monuments," Report no. 30 Statistical analysis of 8 year materials exposure and acceptable deterioration and pollution levels, Swedish Corrosion Institute, Stockholm, Sweden, 1998.

[31] B. Stöckle, A. Krätschmer, C. Gruber, and G. Pöhlmann, "UNECE international co-operative programme on effects on materials, including historic and cultural monuments," Report no. 32 Results from the exposure of patinated and waxed bronze, Bavarian State Conservation Office, Münich, Germany, 1998.

[32] A. Krätschmer and B. Stöckle, "UNECE international co-operative programme on effects on materials, including historic and cultural monuments," Report no. 33 Results from XRD analysis of copper corrosion products, Bavarian State Conservation Office, Münich, Germany, 1998.

[33] J. F. Henriksen and K. Arnesen, "UNECE international co-operative programme on effects on materials, including historic and cultural monuments," Report no. 34 Environmental data report. September 1995 to October 1998, Norwegian Institute for Air Research (NILU), Kjeller, Norway, 2000.

[34] D. Knotkova, K. Kreislova, P. Boschek, J. Kvapil, and G. Holubova, "UNECE international co-operative programme on effects on materials, including historic and cultural monuments," Report no. 35 Results from the multipollutant programme: corrosion attack on carbon steel after 1 and 2 years of exposure (1997–1999), SVUOM Ltd., Prague, Czech Republic, 2001.

[35] A. Leuenberger and M. Faller, "UNECE international co-operative programme on effects on materials, including historic and cultural monuments," Report no. 36 Results from the multipollutant programme: corrosion attack on zinc after 1 and 2 years of exposure (1997–1999), Swiss Federal Laboratories for Materials Testing and Research (EMPA), Dübendorf, Switzerland, 2001.

[36] B. Singer, E. Woznik, A. Krätschmer, and A. Doktor, "UNECE international co-operative programme on effects on materials, including historic and cultural monuments," Report no. 37 Results from the multipollutant programme: corrosion attack on copper and bronze after 1 and 2 years of exposure (1997–1999), Bavarian State Department of Historical Monuments, Münich, Germany, 2001.

[37] E. Garrod and T. Yates, "UNECE international co-operative programme on effects on materials, including historic and cultural monuments," Report no. 38 Results from the multipollutant programme: corrosion attack on limestone after 1 and 2 years of exposure (1997–1999), Building Research Establishment Ltd. (BRE), Garston, UK, 2001.

[38] J. F. Henriksen and O. Anda, "UNECE international co-operative programme on effects on materials, including historic and cultural monuments," Report no. 39 Results from the multipollutant programme: corrosion attack on painted steel after 1 and 2 years of exposure (1997–1999), Norwegian Institute for Air Research (NILU), Kjeller, Norway, 2000.

[39] J. F. Henriksen and K. Arnesen, "UNECE international co-operative programme on effects on materials, including historic and cultural monuments," Report no. 40 Environmental data report. November 1998 to October 1999, Norwegian Institute for Air Research (NILU), Kjeller, Norway, 2001.

[40] J. F. Henriksen and K. Arnesen, "UNECE international co-operative programme on effects on materials, including historic and cultural monuments," Report no. 41 Final environmental data report. November 1997 to October 2001, Norwegian Institute for Air Research (NILU), Kjeller, Norway, 2003.

[41] D. Knotkova, K. Kreislova, J. Kvapil, G. Holubova, and M. Bubenickova, "UNECE international co-operative programme on effects on materials, including historic and cultural monuments," Report no. 42 Results from the multipollutant programme: corrosion attack on carbon steel after 1, 2 and 4 years of exposure (1997–2001), SVUOM Ltd., Prague, Czech Republic, 2003.

[42] D. Reiss, M. Faller, and O. Guseva, "UNECE international co-operative programme on effects on materials, including historic and cultural monuments," Report no. 43 Results from the multipollutant programme: corrosion attack on zinc after 1, 2 and 4 years of exposure (1997–2001), Swiss Federal Laboratories for Materials Testing and Research (EMPA), Dübendorf, Switzerland, 2003.

[43] B. Singer, A. Doktor, and E. Woznik, "UNECE international co-operative programme on effects on materials, including historic and cultural monuments," Report no. 44 Results from the multipollutant programme: Corrosion attack on copper and bronze after 1, 2 and 4 years of exposure (1997–2001), Bavarian State Department of Historical Monuments, Münich, Germany, 2003.

[44] E. Garrod and T. Yates, "UNECE international co-operative programme on effects on materials, including historic and cultural monuments," Report no. 45 Results from the multipollutant programme: Corrosion attack on limestone after

1, 2 and 4 years of exposure (1997–2001), Building Research Establishment Ltd. (BRE), Garston, Watford, UK, 2003.

[45] O. Anda and J. F. Henriksen, "UNECE international co-operative programme on effects on materials, including historic and cultural monuments," Report no. 46 Results from the multipollutant programme: corrosion attack on painted steel after 1, 2 and 4 years of exposure (1997–2001), Norwegian Institute for Air Research (NILU), Kjeller, Norway, 2003.

[46] D. Knotkova, K. Kreislova, J. Kvapil, and G. Holubova, "UNECE international co-operative programme on effects on materials, including historic and cultural monuments," Report no. 47 Trends of corrosivity based on corrosion rates and pollution data. Part 3, SVUOM Ltd., Prague, Czech Republic, 2003.

[47] M. Melcher and M. Schreiner, "UNECE international co-operative programme on effects on materials, including historic and cultural monuments," Report no. 48 Results from the multipollutant programme: Evaluation of the decay to glass samples of medieval composition after 3, 4, 5 and 6 years of exposure. Part A: results of the sheltered exposure, Institute of Sciences and Technologies in Art, Academy of Fine Arts, Vienna, Austria, 2003.

[48] M. Melcher and M. Schreiner, "UNECE international co-operative programme on effects on materials, including historic and cultural monuments," Report no. 49 Results from the multipollutant programme: evaluation of the decay to glass samples of medieval composition after 3, 4, 5 and 6 years of exposure. Part B: results of the unsheltered exposure, Institute of Sciences and Technologies in Art, Academy of Fine Arts, Vienna, Austria, 2004.

[49] J. F. Henriksen, K. Arnesen, and M. Ferm, "UNECE international co-operative programme on effects on materials, including historic and cultural monuments," Report no. 50 Environmental data report. November 2002 to December 2003, Norwegian Institute for Air Research (NILU), Kjeller, Norway, 2004.

[50] J. Tidblad and V. Kucera, "UNECE international co-operative programme on effects on materials, including historic and cultural monuments," Report no. 51 Technical manual for the trend exposure programme 2005-2006, Corrosion and Metals Research Institute (KIMAB), Stockholm, Sweden, 2006.

[51] T. Grøntoft, K. Arnesen, and M. Ferm, "UNECE international co-operative programme on effects on materials, including historic and cultural monuments," Report no. 52 Environmental data report. October 2005 to December 2006, Norwegian Institute for Air Research (NILU), Kjeller, Norway, 2007.

[52] K. Kreislova, D. Knotkova, J. Kvapil, and H. Divisova, "UNECE international co-operative programme on effects on materials, including historic and cultural monuments," Report no. 53 Results from the 2005-2006 trend exposure programme. Corrosion attack of carbon steel after 1 year of exposure (2005-06), SVUOM Ltd., Prague, Czech Republic, 2007.

[53] D. Reiss and M. Faller, "UNECE international co-operative programme on effects on materials, including historic and cultural monuments," Report no. 54 Results from the 2005-2006 trend exposure programme. Corrosion attack of zinc after 1 year of exposure, Swiss Federal Laboratories for Materials Testing and Research (EMPA), Dübendorf, Switzerland, 2007.

[54] T. Yates, "UNECE international co-operative programme on effects on materials, including historic and cultural monuments," Report no. 55 Results from the 2005-2006 trend exposure programme. Corrosion attack of limestone after 1 year of exposure, Building Research Establishment Ltd. (BRE), Garston, Watford, UK, 2007.

[55] J. Tidblad, T. Grøntoft, K. Kreislova, M. Faller, and T. Yates, "UNECE international co-operative programme on effects on materials, including historic and cultural monuments," Report no. 56 Trends in pollution and corrosion of carbon steel, zinc and limestone 1987–2006, Swerea KIMAB AB, Stockholm, Sweden, 2008.

[56] D. de la Fuente, F. Viejo, J. M. Vega, and M. Morcillo, "UNECE international co-operative programme on effects on materials, including historic and cultural monuments," Report no. 57 Case study on assessment of stock at risk and mapping areas of increased corrosion risk in Madrid, National Centre for Metallurgical Research (CENIM/CSIC), Madrid, Spain, 2008.

[57] J. Tidblad, "UNECE international co-operative programme on effects on materials, including historic and cultural monuments," Report no. 58 Technical manual for the trend exposure programme 2008-2009, Swerea KIMAB AB, Stockholm, Sweden, 2009.

[58] T. Lombardo and A. Ionescu, "UNECE international co-operative programme on effects on materials, including historic and cultural monuments," Report no. 59 Soiling of exposed materials and dose-response functions for modern glass, Laboratoire Interuniversitaire des Systèmes Atmosphérique (LISA), Paris, France, 2009.

[59] S. Doytchinov, A. Screpanti, and G. Leggeri, "UNECE international co-operative programme on effects on materials, including historic and cultural monuments," Report no. 60 Combined stock at risk and mapping for selected urban areas of Italy. Italian national agency for new technologies, Energy and the Environment (ENEA), Rome, Italy, 2009.

[60] J. Tidblad, T. Yates, S. Doytchinov, M. Faller, and K. Kreislova, "UNECE international co-operative programme on effects on materials, including historic and cultural monuments," Report no. 61 Assessment of stock of materials at risk including cultural heritage, Swerea KIMAB AB, Stockholm, Sweden, 2010.

[61] J. Tidblad, K. Kreislova, M. Faller, T. Yates, T. Lombardo, and T. Grøntoft, "UNECE international co-operative programme on effects on materials, including historic and cultural monuments," Report no. 62 Results from the 2008-2009 trend exposure programme, Swerea KIMAB AB, Stockholm, Sweden, 2010.

[62] S. Doytchinov, A. Screpanti, and G. Leggeri, "UNECE international co-operative programme on effects on materials, including historic and cultural monuments," Report no. 63 Combined stock at risk and mapping for Italy at the national level. Italian national agency for new technologies, Energy and the Environment (ENEA), Rome, Italy, 2010.

[63] J. Tidblad, D. De la Fuente, M. Faller, and K. Kreislova, "UNECE international co-operative programme on effects on materials, including historic and cultural monuments," Report no. 64 Validation of dose-response functions for the SO2 dominating and multi-pollutant situation, Swerea KIMAB AB, Stockholm, Sweden, 2010.

[64] J. Tidblad, M. Faller, T. Grøntoft et al., "UNECE international co-operative programme on effects on materials, including historic and cultural monuments," Report no. 65 Economic assessment of corrosion and soiling of materials including cultural heritage, Swerea KIMAB AB, Stockholm, Sweden, 2010.

[65] J. Tidblad et al., "UNECE international co-operative programme on effects on materials, including historic and

cultural monuments," Report no. 66 Trends in pollution, corrosion and soiling 1987–2009, Swerea KIMAB AB, Stockholm, Sweden, 2011.

[66] T. Grøntoft et al., "UNECE international co-operative programme on effects on materials, including historic and cultural monuments," Report no. 67 Environmental data report. October 2008 to October 2009, Norwegian Institute for Air Research (NILU), Kjeller, Norway, 2011.

[67] http://www.corr-institute.se/ICP-Materials/.

[68] J. Sliggers and W. Kakebeeke, "Clearing the air. 25 years of the Convention on Long-range Transboundary Air Pollution," ECE/EB.AIR/84, UNECE, 2004.

[69] http://www.unece.org/env/lrtap/.

[70] B. Bolin, L. Granat, L. Ingelstam et al., "Air pollution across national boundaries. The impact on the environment of sulphur in air and precipitation," Swede's case study for the United Nations conference on the human environment, Norstedt & Sons, Stockholm, Sweden, 1971.

[71] http://www.corr-institute.se/MULTI-ASSESS.

[72] J. Watt, J. Tidblad, V. Kucera, and R. Hamilton, *The Effects of Air Pollution on Cultural Heritage*, Springer, 2009.

[73] V. Kucera et al., Model for multi-pollutant impact and assessment of threshold levels for cultural heritage (MULTI-ASSESS) EU project EVK4-CT-2001-00044, Deliverable D3.1 Evaluation of corrosion attack from the broad field exposure programme, 2004.

[74] J. Tidblad, K. Kreislova, D. Knotkova, and V. Kucera, "Exposure of weathering steels in the UN ECE ICP materials programme," in *Proceedings of the International Workshop on Atmospheric Corrosion and Weathering Steels*, Cartagena, Colombia, 2004.

[75] J. Tidblad, C. Leygraf, and V. Kucera, "Acid deposition effects on materials. Evaluation of nickel and copper," *Journal of the Electrochemical Society*, vol. 138, no. 12, pp. 3592–3598, 1991.

[76] J. Tidblad, C. Leygraf, and V. Kucera, "Acid deposition effects on materials. Evaluation of silver after 4 years of exposure," in *Proceedings of the 12th Scandinavian Corrosion Congress (Eurocorr '92)*, vol. 179, Espoo, Finland, June 1992.

[77] J. Tidblad, C. Leygraf, and V. Kucera, "Acid deposition effects on materials: evaluation of nickel after four years of exposure," *Journal of the Electrochemical Society*, vol. 140, no. 7, pp. 1912–1916, 1993.

[78] J. Tidblad, *Atmospheric Corrosion of Ni, Cu, Ag and Sn by acidifying pollutants in sheltered environments. A combined statistical and surface analysis*, Ph.D. thesis, Royal Institute of Technology, Stockholm, Sweden, 1994.

[79] J. Tidblad, C. Leygraf, and V. Kucera, "Acid deposition effects of materials. Evaluation of electric contact materials after four years of exposure," *Atmospheric Corrosion (ASTM STP 1239)*, pp. 11–25, 1995.

[80] G. Woisetschläger, *SEM investigations of weathered potash-lime-silica glass in the international co-operative programme on assessment and monitoring of air pollution effects of the economic commission for Europe within the united nations*, diploma thesis, Vienna University of Technology, Vienna, Austria, 1995.

[81] G. Woisetschläger, *Weathering of medieval potash-lime-silca glass in the international co-operative programme on assessment and monitoring of air pollution effects of the economic commission for Europe within the united nations*, Ph.D. thesis, Vienna University of Technology, Vienna, Austria, 1998.

[82] M. Dutz, *Untersuchungen der korrosionsvorgänge von natürlich verwitterten kalk-kali-silicatgläsern mittels elektronenstrahl (ESMA) und kernreaktionsanalyse (NRA)*, diploma thesis, Vienna University of Technology, Vienna, Austria, 1995.

[83] M. Melcher, *Weathering of low-durability potash-lime-silica glass*, Ph.D. thesis, Vienna University of Technology, Vienna, Austria, 2005.

[84] G. Woisetschläger, M. Dutz, S. Paul, and M. Schreiner, "Weathering phenomena on naturally weathered potash-lime-silica-glass with medieval composition studied by secondary electron microscopy and energy dispersive microanalysis," *Microchimica Acta*, vol. 135, no. 3-4, pp. 121–130, 2000.

[85] M. Melcher and M. Schreiner, "Statistical evaluation of potash-lime-silica glass weathering," *Analytical and Bioanalytical Chemistry*, vol. 379, no. 4, pp. 628–639, 2004.

[86] M. Melcher and M. Schreiner, "Evaluation procedure for leaching studies on naturally weathered potash-lime-silica glasses with medieval composition by scanning electron microscopy," *Journal of Non-Crystalline Solids*, vol. 351, no. 14-15, pp. 1210–1225, 2005.

[87] M. Melcher, M. Schreiner, and K. Kreislova, "Artificial weathering of model glasses with medieval composition—an empirical study on the influence of particulates," *Physics and Chemistry of Glasses B*, vol. 49, no. 6, pp. 346–356, 2008.

[88] J. Tidblad, V. Kucera, D. Persson, and B. Dolozel, "Decay of polymer materials. Preliminary dose-response functions after 4 years of exposure. Natural and artificial ageing of polymers," in *Proceedings of the 1st European Weathering Symposium*, pp. 321–339, Gesellschaft für Umweltsimulation, 2004.

[89] http://www.rivm.nl/en/themasites/icpmm/manual-and-downloads/.

[90] J. Tidblad, V. Kucera, A. A. Mikhailov et al., "UN ECE ICP materials. Dose-response functions on dry and wet acid deposition effects after 8 years of exposure," *Water, Air and Soil Pollution*, vol. 130, no. 1–4, pp. 1457–1462, 2001.

[91] V. Kucera, J. Tidblad, K. Kreislova et al., "UN/ECE ICP materials dose-response functions for the multi-pollutant situation," *Water, Air, and Soil Pollution*, vol. 7, no. 1–3, pp. 249–258, 2007.

[92] F. Samie, J. Tidblad, V. Kucera, and C. Leygraf, "Atmospheric corrosion effects of HNO3. A comparison of laboratory and field exposed copper, zinc and carbon steel," *Journal of the Electrochemical Society*, vol. 154, no. 5, pp. C249–C254, 2007.

[93] M. Ferm, F. De Santis, and C. Varotsos, "Nitric acid measurements in connection with corrosion studies," *Atmospheric Environment*, vol. 39, no. 35, pp. 6664–6672, 2005.

[94] M. Ferm, J. Watt, S. O'Hanlon, F. De Santis, and C. Varotsos, "Deposition measurement of particulate matter in connection with corrosion studies," *Analytical and Bioanalytical Chemistry*, vol. 384, no. 6, pp. 1320–1330, 2006.

[95] T. Lombardo, A. Ionescu, A. Chabas, R.-A. Lefèvre, P. Ausset, and Y. Candau, "Dose-response function for the soiling of silica-soda-lime glass due to dry deposition," *The Science of the Total Environment*, vol. 408, no. 4, pp. 976–984, 2010.

[96] D. de la Fuente, J. M. Vega, F. Viejo, I. Díaz, and M. Morcillo, "City scale assessment model for air pollution effects on the cultural heritage," *Atmospheric Environment*, vol. 45, no. 6, pp. 1242–1250, 2011.

[97] A. C. Le Gall, S. Doytchinov, R. Fischer et al., "A WGE analysis of the achievements, potential benefits and damages on health, materials and the environment of Gothenburg Protocol scenarios," in *Proceedings of the 8th International Conference on Acid Deposition (ACID RAIN '11)*, Beijing, China, June 2011.

Hindawi Publishing Corporation
International Journal of Corrosion
Volume 2012, Article ID 812192, 9 pages
doi:10.1155/2012/812192

Review Article

Some Clarifications Regarding Literature on Atmospheric Corrosion of Weathering Steels

I. Díaz, H. Cano, B. Chico, D. de la Fuente, and M. Morcillo

Department of Surface Engineering, Corrosion, and Durability, National Centre for Metallurgical Research (CENIM/CSIC), Avenida Gregorio del Amo 8, 28040 Madrid, Spain

Correspondence should be addressed to I. Díaz, ivan.diaz@cenim.csic.es

Received 19 July 2011; Accepted 20 September 2011

Academic Editor: Alejandro R. Di Sarli

Extensive research work has thrown light on the requisites for a protective rust layer to form on weathering steels (WSs) in the atmosphere, one of the most important is the existence of wet/dry cycling. However, the abundant literature on WS behaviour in different atmospheres can sometimes be confusing and lacks clear criteria regarding certain aspects that are addressed in the present paper. What corrosion models best fit the obtained data? How long does it take for the rust layer to stabilize? What is the morphology and structure of the protective rust layer? What is an acceptable corrosion rate for unpainted WS? What are the guideline environmental conditions, time of wetness (TOW), SO_2, and Cl^-, for unpainted WS? The paper makes a review of the bibliography on this issue.

1. Introduction

Weathering steels (WS), also known as low-alloy steels, are mild steels with a carbon content of less than 0.2% wt, to which mainly Cu, Cr, Ni, P, Si, and Mn are added as alloying elements to a total of no more than 3.5% wt [1]. The enhanced corrosion resistance of WS is due to the formation of a dense and well-adhering corrosion product layer known as patina. Besides possessing greater mechanical strength and corrosion resistance than mild steel, the patina is also valued for its attractive appearance and self-healing abilities. The main applications for WS include civil structures such as bridges and other load-bearing structures, road installations, electricity posts, utility towers, guide rails, ornamental sculptures, façades, and roofing.

The recent introduction of high-performance steel, a new high-strength WS that does not require painting, has dramatically increased the number of steel bridges being built throughout the world, which has approximately trebled in the last ten years and now accounts for more than 15% of the market [2]. WS is an attractive material that reduces the life cycle cost of steel structures, which remain in service for long periods of time [3].

Extensive research work has thrown light on the requisites for the protective rust layer to form. It is now well accepted that wet/dry cycling is necessary to form a dense and adherent rust layer, with rainwater washing the steel surface well, accumulated moisture draining easily, and a fast drying action. Surfaces protected from the sun and rain (sheltered) tend to form loose and poorly compacted rust, while surfaces freely exposed to the sun and rain produce more compact and protective rust layers. The structures should be free of interstices, crevices, cavities, and other places where water can collect, as corrosion would progress without the formation of a protective patina. It is also not advisable to use bare weathering steels in indoor atmospheres due to the lack of alternate wetting and drying cycles which are necessary to physically consolidate the rust film, or in marine atmospheres where the protective patina does not form.

However, the abundant literature can be sometimes confusing and lacks clear criteria regarding certain concepts that are addressed in the present paper, namely:

(i) what laws best fit the atmospheric corrosion of WS?

(ii) how long does it take to reach a steady state (stabilization of the rust layer) in which the corrosion rate remains practically constant?

(iii) what is the morphology and structure of the protective rust layer?

(iv) what is an acceptable corrosion rate for the use of unpainted WS?

(v) what are the guideline environmental conditions (TOW, SO_2, and Cl^-) for the use of unpainted WS?

Each of these items is reviewed below.

2. Models Governing the Evolution of Atmospheric Corrosion of Weathering Steel with Exposure Time

As the use of weathering steels in civil engineering became more common, it became necessary to estimate in-service corrosion penetration.

Corrosion penetration data is usually fitted to a *power model* involving logarithmic transformation of the exposure time and corrosion penetration. This power function (also called the bilogarithmic law) is widely used to predict the atmospheric corrosion behaviour of metallic materials even after long exposure times, and its accuracy and reliability have been demonstrated by a great number of authors [4–7].

Legault et al. [5, 8] noted that atmospheric corrosion of WS in industrial and marine environments may be described by the expression

$$C = At^n \tag{1}$$

or its logarithmic transformation:

$$\ln C = \ln A + n \ln t, \tag{2}$$

where C is the corrosion after time t, and A and n are constants.

Pourbaix [6] also stated that the bilogarithmic law is valid for different types of atmospheres and for a number of materials and is helpful in extrapolating results of corrosion up to 20–30 years from four-year test results.

The n value can provide a criterion for gauging long-term atmospheric corrosion susceptibility. It gives a measure of the resistance to transport processes within the corrosion product oxide once it has formed [8]. When n is close to 0.5, it can result from an ideal diffusion-controlled mechanism when all the corrosion products remain on the metal surface. This situation seems to occur in slightly polluted inland atmospheres. On the other hand, n values of more than 0.5 arise due to acceleration of the diffusion process (e.g., as a result of rust detachment by erosion, dissolution, flaking, cracking, etc.). This situation is typical of marine atmospheres, even those with low-chloride contents. Conversely, n values of less than 0.5 result from a decrease in the diffusion coefficient with time through recrystallisation, agglomeration, compaction, and so forth of the rust layer [9].

In the special case when $n = 1$, the mean corrosion rate for one-year exposure is equal to A, the intersection of the line on the bilogarithmic plot with the abscissa $t = 1$ year. There is no physical sense in $n > 1$ as $n = 1$ is the limit for unimpeded diffusion (high permeable corrosion products or no layer at all). Values of $n > 1$ occur practically as exceptions, due, for instance, to outliers in the mass loss determinations. As a rule, $n < 1$. Therefore, n could be used as an indicator for the physicochemical behaviour of the corrosion layer and hence for its interactions with the atmospheric environment. The value of n would thus depend both on the metal concerned, the local atmosphere, maximum exposure time, and the exposure conditions.

On the other hand, the parameter A provides a criterion for gauging short-term atmospheric corrosion susceptibility. It provides a measure of the inherent reactivity of a metal surface as reflected in the tendency for that surface to produce a corrosion product layer in a short-term atmospheric exposure [8].

McCuen et al. [10] proposed to improve the *power model* setting numerically A and n coefficients with the nonlinear least-squares method directly to the actual values of the variables C and t, not the logarithms of the variables, since the logarithmic transformation gives too much weight to the penetration data for shorter exposure. This eliminates the overall bias, and more accurately predicts penetration for longer exposure times. They call *numerical power model* to this new model which has the same functional form as the bilogarithmic model.

Nevertheless, they saw that WS corrosion penetration data revealed behaviour differences that could not all be explained by the parabolic model and thus preferred a composite model (*power-linear model*) consisting of a power function for short exposure times, up to 3 to 5 years, followed by a linear function for longer exposure times. This model is similar to that used to develop standard ISO 9224 [11], which envisages two exposure periods with different corrosion kinetics. In the first period, covering the first ten years of exposure, the growth law is parabolic (average corrosion rate, r_{av}), while in second period, for times of more than 10 years, the behaviour is linear (steady state corrosion rate, r_{lin}).

ISO 9224 [11] offers information on guiding corrosion values for carbon steel and weathering steel (Table 1) in each time period according to the atmospheric corrosivity as defined in ISO 9223 [12]. The guiding corrosion values are based on experience obtained with a large number of exposure sites and service performances.

The question of whether this law provides a better prediction of WS corrosion cannot be fully answered until a greater volume of data is available for analysis, with reference to exposure times of at least 20 years. McCuen and Albrecht compared both models (the power model and the power-linear model) using atmospheric corrosion data reported for WS in the United States and concluded that the experimental data fitted the power-linear model better than the power model and thus provided more accurate predictions of long-term atmospheric corrosion [13].

Finally, Klinesmith et al. [14] mention that all variation related to environmental conditions appears as error variation in the time-dependent models for models that predict corrosion loss as a function of time only. Further, time-dependent models will yield inaccurate predictions when used to estimate corrosion loss in environments that are different from the environment where the model was

Table 1: Guiding corrosion values for corrosion rates (r_{av}, r_{lin}) of carbon steel and weathering steel in atmospheres of various corrosivity categories.

Metal	Average corrosion rate (r_{av}) during the first 10 years for the following corrosivity categories (ISO 9223)				
	C1	C2	C3	C4	C5
Carbon steel	$r_{av} \leq 0.5$	$0.5 < r_{av} \leq 5$	$5 < r_{av} \leq 12$	$12 < r_{av} \leq 30$	$30 < r_{av} \leq 100$
Weathering steel	$r_{av} \leq 0.1$	$0.1 < r_{av} \leq 2$	$2 < r_{av} \leq 8$	$8 < r_{av} \leq 15$	$15 < r_{av} \leq 80$
Metal	Steady state corrosion rate (r_{lin}) for the following corrosivity categories (ISO 9223)				
	C1	C2	C3	C4	C5
Carbon steel	$r_{lin} \leq 0.1$	$0.1 < r_{lin} \leq 1.5$	$1.5 < r_{lin} \leq 6$	$6 < r_{lin} \leq 20$	$20 < r_{lin} \leq 90$
Weathering steel	$r_{lin} \leq 0.1$	$0.1 < r_{lin} \leq 1$	$1 < r_{lin} \leq 5$	$5 < r_{lin} \leq 10$	$10 < r_{lin} \leq 80$

calibrated. To overcome the problem noted, they propose a model that incorporates multiple environmental factors such as TOW, SO_2, Cl^-, and temperature (T):

$$C = At^B \left(\frac{\text{TOW}}{D}\right)^E \left(1 + \frac{\text{SO}_2}{F}\right)^G \left(1 + \frac{\text{Cl}}{H}\right)^I e^{J(T+T_0)}, \quad (3)$$

where A, B, D, E, F, G, H, I, J, and T_0 are empirical coefficients.

The model was formulated for different metals and the results indicate that it was reliable for use in a broad range of conditions or locations.

In spite of that, recent studies on the long-term atmospheric corrosion of WS continue to use the power function because of its simplicity [6, 15, 16], although ignoring the linear part will introduce considerable error in thickness estimates for long exposure times.

3. Rust Layer Stabilisation Time

Information on this aspect is highly erratic and variable, going from claims that a protective patina can be seen to be forming after as little as 6 weeks exposure in environments with low pollution to reports of stabilisation times of "a few years," one year, 2-3 years, 8 years, and so forth.

The time taken to reach a steady state of atmospheric corrosion will obviously depend on the environmental conditions of the atmosphere where the steel is exposed, and to address this issue it is important to have abundant information on the effect of climatic and atmospheric pollution variables on WS corrosion resistance. However, the fact is that unfortunately there is no solid grounding (supported by ample experimentation) upon which to base relationships between atmospheric exposure and WS corrosion variables.

Despite the scarcity of information, a review has been made of published field data on the atmospheric corrosion of WS in different atmospheres, especially for long exposure times.

Table 2 offers a compendium of data encountered in the literature which may be useful in this respect. One factor of uncertainty is that atmospheres are mostly classified in purely qualitative terms (rural, urban, industrial, or marine), based on a subjective appreciation of pollution factors and omitting the humidity variable. On the other hand, although there is a large amount of data on behaviour in the first years of exposure, there is an ostensible lack of information on exposure times of more than 20 years.

The plotting of corrosion versus exposure time has allowed to estimate the time necessary for stabilisation (steady state) of the rust layer, which would indicate the time necessary for the formation of protective layers (column 6). Indeed, a look at Table 2 allows observing that after very short exposure times (3–5 years) stabilised (protective) rust layers are commonly formed in rural and urban atmospheres. Longer exposure times (5–10 years) are usually required in industrial atmospheres. With regard to marine atmospheres, although little information is available, corrosion rates are seen to be higher, and the time taken to reach the steady state, if it is reached, tends to be longer, in excess of 15 years.

Table 2 also offers important information on aspects such as the effect of the type of atmosphere on WS corrosion, specifically, about the corrosivity category (column 5) as a function of 1st-year corrosion, long-term WS corrosion rates (column 7), and the relationship between carbon steel corrosion and WS corrosion (column 8), aspects on which reported data in the literature are highly variable.

In relation to the influence of the type of atmosphere in the corrosion of weathering steel, as in the case of carbon steel, it can clearly be seen how WS corrosion rises going from a practically pollution-free rural atmosphere (C2) to an urban atmosphere (C2-C3) and from there to industrial and marine atmospheres (C3-C4).

Particular mention should be made of the effect of atmospheric SO_2 pollution on WS corrosion, where the existing literature is rather confusing, from those who say that WS is less sensitive to SO_2 than carbon steel, especially for long exposure time, to those who believe that "weathering steels need access to SO_2 or sulphate-containing aerosols to improve their corrosion resistance," [28] or "it is generally accepted that a low but finite concentration of SO_2 in the atmosphere can actually assist the formation of a protective layer on WS." In the first case, Satake and Moroishi [29] report a close relationship between corrosion losses and SO_2 contents in the air in the first year of exposure but which disappears in the fifth year of exposure. On the contrary, ISO 9223 [12] notes that "in atmospheres with SO_2 pollution a more protective rust layer is formed." The literature also reports that copper in WS can form small amounts of relatively insoluble copper hydroxy sulphates, such as

Table 2: Compendium of bibliographic information on evolution of atmospheric corrosion of conventional WS with time of exposure.

Reference	Test site	Country	Atmosphere	Corrosivity category (ISO 9223) [12]	Time (years) for steady-state condition	At the longest exposure time (years)	
						Corrosion rate (μm/y)	R^* (CS/WS)
[17]	South Bend	USA	Rural	C2	5–10	1.7 (15.5 y)	4.6 (15.5 y)
[18]	Sailorsburg	USA	Rural	C2	5–10	3.4 (16 y)	3.5 (16 y)
[19]	Potter County	USA	Rural	C2	3	2.5 (8–16 y)	2.9 (8–16 y)
[17]	State College	USA	Rural	C3	3	7.3 (7 y)	1.9 (7 y)
[20]	Cincinnati	USA	Urban	C2	5	4.8 (5.3 y)	1.5 (5.3 y)
[20]	Detroit	USA	Urban	C2	5–10	9.2 (5.3 y)	1.5 (5.3 y)
[20]	Los Angeles	USA	Urban	C2	5	4.4 (5.3 y)	1.1 (5.3 y)
[20]	Philadelphia	USA	Urban	C2	5	6.3 (5.3 y)	1.5 (5.3 y)
[20]	Washington	USA	Urban	C2	5	4.9 (5.3 y)	1.6 (5.3 y)
[21]	Hurbanovo	Czech Rep.	Urban, 41 mg/(m^2 d) of SO_2	C2-C3	≈3	2 (5–10 y)	2-3 (5–10 y)
[21]	Praha	Czech Rep.	Urban, 86 mg/(m^2 d) of SO_2	C3	≈3	3 (5–10 y)	3-4 (5–10 y)
[22]	Nat. Tsing-Hua Univ.	China	Urban, 60 mg/(m^2 d) of SO_2	C3	≈5	22 (5 y)	1.5 (5 y)
[21]	Kopisty	Czech Rep.	Industrial, 129 mg/(m^2 d) of SO_2	C4	5–10	23 (5 y)	2 (5 y)
[22]	China Steel Corp.	China	Industrial, 87 mg/(m^2 d) of SO_2	C3	≈3	11.7 (6 y)	3 (6 y)
[23]	Amagasaki	Japan	Industrial, 152 mg/(m^2 d) of SO_2	C3	5–10	10.2–14.6 (5–7 y)	2.4–3.7 (5–7 y)
[23]	Kitakyushu	Japan	Industrial, 172 mg/(m^2 d) of SO_2	C3	5–10	13.2 (5 y)	2.7 (5 y)
[17]	Kearny (1940)	USA	Industrial	C3	5–10	2.8 (20 y)	5.9 (20 y)
[19]	Kearny (1970)	USA	Industrial	C3	—	1.5 (8–16 y)	2.1 (8–16 y)
[24]	Newark	USA	Industrial	C3-C4	3	10.3 (7 y)	1.9 (7 y)
[24]	Whiting	USA	Industrial	C3-C4	3	10.3 (7 y)	1.8 (7 y)
[25]	Rankin	USA	Industrial	C3	≈8	4.20 (17 y)	—
[25]	Rankin	USA	Industrial	C3	5–10	7.74 (10 y)	4.31 (10 y)
[25]	Columbus	USA	Industrial	C3	5–10	7.72 (10 y)	2.28 (10 y)
[25]	Bethlehem	USA	Industrial	C3	5	6.54 (10 y)	3.13 (10 y)
[17]	Kure Beach (250 m)	USA	Marine, 91 mg/(m^2 d) of Cl^-	C2-C3	>10	3.5 (15.5 y)	2.3 (15.5 y)
[26]	Kure Beach (250 m)	USA	Marine, 91 mg/(m^2 d) of Cl^-	C2-C3	>15	7.5 (16 y)	—
[24]	Kure Beach (25 m)	USA	Marine, 485 mg/(m^2 d) of Cl^-	C3	7	14.6 (7 y)	5.7 (7 y)
[24]	Point Reyes	USA	Marine	C4	7	18.0 (7 y)	3.3 (7 y)
[27]	Miraflores	Panama	Marine	C3	>15	6.8 (16 y)	2.7 (16 y)
[27]	Limon Bay	Panama	Marine	C3	>15	12.7 (16 y)	2.0 (16 y)
[13]	Block Island	USA	Marine	C2-C3	>17	12.7 (17.1 y)	—

R^*: ratio between carbon steel (CS) corrosion and weathering steel (WS) corrosion.
—: not available.

$[Cu_4(SO_4)(OH)_6]$ or $[Cu_3(SO_4)(OH)_4]$. These compounds can precipitate in pores of the rust layer, thereby improving the barrier effect of the patina [28].

Studies into the effect of SO_2 pollution in the atmosphere on WS corrosion are very scarce. Perhaps the most important information in this respect is that obtained in an 8-year study performed at numerous locations within the framework of the UNECE International Cooperative Programme on effects on materials, including Historic and Cultural monuments [30]. Figure 1 plots the WS corrosion rate after 8 years of exposure versus the SO_2 concentration in the atmosphere, and a clear effect of SO_2 in the atmospheric corrosion of WS is observed. According to Leygraf and Gradael, it seems that a certain amount of deposited SO_2 is beneficial. However, large amounts result in intense acidification of the aqueous layer, triggering dissolution and hindering precipitation [28].

With regard to marine atmospheres, although little information is available (see Table 2), corrosion rates are seen to be higher and the time taken to reach the steady state, if it is reached, tends to be longer, in excess of 15 years as it was mentioned previously. The action of chloride ions in this type of atmosphere seems to hinder the formation of protective rust layers, thus impeding the use of conventional WS.

Another aspect about which bibliographic information is highly variable is the relationship between mild steel corrosion rate and WS corrosion rate for different exposure times and atmosphere types. It is common to find general statements in the literature such as: "WS has to 4, 5 to 8, 10, and so forth, times more corrosion resistance than carbon steel," or "in comparison to carbon steels, WS may have corrosion rates of more than one order of magnitude less, depending on the environmental conditions." That relationship obviously depends again on the environmental conditions where both materials are exposed and the time of exposure. For this reason, the last column in Table 2 shows the relationship R between carbon steel (CS) corrosion and conventional WS corrosion for the longest exposure time in each of the atmospheres for which information is available in the reviewed literature. The average values yield relationships of 2.3 (rural-urban atmospheres), 2.9 (industrial atmospheres), and 3.2 (marine atmosphere). The lack of precision is great, and a certain tendency is seen for the value of this relationship to rise with time, which means that the beneficial effects of WS are increasing. It is also noted that the reduction in WS corrosion seems to be greater in the most aggressive atmospheres (industrial or marine).

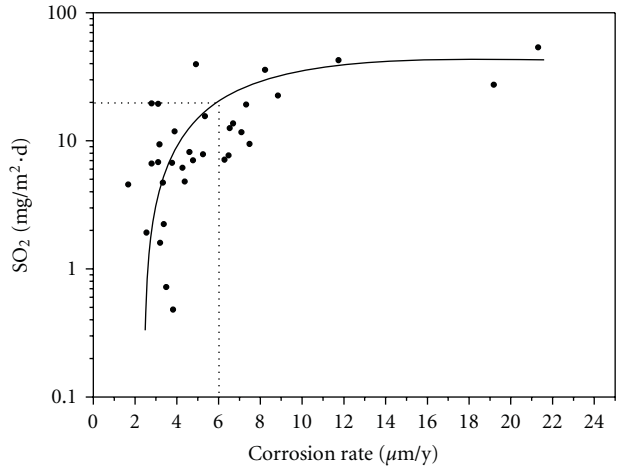

Figure 1: Variation of atmospheric corrosion rate for conventional weathering steel with SO_2 content in the atmosphere, constructed from date provided by UNECE, after 8 years of exposure.

4. Morphology of the Protective Rust Layer

The formation of the protective rust layer on weathering steels is not yet completely understood. In the late 1960s, researchers suggested that the stratification of rust layers was an intrinsic property of protective rusts formed on WS. The work of Okada [31] is perhaps the most commonly cited in this respect, where the authors show that unlike carbon steel, upon which only one stratum of rust is formed, on WS, two strata of rust may be observed after a certain exposure time, consisting of an internal layer with protective characteristics and an unprotective outer layer. Similarly, Leygragh and Gradael [28] and Zhang et al. [9] state that the structure of rust on WS is different from that on iron or carbon steels. It is characterised by a double-layer structure, with the inner phase providing a greater barrier to oxygen and water than the outer phase. The outer phase is flaky and poorly adherent, whereas the inner phase adheres well.

Microscopic observation performed by Yamashita et al. [32] and Okada [31] found that the rust layer can be divided into two layers: one corresponds to the outer layer which is optically active, and the other is the inner layer which is optically isotropic (darkened). On the other hand, the surface rust formed on the mild steel consists of the mottled structure consisting of the optically active and isotropic corrosion products. The optically isotropic layer was mainly composed of amorphous spinel-type iron oxide and the optically active layer was γ-FeOOH. Raman et al. [33] and Suzuki et al. [34] described that the outer layer of WS contains several different crystalline oxyhydroxides, including lepidocrocite (γ-FeOOH), goethite (α-FeOOH), akaganeite (β-FeOOH), feroxyhyte (δ-FeOOH), maghemite (γ-Fe_2O_3), magnetite (Fe_3O_4), and ferrihydrite ($Fe_5HO_8\cdot 4H_2O$), and an inner region, consisting primarily of dense amorphous FeOOH with some crystalline Fe_3O_4 (Figure 2).

Dillmann et al. [35] studied in detail that the major phases of the rust layers are magnetite, goethite, and lepidocrocite. Lepidocrocite seems to be more present in the outer layer and goethite seems to be the major constituent of the inner layer. Furthermore, Zhang et al. [9] pointed out that the inner rust layer is enriched in some kind of alloying elements just like Cr, Cu, and other elements, whereas the outer layer, which is distributed with cracks and pores, could not inhibit the entrance of the corrosive electrolyte.

Now it is generally agreed that both CS and WS form rusts that tend to stratify with exposure time [36]. Both common carbon steels and WS present a rust layer that is in turn composed of two sublayers, a reddish outer layer and a dark grey inner layer (polarised light). This stratification is independent of the degree of protection afforded by the rust.

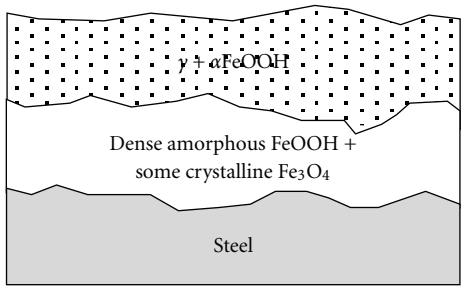

Figure 2: Dual nature of the rust layer.

The composition and morphology of the protective patina formed on WS is very different to the coating formed on carbon steel. The difference between the rust layers formed on carbon steel and on WS is that the α-phase (goethite phase) on the latter forms a densely packed and uniform layer of nanometre-sized particles, which are closely attached to the underlying steel substrate. On carbon steel, however, the distribution of phases is more heterogeneous, resulting in a rust layer with a mottled structure. The corrosion protection ability of WS is mainly attributed to this dense α-phase whose formation is stimulated by dry-wet-dry cycling [3].

According to Yamashita and Uchida [37], the protective rust layer on WS is usually formed spontaneously after a certain number of years of exposure. Until the protective ability of the rust layer emerges, the WS corrosion rate is not especially low. Furthermore, the protective rust layer cannot form in coastal environments where the amount of airborne sea-salt particles is relatively high. The higher the chloride deposition rate in marine atmospheres, the greater the degree of flaking observed, with loosely adherent flaky rust favouring rust film breakdown (detachment, spalling) and the initiation of fresh attack. The morphologic characteristics of the protective patina will therefore depend on the type of environment (rural, urban, industrial, or marine), WS composition, years of exposure, relative humidity, temperature, and pollutants (SO_2, Cl^-, etc.) as the main factors governing the formation and transformation of the protective layer.

5. Allowable Corrosion Rate for Unpainted Weathering Steel

In 1962, Larrabe and Coburn [17] suggested that an average WS corrosion loss of 2-3 mils (25–75 μm) in 15 years in a given atmosphere (i.e., 1.7–5 μm/y) would be sufficiently low for this steel to be used in the atmosphere without being painted.

In Japan, conventional WS specified as Japan Industrial Standard G 3114 SMA (JIS-SMA Weathering Steel), which is almost the same as that first commercialised by US Steel Corporation in the 1930s, can be used for bridges in environments where less than 0.3 mm corrosion loss per side is expected in 50 years of exposure, that is, 6 μm/y [38]. It is important to note that 50 years does not mean bridge lifetime and that 0.3 mm of corrosion loss does not define the criteria of structural stability. These values are used to define the corrosivity of the atmosphere, and in general steel structures can be said to be sufficiently durable to accommodate a great deal of corrosion before any risk of collapse. Conventional WS is currently considered in Japan to be appropriate for bridges in environments where corrosion loss on one side of a girder is less than 0.5 mm in 100 years of exposure, that is, 5 μm/y [39].

In USA, according to Cook [40], the acceptable corrosion rate for weathering steel in medium corrosivity locations is 120 μm maximum for 20 years of exposure, that is, 6 μm/y again. Due to the development of rust patina during the lifetime of a structure that incorporates unpainted WS, a corrosion allowance should be made on each exposed surface, representing a loss of thickness of the material used for structural purposes [41]:

(i) for atmospheric conditions defined by ISO 9223 [12] as class C1, C2, or C3 ("mild" environments for WS), the corrosion allowance should be 1 mm per surface, while for class C4 on C5 ("Severe" environments for WS), the corrosion allowance shall be 1.5 mm per surface,

(ii) for the "interior" surface of box sections, the allowance shall be 0.5 mm.

Following the same criterion as Japan and USA for the use of unpainted WS allowing a maximum atmospheric corrosion rate for steel of 6 μm/y in long-term exposures, the seventh column in Table 2 presents information on this aspect. According to the information contained in Table 2, conventional WS may be used in rural and urban areas without excessive SO_2 pollution where the WS corrosion rate at the end of the exposure period is usually less than 6 μm/y; however, it should not be used in industrial or marine atmospheres because long-term WS corrosion rate has higher values, usually in excess of 6 μm/y. It should nevertheless be noted that the available information corresponds to relatively short exposure times in which, as has been commented above, WS still presents high corrosion rates and where protective rust layers have not perhaps yet had time to form.

6. Guideline Levels for Environmental Parameters (TOW, SO_2, and Cl^-) for the Use of Conventional Weathering Steel

6.1. Japan. An application guideline for unpainted WS has been prepared based on the results of surveys and examinations, including the long-term exposure tests carried out from 1981 to 1993 by three organisations: the Public Works Research Institute of the Construction Ministry, the Japan Association of Steel Bridge Construction, and the Kozai Club [38]. Figure 3 shows the relationship between atmospheric salinity and WS corrosion (per exposed surface), differentiating between two zones according to the adherent or nonadherent nature of the rust formed. Salinity measurements were obtained by the gauze method (JIS-Z-2381) [42]. Bearing in mind the maximum corrosion rate permitted for the use of WS, 6 μm/y, an NaCl critical level of 0.05 mg/(dm^2 d) or 3 mg/(m^2 d) of Cl^- is established for

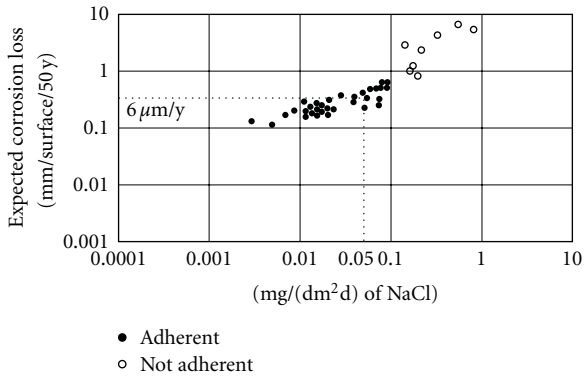

Figure 3: Influence of air-born salts (atmospheric salinity) on the stability of the protective layer of corrosion products formed on WS.

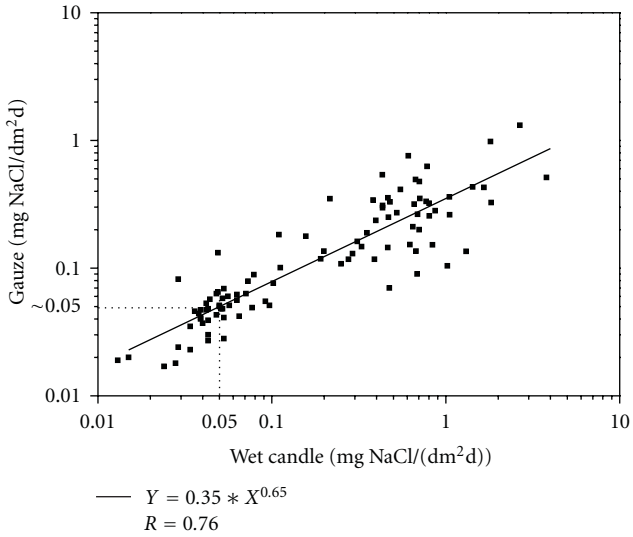

Figure 4: Relationship between measurements obtained by the wet candle method and the gauze method.

airborne salt [43]. At the present time the NaCl limit is set at 0.1 mg/(dm^2 d) or 6 mg/(m^2 d) of Cl^- and there is even talks of a range of 0.1-0.2 mg/(dm^2 d) of NaCl or 6–12 mg/(m^2 d) of Cl^-, depending on the conditions of usage [44].

6.2. United Kingdom. The United Kingdom Department of Transport Standard BD 7 [41], "Use of WS for highway structures," suggested in 1981 that uncoated WS should not be used when:

(1) the chloride level exceeds 0.1 mg/(dm^2 d) or 10 mg/(m^2 d),

(2) the yearly average time of wetness exceeds 60%,

(3) the threshold level for sulphur trioxide exceeds 2.1 mg/(dm^2 d) or 168 mg/(m^2 d) of SO_2.

The 2001 edition of BD 7 established new critical levels for Cl^- and SO_2. A salinity classification of S3 ($\geq$300 mg/(m^2 d) of Cl^-) and SO_2 levels above P3 ($\geq$200 mg/(m^2 d)) should be avoided for use of uncoated WS.

6.3. USA. According to United States government guidelines [45], the following conditions should be avoided if WS is used: Chloride deposition >50 mg/(m^2 d), sulphur dioxide deposition >168 mg/(m^2 d), as United Kingdom (Standard BD 7 [41]), and average time of wetness >60%. The time of wetness is here defined as the time during which the relative humidity is >80% and the temperature is >0°C. Environmental data has been obtained in accordance with ISO 9223 [12]. Unlike in Japan, atmospheric salinity data has been obtained by the wet candle method (ISO 9223) [12]. The relationship between the data obtained with these two techniques, the gauze method and the wet candle method [46], is displayed in Figure 4 for NaCl levels between 0.013 y 3.8 mg/(dm^2 d), obtained by the wet candle method [47].

It shows that the wet candle method is more sensitive to the presence of NaCl, capturing greater amount of aerosol that the gauze method for NaCl levels higher than 0.05 mg/(dm^2 d).

Unlike the effect of atmospheric salinity on WS corrosion, for which valuable information was obtained in 12-year exposure tests carried out to classify the severity of environments in Japan (Figure 3), no similar study concerning the effect of atmospheric SO_2 has been found in the literature. Nevertheless, the graph in Figure 1 draws on interesting results obtained by UNECE [30] for the case of weathering steel exposed for 8 years in numerous atmospheres in Europe and America. The graph excludes sites where the atmospheric salinity or time of wetness is excessively high for protective rust layers to form ($\geq$6 mg/L of Cl^- in rain water and TOW in excess of 5500 h/y). This graph allows a critical level of around 20 mg/(m^2 d) of SO_2 to be established, in accordance with the criterion for the use of unpainted WS in atmospheric exposure (6 μm/y).

In another study performed in the former Czechoslovakia by Knotkova et al. at different testing sites with high-SO_2 pollution, an SO_2 critical level of 90 mg/(m^2 d) was established for the use of WS in this type of atmospheres [21], much higher than the obtained level from Figure 1.

7. Conclusions

From the bibliographic review performed, the following conclusions may be drawn.

(i) Although the power function ($C = At^n$) seems to provide a good fit of the evolution of atmospheric corrosion of weathering steels with exposure time, the power-linear model provides better predictions for long-term exposure times.

(ii) The time taken for the rust layer to stabilise obviously depends on the environmental conditions of exposure: 3–5 years for rural or urban atmospheres; 5–10 years for industrial atmospheres; >15 years for marine atmospheres, if a steady state is ever actually reached in this type of atmosphere. Atmospheres polluted with SO_2, if not strongly polluted (>90 mg/(m^2 d) of SO_2), promote earlier stabilisation of the rust layers, ($\approx$3 years) possibly due to the

sealing of internal porosity in the rust by corrosion products formed between SO_2 and copper in the WS.

(iii) With regard to the morphology of the rust layers formed in the atmosphere, two sublayers are formed on both carbon steel and WS, the innermost being responsible for the protective properties of the rust in the case of WS.

(iv) There seems to be general agreement on the allowable corrosion rate (6 μm/y) for the use of unpainted WS in the atmosphere.

(v) There is a lack of unified criteria on guideline environmental conditions (SO_2, Cl^-) for the use of unpainted WS. The chloride level allowed in Japan seems to be excessively low (6 mg/(m^2 d)) and excessively high ($\geq$300 mg/(m^2 d)) in United Kingdom, while the SO_2 levels allowed in the United Kingdom and USA seem excessively high (200 and 168 mg/(m^2 d)), respectively.

References

[1] T. Murata, "Weathering steel," in *Uhlig's Corrosion Handbook*, R. W. Revie, Ed., J. Wiley & Sons, New York, NY, USA, 2000.

[2] I. Kage, K. Matsui, and F. Kawabata, "Minimum maintenance steel plates and their application technologies for bridge—life cycle cost reduction technologies with environmental safeguards for preserving social infrastructure assets," *JFE Technical Report*, no. 5, pp. 37–44, 2005.

[3] D. C. Cook, "Spectroscopic identification of protective and non-protective corrosion coatings on steel structures in marine environments," *Corrosion Science*, vol. 47, no. 10, pp. 2550–2570, 2005.

[4] K. Bohnenkamp, G. Burgmann, and W. Schwenk, "Investigations of the atmospheric corrosion of plain carbon and low alloy steels in industrial, rural and sea air," *Stahl und Eisen*, vol. 93, no. 22, pp. 1054–1060, 1973.

[5] R. A. Legault and A. G. Preban, "Kinetics of the atmospheric corrosion of low-alloy steels in an industrial environment," *Corrosion*, vol. 31, no. 4, pp. 117–122, 1975.

[6] M. Pourbaix, "The linear bilogarithmic law for atmospheric corrosion," in *Atmospheric Corrosion*, W. H. Ailor, Ed., J. Wiley & Sons, New York, NY, USA, 1982.

[7] S. Feliu and M. Morcillo, "Atmospheric corrosion testing in spain," in *Atmospheric Corrosion*, W. H. Ailor, Ed., pp. 913–922, J. Wiley & Sons, New York, NY, USA, 1982.

[8] R. A. Legault and V. P. Pearson, "Atmospheric Corrosion in Marine Environments," *National Association of Corrosion Engineers*, vol. 34, no. 12, pp. 433–437, 1978.

[9] Q. C. Zhang, J. S. Wu, J. J. Wang, W. L. Zheng, J. G. Chen, and A. B. Li, "Corrosion behavior of weathering steel in marine atmosphere," *Materials Chemistry and Physics*, vol. 77, no. 2, pp. 603–608, 2003.

[10] R. H. McCuen, P. Albrecht, and J. G. Cheng, "A New approach to power-model regression of corrosion penetration data," in *Corrosion Form and control for Infrastructure*, V. Chaker, Ed., ASTM STP 1137, American Society for Testing and Materials, Philadelphia, Pa, USA, 1992.

[11] ISO 9224, *Corrosion of Metals and Alloys—Corrosivity of Atmospheres—Guiding Values for the Corrosivity Categories*, Geneve, Switzerland, 1992.

[12] ISO 9223, *Corrosion of Metals and Alloys—Corrosivity of Atmospheres—Classification*, Geneve, Switzerland, 1992.

[13] R. H. McCuen and P. Albrecht, "Composite modeling of atmospheric corrosion penetration data," in *Application of Accelerated Corrosion Test to Service Life Prediction of Materials*, G. Cragnolino and N. Sriddhar, Eds., ASTM STP 1194, ASTM, Philadelphia, Pa, USA, 1994.

[14] D. E. Klinesmith, R. H. McCuen, and P. Albrecht, "Effect of environmental conditions on corrosion rates," *Journal of Materials in Civil Engineering*, vol. 19, no. 2, pp. 121–129, 2007.

[15] H. E. Townsend, "Effects of alloying elements on the corrosion of steel in industrial atmospheres," *Corrosion*, vol. 57, no. 6, pp. 497–501, 2001.

[16] S. W. Dean, D. Knotkova, and K. Kresilova, *ISOCORRAG International Atmospheric Exposure Program: Summary of Results ASTM Data Series 71*, ASTM International, West Conshohorken, Pa, USA, 2010.

[17] C. P. Larrabe and S. K. Coburn, *Proceedings of the 5th International Congress on Metal Corrosion*, London, UK, 1962.

[18] H. E. Townsend and J. C. Zoccola, "Eight-year atmospheric corrosion performance of weathering steel in industrial, rural and marine environments," in *Atmospheric Corrosion*, S. W. Dean Jr. and E. C. Rhea, Eds., ASTM STP 767, ASTM, Philadelphia, Pa, USA, 1982.

[19] S. K. Coburn, M. E. Komp, and S. C. Lore, *Atmospheric Corrosion*, ASTM STP 1239, ASTM, Philadelphia, Pa, USA, 1995.

[20] F. H. Haynie and J. B. Upham, "Effects of atmospheric pollutans on corrosion behavior of steels," *Material Performance*, vol. 10, no. 11, pp. 18–21, 1971.

[21] D. Knotkova, J. Vlckova, and J. Honzak, "Atmospheric corrosion of weathering steels," in *Atmospheric Corrosion*, S. W. Dean Jr. and E. C. Rhea, Eds., ASTM STP 767, ASTM, Philadelphia, Pa, USA, 1982.

[22] J. H. Wang, F. I. Wei, Y. S. Chang, and H. C. Shih, "The corrosion mechanisms of carbon steel and weathering steel in SO_2 polluted atmospheres," *Materials Chemistry and Physics*, vol. 47, no. 1, pp. 1–8, 1997.

[23] T. Moroishi and J. Satake, "Effect of alloying elements on atmospheric corrosion of high tensile strength steels," *Journal of the Iron and Steel Institute of Japan*, vol. 59, no. 2, pp. 293–300, 1973.

[24] G. B. Mannweiler, *Corrosion Test Results on Fifteen Ferrous Metals After Seven-Year Atmospheric Exposure*, ASTM STP 435, ASTM, Philadelphia, Pa, USA, 1968.

[25] B. J. Horton, *The Composition, Structure and Growth of Atmospheric Rust on Various Steels*, University Lehigh, 1964.

[26] H. R. Copson, "Long-time atmospheric corrosion test on low-alloy steels," *Proceedings ASTM*, vol. 60, 1960.

[27] C. R. Southwell, J. D. Bultman, and A. L. Alexander, "Corrosion of metals in tropical environments—final report of 16-year exposures," *Materials Performance*, vol. 15, no. 7, pp. 9–26, 1976.

[28] C. Leygraf and T. Gradael, *Atmospheric Corrosion, Electrochemical Society Series*, J. Wiley & Sons, New York, USA, 2000.

[29] J. Satake and T. Moroishi, *Proceedings of the 5th International Congress on Metal Corrosion*, NACE, Houston, Tex, USA, 1974.

[30] J. Tidblad, V. Kucera, and A. A. Mikhailov, *UNECE International Cooperative Programme of Effects on Materials, Including Historic and Cultural Monuments*, Report No. 30: Statistical Analysis of 8 Year Materials Exposure and Acceptable Deterioration and Pollution Levels.

[31] H. Okada, *Proceedings of the 4th International Congress on Metal Corrosion*, NACE, Houston, Tex, USA, 1972.

[32] M. Yamashita, H. Miyuki, Y. Matsuda, H. Nagano, and T. Misawa, "The long term growth of the protective rust layer formed on weathering steel by atmospheric corrosion during a quarter of a century," *Corrosion Science*, vol. 36, no. 2, pp. 283–299, 1994.

[33] A. Raman, S. Nasrazadani, and L. Sharma, "Morphology of rust phases formed on weathering steels in various laboratory corrosion tests," *Metallography*, vol. 22, no. 1, pp. 79–96, 1989.

[34] I. Suzuki, Y. Hisamatsu, and N. Masuko, "Nature of atmospheric rust on iron," *Journal of the Electrochemical Society*, vol. 127, no. 10, pp. 2210–2215, 1980.

[35] P. Dillmann, F. Mazaudier, and S. Hoerlé, "Advances in understanding atmospheric corrosion of iron: I. Rust characterisation of ancient ferrous artefacts exposed to indoor atmospheric corrosion," *Corrosion Science*, vol. 46, no. 6, pp. 1401–1429, 2004.

[36] L. M. Ocampo, "Influência dos elementos de liga Na corrosão de aços patináveis," in *Engenharia Metalúrgica e de Materiais*, p. 145, Universidade Federal do Rio de Janeiro, Rio de Janeiro, Brazil, 2005.

[37] M. Yamashita and H. Uchida, "Recent research and development in solving atmospheric corrosion problems of steel industries in Japan," *Hyperfine Interactions*, vol. 139-140, no. 1–4, pp. 153–166, 2002.

[38] K. Club, Ed., "Guideline for desing and construccion of bridges by weathering steel," Tech. Rep., Tokio, Japan, 1993.

[39] "Specification for highway bridges," in *Japan Road Association*, Tokio, Japan, 2002.

[40] D. C. Cook, *The Corrosion of High Performance Steel in Adverse Environments*, ISIAME, 2004.

[41] *BD7-01, Wetahering Steel for Highway Structures*, vol. 2, section 3, part 8 of *Desing Manual for Roads and Bridges*, The United Kingdom Department of Transport, London, UK, 2001.

[42] *Recommended Practice for Weathering Test*, JIS-Z-2381, Japan Industrial Standard, 1987.

[43] M. Takabe, M. Ohya, and S. Ajiki, "Estimation of quantity of Cl^- from deicing salts on weathering steels used for bridges," *Steel Structures*, vol. 8, pp. 73–81, 2008.

[44] S. S. Kim, "Appropriate environmental sphere of application for unpainted weathering steel," *Journal of Industrial and Engineering Chemistry*, vol. 9, no. 2, pp. 212–218, 2003.

[45] *Technical Advisory 5140.22, Uncoated Weathering Steel in Structures*, US Department of Transportation, Federal Highway Administration, 1989.

[46] *Standard Test Method for Determining Atmospheric Chloride Deposition Rate by Wet Candle Method*, ASTM G140-96, ASTM, Philadelphia, Pa, USA, 1996.

[47] S. W. Dean, "Atmospheric," in *Corrosion test and Standards, Application and Interpretation*, R. Baboian, Ed., pp. 116–125, ASTM, Philadelphia, Pa, USA, 1995.